6-19-2017

A Finite Element Analysis of Maxillary Centers of Resistance

Edward A. Cronauer
ecronauer@uchc.edu

A Finite Element Analysis of Maxillary Centers of Resistance

Edward Anthony Cronauer

B.A., Duke University, 2009
D.M.D., University of Florida, 2014

A Thesis

Submitted in Partial Fulfillment of the

Requirements for the Degree of

Master of Dental Science

At the

University of Connecticut

2017

2017

Approval Page

Master of Dental Science Thesis

A Finite Element Analysis of Maxillary Centers of Resistance

Presented by

Edward Anthony Cronauer, B.A., D.M.D

Major Advisor: _____

Dr. Madhur Upadhyay, B.D.S., M.D.S., M.Dent.Sc.

Associate Advisor: _____

Dr. David M. Pierce, M.S., Ph.D.

Associate Advisor: _____

Dr. Satyashankara Aditya Tadinada, B.D.S., M.Dent.Sc.

University of Connecticut

2017

I. Table of Contents

II. Abstract

Introduction: Orthodontic tooth movement involves the application of forces to particular teeth to achieve movement in a desired direction. The applied forces have magnitude and direction that, when applied to teeth, can result in translation, rotation, or, as in most cases, a combination of the two.[1] This resulting movement depends on the point of application of this force vector to the tooth.

The center of mass of a body is the point through which a force would cause pure translation of the object. Because teeth are not free in space but rather partially restricted from movement by the periodontal ligament and alveolar bone, the traditional "center of mass" of a tooth is redefined as the center of resistance (CR).[1] A force through the center of resistance of a tooth would cause pure translation of the tooth through bone without rotation.[1] Thus, forces applied away from the center of resistance would not achieve translation and would cause effects that may or may not be desirable.

Because the center of resistance is dependent upon root length, root morphology, and alveolar bone height,[1, 2] it is difficult to know, with sure accuracy, the center of resistance for every patient. Additionally, when more than one tooth is involved in the application of force, the center of resistance differs and can become far more difficult to determine.

Previous investigations involved a number of techniques to estimate the center of resistance of a tooth or segment of teeth. These methods range from traditional radiographic and physical measurements and calculations,[3, 4] to in vitro studies on models or cadaveric specimens,[5] to more modern techniques such as finite element analysis with three dimensional images.[6, 7, 8, 9, 10, 11, 12, 13]

Finite element analysis is a computer-based method of resolving stresses and strains in systems that range from simple structures to complicated 3D objects. It is an important tool in the engineering field and is becoming more popular in other fields each year as technology improves and becomes more affordable and accessible. Finite element analysis is an ideal tool to examine biological three dimensional structures, such as teeth, PDL, and bone, in order to determine the center of resistance.[9, 10]

In the current literature, most finite element studies are conducted on models or a single tooth using high-dose micro CT scans. Little has been done with newer, lower-dose, and lower resolution CBCT imaging. Additionally, very little is described about the materials and methods used to develop these models for finite element analysis, and no study has looked at a patient's entire maxillary dentition. Investigators are left to determine the proper workflow and tools from scratch for each project undertaken costing research time and resources. As a secondary result, finite element studies contain significant variability in the procedures used for analysis. This study used routine, low-dose CBCT patient images and developed a toolset and workflow to generate finite element models for analysis. Additionally, ten patient models were developed that can be used for finite element analysis in future studies.

Materials and Methods: CBCT images were the source of three dimensional data from patients. These volumes were manipulated in software to extract 3D biological structures relevant to determining the center of resistance of the maxillary teeth, similar to methods employed in other studies using Mimics software for segmentation.[7, 12] These segmented objects were then cleaned and converted into a virtual mesh made up of small, standard, uniform triangles consisting of nodes and edges with 3matic software. The models were further converted into a solid mesh of tetrahedrons with mid-side nodes on each edge for use in finite element analysis. The solid mesh models were loaded into engineering software, Abaqus, which

was used to pre-process the models to create an assembly, set some material properties, set interaction conditions, boundary conditions, and place loads. The loads, when analyzed, will simulate the stresses and strains on the system. With this data, the center of resistance can be determined for a desired tooth or group of teeth based off the stresses and strains in the model.

Results: The results of this study are a detailed workflow for generating finite element models using CBCT patient images. Software tools and values used in the model generation are described. Ten patient models were created from CBCT patient images for use in finite element analysis.

Conclusions: This study concluded that CBCT images are acceptable for use in generating finite element models for analysis and that a consistent workflow for generating models can be established. Although the processing time required for a model is relatively lengthy, as scans improve, software becomes more efficient, and algorithms become smarter, processes such as these should become easier and faster. This study is an early look into what could be the sequence of steps to a personalized orthodontic treatment plan.[14]

I. Introduction

A. Background and Literature Review

Orthodontics is a specialty of dentistry that is entrenched in mechanics and physics. It is in the unique position of treating a variety of patients with variable malocclusions to a defined set of treatment goals. To achieve the desired treatment result, the crux of treatment is planning out and implementing the means to that end.

Orthodontic treatment involves applying various forces at different points on teeth to achieve biological movements that result in repositioning of the teeth into a desired functional and esthetic orientation. The overall force systems implemented in orthodontic tooth movement are far from simple fulcrum and lever systems that can be calculated on a piece of paper. When a force is applied to a tooth, segment, or whole arch, it is important to know the center of resistance of the body in order to be able to better understand and predict the movement that will take place.[1]

Smith and Burstone[1] equate the center of gravity for a body suspended in space to the center of resistance of a restrained body. Maintained in bone by the periodontal ligament, a tooth encapsulates the center of resistance – the point through which a force causes translation.[1] For decades, the orthodontic field has been revisiting research regarding the location of the center of resistance of a given tooth, segment, or arch.[1, 2, 3, 4, 5, 7, 10, 11, 13, 15, 16] Great variation in location stems from the morphology of the teeth, the role of the periodontal ligament, alveolar bone height, and the biology of the bone and remodeling characteristics.[2]

As a result of these factors, determining the center of resistance and predicting tooth movement for a given application of force proves to be difficult. Early investigations determined rough positions for the center of resistance for certain teeth to be about one third the root length

from the alveolar bone crest.[4, 1] These studies were limited to few teeth at a time and determined the locations of the center of resistance based off generic anatomical data for teeth, measurements from two dimensional radiographs, and calculations on two dimensional drawings. Consequently, involving multiple teeth within the arch or between the arches exponentially complicates the system. Clinically predicting tooth movements from a particular application of force then becomes more a matter of clinical experience and trial and error than a calculation.

However, with the advent of new technology came the ability to model more complicated systems. In the 1980's, computers and novel technologies began to be employed to test the validity of previously estimated locations for the center of resistance and to improve current modeling to achieve more accurate numbers.[4, 6]

With today's technology and the pace of improvement, more and more accurate models are being created. The introduction of computed tomography scanning and cone-beam computed tomography scanning has thrust models and calculations from the two dimensional world into three dimensions. Increases in computer processing power and software complexity have allowed researchers to use 3D radiographs to extract accurate anatomical models for use in advanced software to segment the teeth, bone, PDL, and various other structures.[7, 8, 10, 11, 12, 13, 17]

These segmented structures can be converted into a virtual "mesh" for use in engineering software to calculate stresses and strains on the system when a given force is applied. With the stresses and strains simulated on the "anatomic mesh," the center of resistance can be accurately calculated for any combination of teeth in relation to their physiologic positioning within the bone and periodontal ligament. For the clinician, a clear, straightforward "heat-map" of the centers of resistance of the maxillary teeth from anterior to posterior teeth would be an invaluable clinical tool to better plan tooth movements and predict side effects.

In the current literature, there are no studies demonstrating the positional changes of the center of resistance as teeth are sequentially added into an arch wire segment. Most literature examines the center of resistance of a single tooth,[2, 4] the anterior segment (either lateral incisor to lateral incisor or canine to canine),[11, 15, 16] or the whole maxillary arch together.[10] Some of the current literature uses generic models or three dimensional scans of dentoform models rather than human data.[4, 10] Additionally, with the advent of temporary anchorage devices and their use for intrusion of posterior teeth, there are no studies that describe the center of resistance of the posterior segment alone. Furthermore, no studies appear to compare results among multiple patients to look for consistency or inconsistency of CR position.

Despite these large gaps in knowledge, the potentially most limiting factor of the current literature is the fact that most of these models have been derived from micro-CT scans of cadaveric specimens or dentoform models. While this form of imaging provides great resolution making model generation very accurate and fairly straightforward with some software, it is very high-dose for the patient, and not routinely used in treatment. Thus, micro-CT is not a realistic nor ethical modality for scanning patients to get an image of an arch of teeth for model generation and finite element analysis.

Fortunately, relatively new imaging technology has changed this barrier with the advent of cone-beam computed tomography (CBCT). CBCT is a far lower dose radiation to the patient than micro-CT and can acquire a wide range of image sizes, from single tooth scans to whole head scans. Continual progress has also taken place that has consistently and greatly reduced the amount of radiation dose associated with each scan, making CBCT a very viable method for acquiring 3D patient radiographs for analysis and treatment in today's patient-centered care environment. In fact, full-volume CBCT scans on some newer machines match the low radiation dose of a simple 2D panoramic radiograph. This has led some practitioners to opt to scan

patients with CBCT for their initial and final records instead of the traditional lateral cephalometric and panoramic radiographs, since both can be derived from the 3D scan.

Therefore, following the recent trend of patient-centered care, CBCT scans could be used in orthodontics to generate unique, patient-specific models that could be examined with finite element analysis software to determine the center of resistance of a tooth or groups of teeth on a per-patient basis. This could be very beneficial to set up biomechanical plans in complex treatments, such as those that require space closure or molar intrusion. However, CBCT scans do have drawbacks – the lower radiation dose means scan resolutions are not as fine. Voxel sizes on average for CBCT scans are 0.25-0.35mm, which means finer anatomy, such as the periodontal ligament, are not easily visualized, which complicates model generation. Therefore, CBCT scans have not been the primary source for model generation in many of the finite element analysis orthodontic literature.

Additionally, no consistent workflow and very little detail has been described in the literature for creating anatomic models and the steps necessary to analyze them. Each finite element study provides a brief explanation of the software and version used for model generation and a rough outline of the steps used to reach the final analysis. Not only is this insufficient to replicate the research but it also introduces considerable variability among studies in terms of model generation due to the fact that no clear workflow has been published for subsequent studies to use. Essentially, each finite element investigator starts from scratch in developing a protocol, experiments with different software and tools within software programs to generate an acceptable model, attempts to accurately mesh the resulting surface models into a solid model, and then analyzes the solid model based on certain material parameters. Much time is spent learning the software, finding the right tools to generate the model, dealing with errors or

workflow complications that require model regeneration, and handling errors in the engineering software that may require a different approach or tool for model generation.

B. Rationale and Objectives

Understanding the location of the center of resistance of a tooth or group of teeth is invaluable in orthodontics in order to plan and execute tooth movements. Furthermore, awareness of the changes in the location of CR as additional teeth are incorporated into treatment is important to planning good biomechanics and efficient tooth movement. Current studies determine the center of resistance of certain teeth or segments of teeth, but they have mainly been limited to single teeth, a segment of incisors, canine to canine segments, or the whole maxillary arch. Clinicians are left to guess the center of resistance for different groupings of teeth, such as in cases of first or second premolar extraction space closure, tip back mechanics on molars, or posterior intrusion.

Clinicians do not have a clear depiction of these locations, nor do they know how reliable these locations are among patients. Up to this point, no attempt has been made to compare the centers of resistance among patients for consistency or inconsistency using three dimensional data.

To accomplish these analysis goals, one needs a groundwork and plan to follow before even reaching the point of determining the center of resistance. Up to this time, the methods and techniques used in the literature to develop the models for finite element analysis have been unclear, too concise, or simply non-existent.

Therefore, it is the goal of this research project to determine the appropriate segmentation algorithm for segmenting tooth, PDL, and bone out of a low-dose CBCT. Additionally, it is the goal of this research project to establish a protocol, software set, and toolset to generate accurate, viable, water-tight surface models that closely represent a patient's anatomy and also to establish a workflow for converting these surface models to solid meshes for finite element analysis in engineering software to determine the center of resistance of a tooth or set of teeth. With this

information laid out, it will be possible for any future investigator to efficiently use multiple patients' anatomical CBCT data to form models for finite element analysis to determine the center of resistance of various groups of teeth and compare the consistency among patients.

II. Hypotheses and Aims

A. Hypotheses

Hypothesis 1:

Null Hypothesis: Cone-beam computed tomography (CBCT) is a viable alternative to high radiation dose micro-CT imaging in generating anatomical surface models of teeth, PDL, and bone for finite element analysis.

Alternate Hypothesis: Cone-beam computed tomography (CBCT) is not a viable alternative to micro-CT in generating accurate anatomical models of the teeth, PDL, and bone for use in finite element analysis.

Hypothesis 2:

Null Hypothesis: Surface models developed from CBCT scans can be converted to solid mesh models for use in finite element analysis.

Alternate Hypothesis: Surface models developed from CBCT scans cannot be converted to solid mesh models for use in finite element analysis.

B. Specific Aims and Objectives

Specific Aim 1: Determine appropriate segmentation algorithms for developing surface models of tooth, periodontal ligament (PDL), and bone.

Specific Aim 2: Establish a protocol and generate surface models of tooth, periodontal ligament (PDL), and bone from CBCT scans for future use in finite element analysis

Specific Aim 3: Establish a workflow for converting surface models into solid meshes appropriate for finite element analysis.

III. Materials and Methods

A. Study Design

The current study retrospectively examined 10 routine cone-beam computed tomography volumes from patients to determine segmentation algorithms and develop surface models and solid meshes of the teeth, PDL, and bone for calculation of the center of resistance of the maxillary arch and various segments of teeth. The CBCT volumes were randomly selected from a pool of images from the University of Connecticut oral radiology CBCT database. Each CBCT was briefly examined to check if it met the inclusion criteria as discussed below. If it did not meet the criteria, it was discarded and another volume was randomly chosen.

All imaging was de-identified of all patient-related information before use in any part of the study. The imaging was used under institutional approved protocols as determined by the University of Connecticut Health Center institutional review board (IRB).

In order to convert from a CBCT volume into a model that could be analyzed for center of resistance, each volume has to be run through four main stages of processing in three different pieces of software. In the first stage, 3D models are segmented from the gray-value-based CBCT images. In the second stage, the 3D models are cleaned to remove holes, projections, and imperfections and then smoothed. In the third stage, the surface triangulation is optimized and the surface models are remeshed to solid tetrahedral meshes. Additionally, material properties are assigned to each solid element based on the material to which it belongs (i.e. tooth, PDL, bone). Material property assignment and remeshing can also be done in the engineering software of stage 4, but with less flexibility than in stage 3.

Finally, in the fourth stage, models are loaded into engineering software, such as Ansys or Abaqus. The models will be analyzed in conjunction with the engineering department at the University of Connecticut Storrs campus to place loads on the teeth in order to calculate stresses

and strains to determine the center of resistance. Various segments of teeth will be used for analysis. The segments will include the anterior 2-2 segment, 3-3 segment, 4-4 segment, and complete maxilla along with posterior segments from premolars to second molars.

It is important to understand the structure of these 3D models in order to understand the various processing steps – each 3D model is nothing more than a number of points in space that have x, y, and z values assigned to them to define where they belong in space. [Figure III-1]

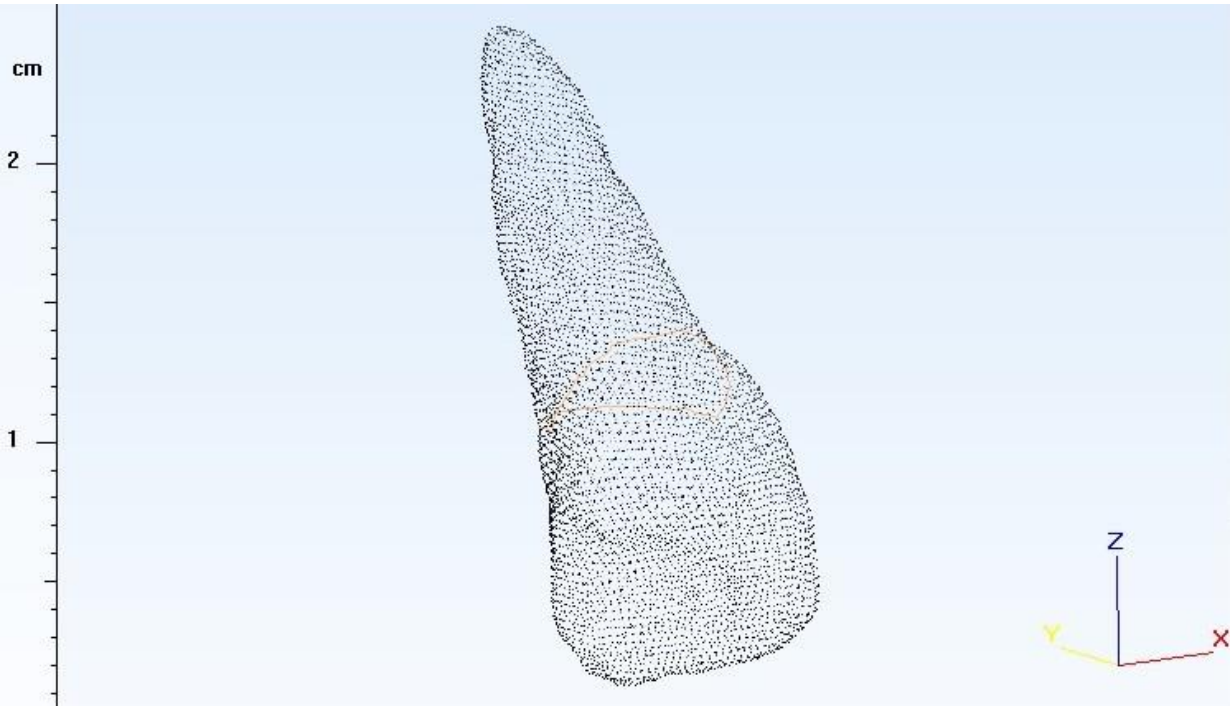

Figure III-1: Point cloud of tooth demonstrating nodes in space

When a surface 3D model is developed, these points or "nodes" are connected together with lines to develop triangles. Thus, the surface models are made up of many triangles with filled surfaces that approximate the overall surface structure of the original anatomical object as defined by the CBCT. [Figure III-2]

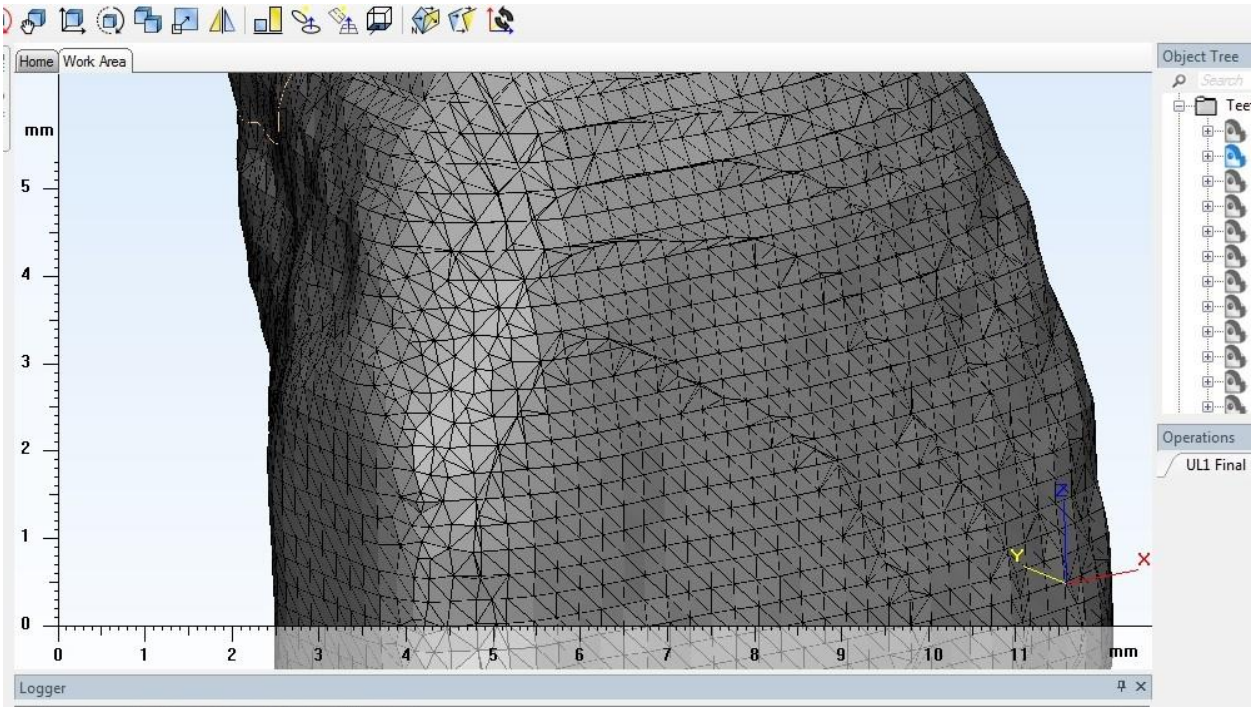

Figure III-2: Nodes connected with wireframes forming triangles and triangle surfaces filled demonstrating object's surface structure

In order to accurately analyze these models in engineering software, such as Ansys or Abaqus, the models must be solid through and through. The surface models, however, are shells and hollow inside. [Figure III-3] Therefore, the surface "meshes" of triangles must be converted to volume "meshes" of solid tetrahedral elements. [Figure III-4]

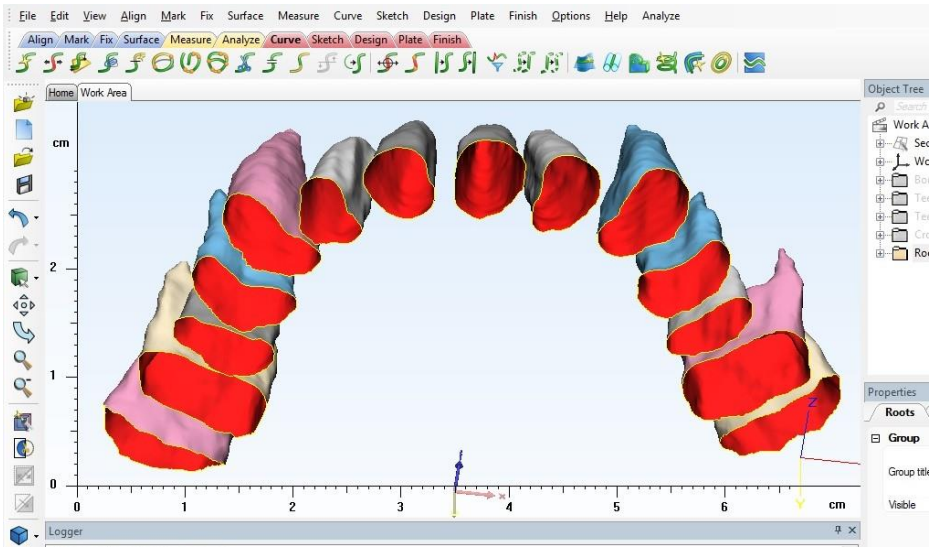

Figure III-3: View of hollow shells after tooth has been cut to leave just the root

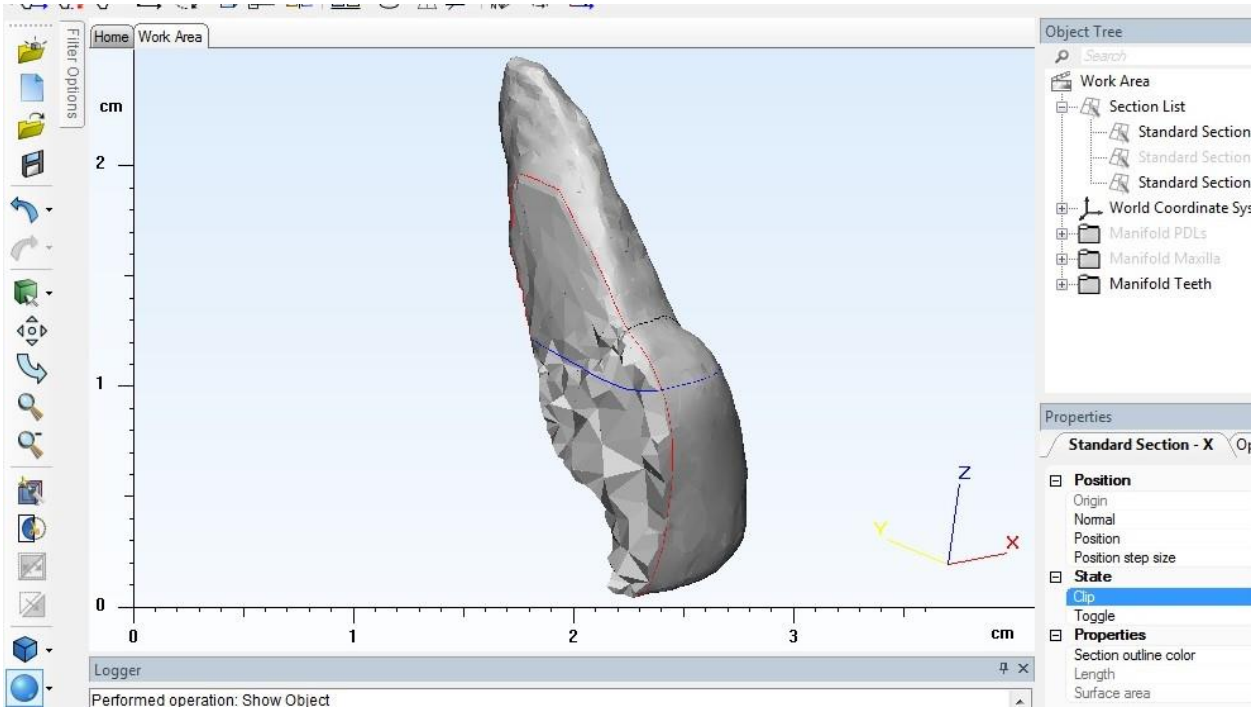

Figure III-4: Transection of tooth showing solid tetrahedral elements

The study is designed to begin in stage 1 with segmentation. CBCT volumes are loaded into Mimics v.19 (Materialise; Leuven, Belgium), which is used to orient the maxilla evenly along the x, y, and z planes and crop the image to include just the maxilla and teeth. [Figure III-5]

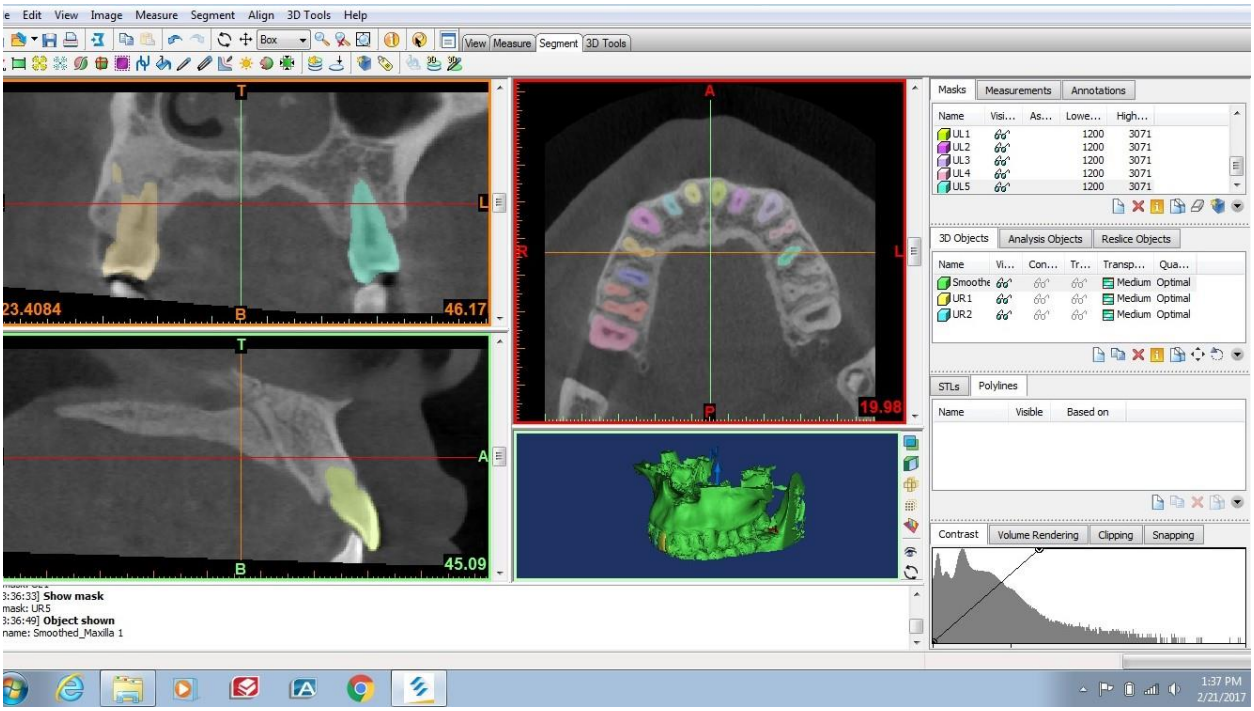

Figure III-5: Layout of Mimics with maxilla cropped and oriented on the x-y axis

Within Mimics, masks of the teeth were individually segmented from the radiograph along with the maxillary bone. [Figure III-6 and Figure III-7]. Once the masks were converted into three dimensional structures, the 3D objects were preliminarily cleaned and smoothed. At this point, they were ready for stage two of processing.

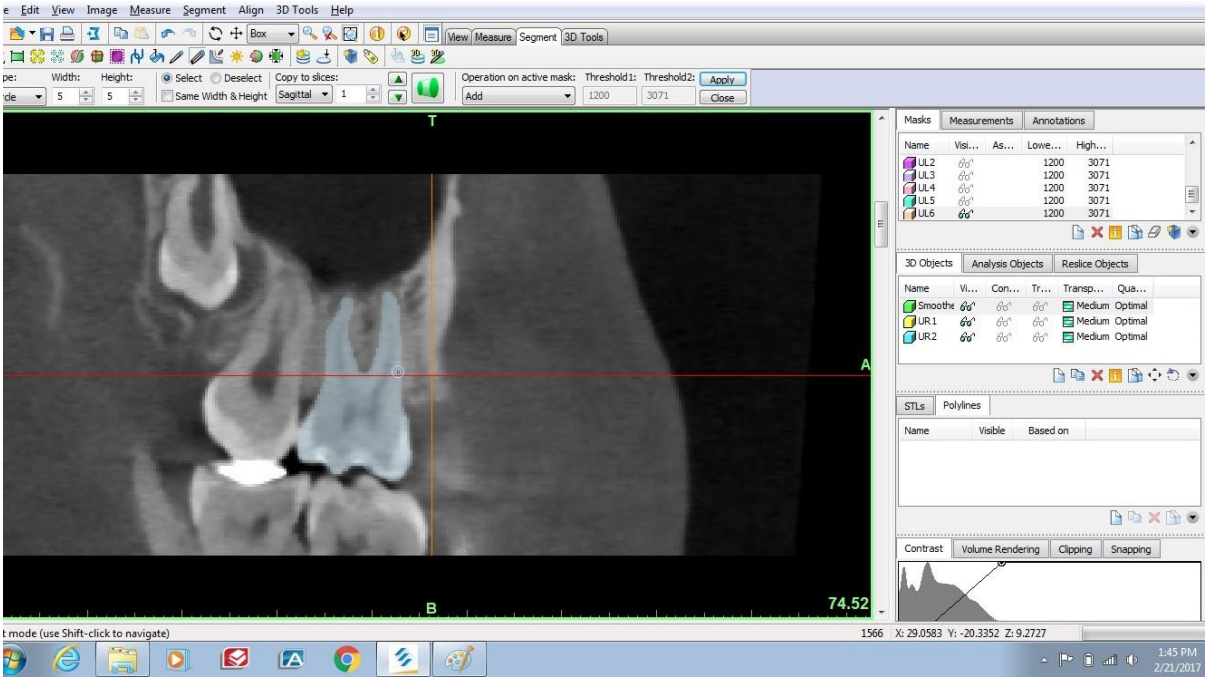

Figure III-6: CBCT sagittal slice of maxillary first molar highlighted for addition to mask

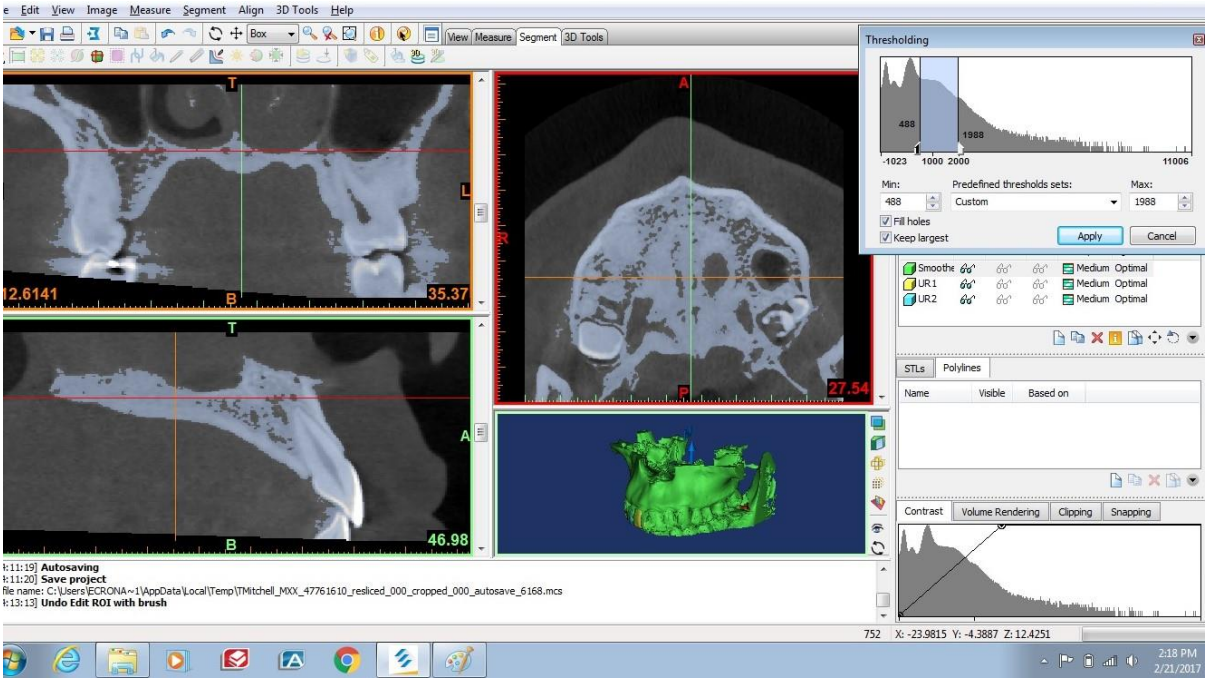

Figure III-7: Mask of maxilla selected via thresholding

The two middle stages (stage 2: surface model optimization and stage 3: volume meshing) were performed in 3matic (Materialise; Leuven, Belgium). The surface model cleaning and optimization were performed using the core tools of the software (figure). Surface and volume meshing was performed using the additional meshing module that is an optional add-on for the software.

Stage 2 consisted of cleaning the surface models of the teeth and bone and additionally generating a PDL structure from the root surface of the teeth, since the PDL was not able to be accurately visualized and segmented from the lower-dose and larger voxel CBCT in Stage 1 using Mimics. Cleaning the surface models included removing small aberrations, such as bumps, holes, or ripples that were the result of the layer by layer segmentation from the CBCT in Mimics. Once the bone and teeth were smoothed, the crown and roots of the teeth were separated. The root structure was then used to "grow" a PDL from the surface 0.2mm in thickness. Because the bone and tooth gray values were very similar on the CBCT, the thresholding to segment the bone model included the tooth roots and crowns all in one model. They were subtracted out of the model in this second stage along with the grown PDL.

Once the tooth, PDL, and bone surface models were completed, they were ready for stage 3: optimizing the surface mesh and converting the models to volume meshes. The goal of optimizing the surface mesh is to develop a surface that is covered with equilateral or near-equilateral triangles. Additionally, another goal is to reduce the number of triangles (consolidate smaller triangles into larger ones) as much as possible to decrease the amount of computing power that will be necessary to analyze the models in the final stage. Once the surface mesh is optimized, then the model can be meshed to a volume. The same goals apply: proportional tetrahedrons and a reduction in the number of tetrahedrons to decrease computing power required for model analysis. The most critical aspect of this stage is that all objects are water

tight and also that all surfaces are coincident. There cannot be any areas of the surface that overlap or intersect at all or the model will fail in the final analysis stage.

Finally stage 4 involved setting the material properties of the models and loading them into Ansys for analysis. The generated finite element meshes were analyzed in conjunction with the engineering department at the University of Connecticut Storrs campus to apply forces to the mesh models in order to calculate the center of resistance of the maxillary teeth. Various segments of teeth will be used for analysis. The segments will include the anterior 2-2 segment, 3-3 segment, 4-4 segment, and complete maxilla. Additionally, this study aims to separately plot the centers of resistance of posterior segments – from premolars to second molars.

B. Procedures

1. Volume Selection and Criteria

Random selection took place from a pool of already exposed CBCT radiographs taken in the University of Connecticut oral radiology clinic. Each selected volume was examined for tooth alignment, missing teeth, voxel size, field of view, and overall quality of the image. Once selected, each volume was completely de-identified of any patient information and cropped to include just the maxilla and teeth.

To qualify for use in the study, each volume had to meet the following inclusion criteria:

- A voxel size of no larger than 350 µm
- A field of view large enough to capture the maxilla and teeth
- Ideal or nearly ideal maxillary tooth alignment with crowding less than 2-3mm
- All teeth present in the arch with the exception of third molars
- No significant arch asymmetry or other deforming factors
- Superior-inferior boundaries: the image must include all of the maxillary tooth crowns and incisal edges inferiorly and the hard palate up to the nasal floor and maxillary sinuses superiorly
- Anterior-posterior boundaries: the image must include the anterior nasal spine and facial surfaces of the maxillary teeth anteriorly and the posterior extent of the hard palate and maxillary tuberosity posteriorly
- No or little scatter or degrading attributes of the image quality due to brackets, restorations, implants, or other artifacts

2. Segmentation

Selected CBCT volumes were exported from the database in which they are stored as DICOM files. For stage 1, the DICOM files were loaded into Mimics software (Materialise; Leuven, Belgium) for segmentation. Each volume was cropped to remove information superior to the hard palate and maxillary sinuses and inferior to the incisal and occlusal surfaces of the maxillary dentition. By nature of maxillary anatomy, images should not require cropping from the anterior. However, data posterior to the maxillary tuberosities, if present, was removed to simplify volume segmentation and manipulation.

Threshold segmentation was used within Mimics to separate desired anatomical structures from the rest of the tissue. Thresholding was initially done using the predefined settings in the software in order to standardize the segmentation for each patient as much as possible. To achieve accurate tooth, root, and bone anatomy, manual manipulation of the segments was employed as necessary to remove any amounts of extraneous tissue incorporated in the segment after using the software's preprogrammed threshold levels.

Segmentation of the PDL was complicated by the resolution of the CBCT. Ideally, segmentation of the PDL would occur by fill of the space between the teeth and bone, unless soft tissue thresholding in the software provided a more accurate and effective representation of the periodontal ligament. Because modeling the PDL thickness as non-uniform[19] and modeling the PDL as a fibrous tissue[20, 21] has been shown in the literature to affect the determination of the CR, ideally segmentation would be performed to be as anatomically accurate as possible. However, this proved difficult. The method of PDL model generation is elucidated stepwise in the final results.

3. Cleaning and Meshing

The two middle stages (stage 2: surface model optimization and stage 3: volume meshing) were performed in 3matic (Materialise; Leuven, Belgium). Before any meshing can be performed, the models segmented from the CBCT were cleaned and optimized using the core tools of the software. Sharp edges, holes, imperfections, and bumps were removed, so that the models were smooth and anatomically representative. This is especially true of the bone, where smoothing and cleaning is important to reduce the number of elements of the final mesh. Extraneous surface anatomy of the bone, such as the septum, hamulus, and pterygoid plates, was trimmed from the model to simplify the final mesh.

Surface models must meet two requirements in order to succeed in the final analysis: 1) models must be "water tight" and 2) model shared surfaces must be coincident with each other. The models were verified for the "water-tight" requirement, patched as necessary, and repaired to reach a final surface model that was viable for meshing. To ensure the surfaces were coincident, model optimization took this necessity into consideration when developing a toolset and workflow.

Once cleaned and anatomically finalized, surface and volume meshing was performed using the additional meshing module that is an optional add-on for the 3matic software. With the remesh module, the surface models were first remeshed to provide a surface of as near equilateral triangles as possible. The number of triangles was then reduced with another algorithm to simplify the model to assure reasonable computational resource requirements. Both the remesh and triangle reduction algorithms maintain surface anatomy, which uses finer triangles to maintain morphologic accuracy on load-bearing surfaces, such as tooth roots, PDL, and lamina dura, while allowing larger elements to make up simpler surfaces.

Once the surface model meshes were remeshed for quality triangles and a reduction of elements, the solid models were generated. This involved using the optional meshing module of 3matic. Similar to the surface optimization, the module has an algorithm that will generate an optimized tetrahedral solid mesh from the surface mesh. The tetrahedrons were grown interiorly with the surface triangles acting as one of the tetrahedral faces of the solid mesh. As the algorithm propagates toward the center of the object, the tetrahedral elements grow in size in order to reduce computational requirements for analysis. This is acceptable, since the majority of the stresses and strains will occur toward the surface of the model. The solid mesh was composed of 10-node tetrahedrons with mid-side nodes placed at the midpoint of each edge of the tetrahedron to increase model analysis accuracy.

Boundary conditions for the model will be set by rigidly fixing the superior portion of the model – the bone representing the anterior maxilla and anterior nasal spine, palatine process of the maxilla, and palatine bone posterior to the maxillary tuberosities.

4. Material Assignment

Part of the requirement for analysis in engineering software is that each solid element has material properties set. The two primary material properties assigned are Young's modulus of elasticity and Poisson's ratio. This is typically done within the engineering software for simpler models, such as a steel beam. However, the 3matic add-on module integrates with Mimics and acts as a bridge between the two pieces of software, providing the ability to assign the material properties homogenously, in a stratified manner, with complicated equations, or via gray values of the source radiograph. Thus, this module was used to assign some material properties.

Solid mesh models were exported from 3matic as Abaqus files. The maxillary bone was imported into Mimics, where material properties were assigned.

Because bone varies in density, various methods have been used to model bone, since Young's modulus will differ for the cortical bone, trabecular bone, and marrow space. Some studies[2] average the Young's moduli for the different bone types and assign one uniform value to all of the bone in the mesh, others[8] assign specific values for the three bone types, and some investigators[13] proportionally assign the modulus on a per-element basis using gray values from the source radiograph. In this study, bone was proportionally assigned the modulus of elasticity using radiograph gray values.

Possibly the most complicated aspect of the finite element modeling is that of the periodontal ligament. The ligament is very thin, with thickness varying from 0.15mm to 0.38mm.[23] In this study, PDLs of uniform 0.2mm thickness were developed. Additionally, the fact that the ligament does not exhibit linear elastic properties further complicates material assignment. Some investigations have simplified modeling by assigning linear elastic properties. However, direct measurement of the ligament's properties[22, 25] and linear versus non-linear finite element analysis[24, 26] has shown that the non-linear model is more physiologically accurate and

provides more consistent results. Many studies have been performed comparing experimental data to finite element analyses using different material parameters. However, most of these studies use various amounts of force and compare the finite element analyses against different experimental sources, such as pigs and humans. [22, 29] Additionally, most of the studies on the periodontal ligament do not provide detailed equations or data for material property assignment in future studies. One study, however, did provide very detailed explanations of their findings, including the parameters and equations for best fitting models that very closely compared to the experimental results.[29]

The study found the V-W and Ogden models as very close fits for the experimental data acquired from the pig specimen.[29] Abaqus, as part of the material property assignment, has the option to implement the Ogden model in the software for assigning material properties. The R^2 correlation coefficient for the Ogden model is 0.99025 for the pig specimen tested by Huang et.al. Thus, the Ogden model was implemented along with the parameters from the Huang et.al. study to set material properties of the PDL in Abaqus.

Finally, the solid meshes of teeth were assigned homogenous material properties. Because the material assignment is homogenous, this study assigned the material properties of the teeth in Abaqus rather than Mimics to avoid the multi-step import/export process involved with Mimics. For the teeth, the Young's modulus was set to 2,040 kg/mm^2, and 0.3 set as Poisson's ratio.[8, 13, 22]

5. Model Pre-Processing for Analysis

After material property assignment, the Abaqus model files will be imported into Abaqus for model pre-processing in preparation for analysis. Pre-processing for any analysis involves a standard set of steps: defining a geometry, assigning material properties, assembling multiple geometries into an assembly, setting steps for the model analysis, defining interactions between the different geometries, setting loads for the model, and meshing the model.

Some of these pre-processing steps were already completed before Abaqus. Because of the processing completed in Mimics and 3matic, the geometries were already developed. Additionally, the geometries were meshed and transformed into a solid using 3matic. Finally, some of the material properties were assigned with the 3matic module.

Because the PDL requires special material assignment, the material properties were assigned to the PDLs in Abaqus [using the blah blah formula]. The teeth, PDLs, and maxillary bone were assembled together in Abaqus, and the shared interfaces (i.e. coincident surfaces) between the teeth and PDLs and also the PDLs and bone were set to be fixed to each other.

Boundary conditions of the model were set such that the horizontal plane coinciding with the top of the maxilla will be constrained with zero degrees of freedom in order to rigidly fix the maxillary bone from movement.

Steps were assigned to the model for each simulation that was to take place – anterior 2-2, 3-3, 4-4, full maxilla, and posterior segments. For each step, interactions were defined for the model that would fix the tooth crown contacts together for those teeth belonging in the group to be analyzed. A 2N load directed posteriorly was placed on the central incisors for all of the models that did not involve posterior segments. For posterior segments, a 2N force was placed

perpendicular to the buccal surface of the central tooth in the segment. If an even number of teeth were present in the segment, the load was placed on the larger of the two teeth.

IV. Results

A. Patient Demographics

Ten patient models were generated for viable use in finite element analysis from the ten CBCT images that were obtained. The models can be viewed in the appendix. The sample consisted of 5 male and 5 female patients whose ages ranged from 11.6 to 61.2 years. The average age of the patients was 31.3 years and the median age was 20.9 years. [Table 1]

Table 1

Patient	Gender	Age	Voxel Size (mm)
1	M	18.90	0.27
2	F	18.39	0.33
3	F	15.92	0.27
4	M	49.95	0.33
5	M	22.89	0.20
6	M	16.90	0.27
7	F	61.16	0.27
8	F	11.58	0.30
9	M	60.87	0.27
10	F	37.28	0.27

As mentioned earlier, micro CT makes for easier model generation due to the increased resolution of the scan and greater ease of distinguishing between tissues, but the tradeoff is a higher radiation dose to the patient. In this study, lower dose CBCT images were used. The results show that lower dose CBCT images are viable for generation of successful models. The following detailed workflow and toolset is part of the results derived from this study. These steps were used to generate each finite element model and can be implemented reliably in future studies for consistent model generation.

B. Generated Workflow and Toolset

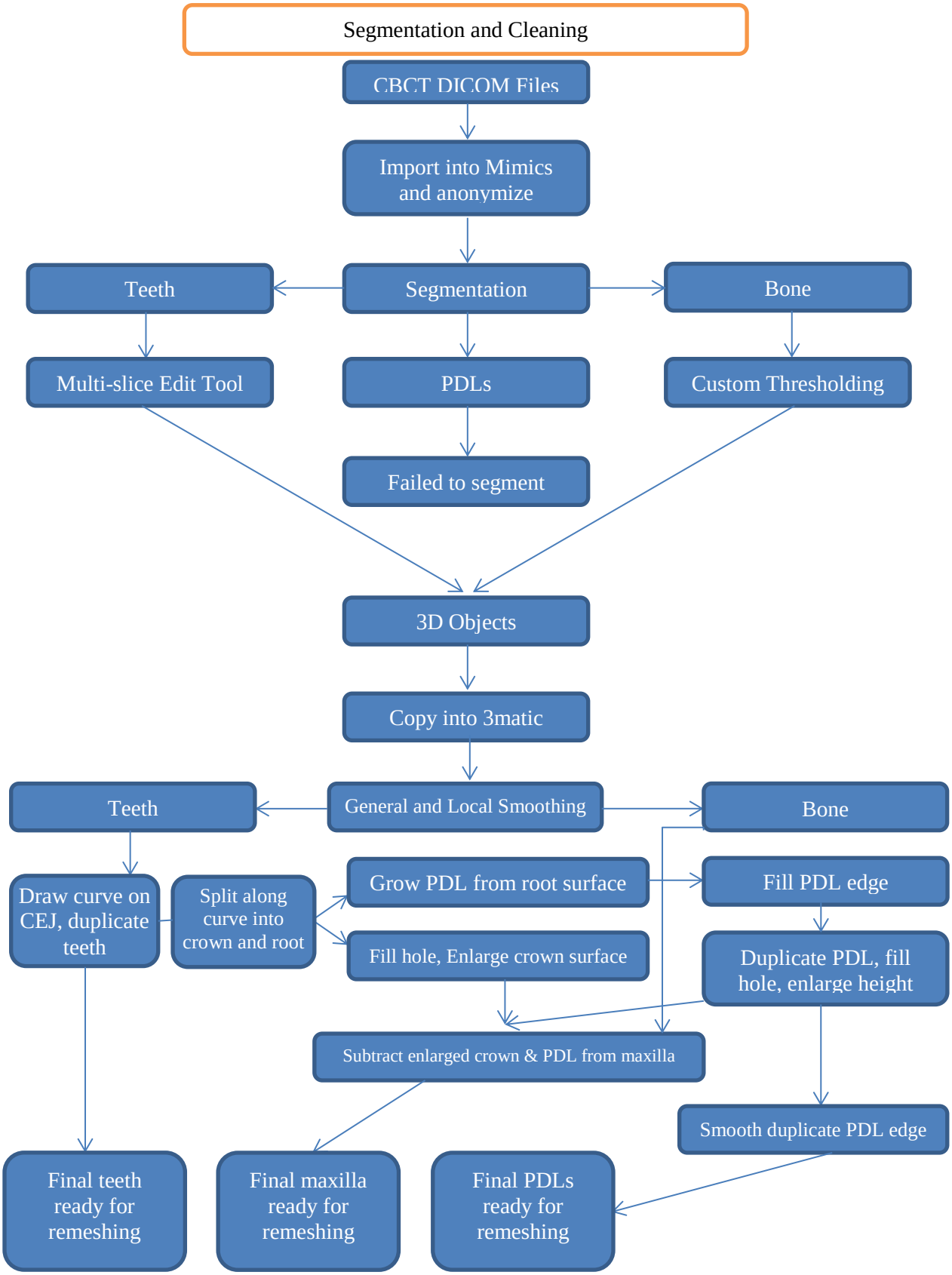


Remeshing and Volume Mesh Creation
Final Teeth
Final Maxilla
Final PDLs
Adaptive Remesh
Quality Preserving Reduce Triangles
Create Volume Mesh
Export as Abaqus/Ansys file
Import teeth & maxilla into Mimics
Assign material properties to teeth and bone
Save and export files
Import Tooth, PDL, and Bone files into Abaqus / Ansys for finite element analysis pre-processing

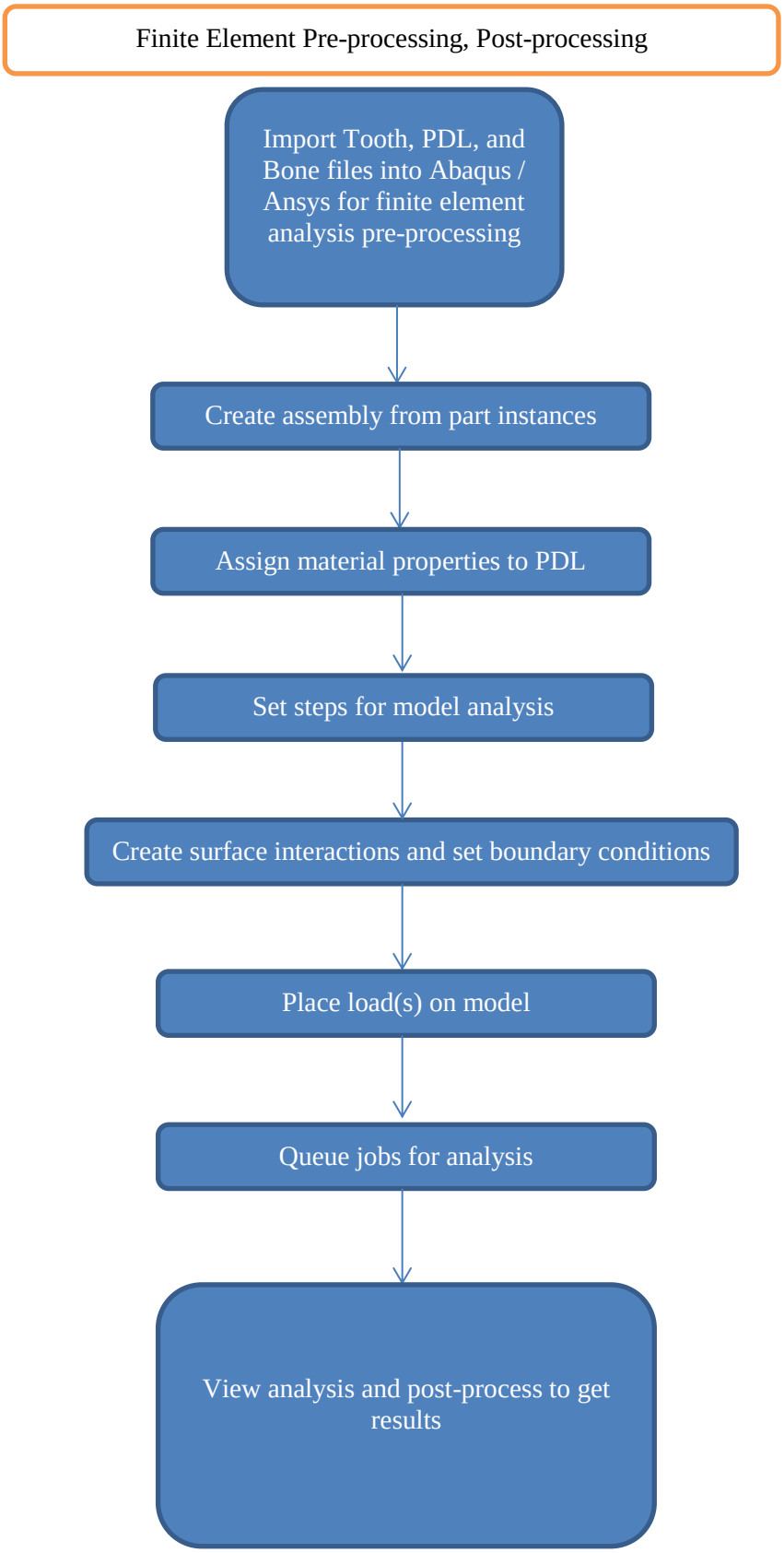
Finite Element Pre-processing, Post-processing
Import Tooth, PDL, and Bone files into Abaqus / Ansys for finite element analysis pre-processing
Create assembly from part instances
Assign material properties to PDL
Set steps for model analysis
Create surface interactions and set boundary conditions
Place load(s) on model
Queue jobs for analysis
View analysis and post-process to get results

C. Generated Workflow and Toolset – Explained in Detail

Three separate software programs were determined for use in model generation: Mimics (Materialise; Leuven, Belgium), 3matic (Materialise; Leuven, Belgium), and Abaqus (Dassault Systèmes; Vélizy-Villacoublay Cedex, France). The workflow generated consists of the following steps detailed below.

1. Segmentation:

CBCT raw DICOM files were first imported into Mimics [Figure IV-1]. Once loaded into Mimics, the files were anonymized to remove all patient data via a tool in Mimics (File → Anonymize Project). Once complete, the CBCT field was cropped (Image → Crop Project…) to include just the maxillary bone and teeth with the superior portion of the image ending at about the nasal floor, the posterior portion ending just behind the maxillary tuberosities, and the inferior portion ending just below the maxillary tooth crowns [Figure IV-2].

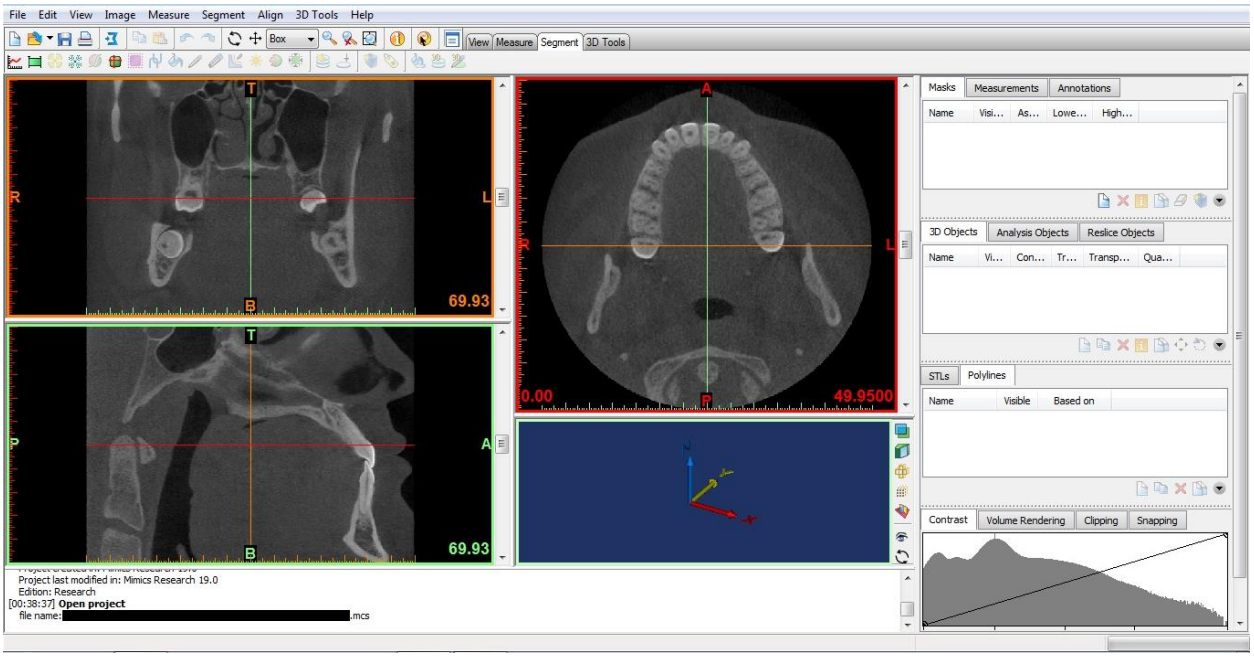

Figure IV-1: CBCT imported into Mimics from raw DICOM data

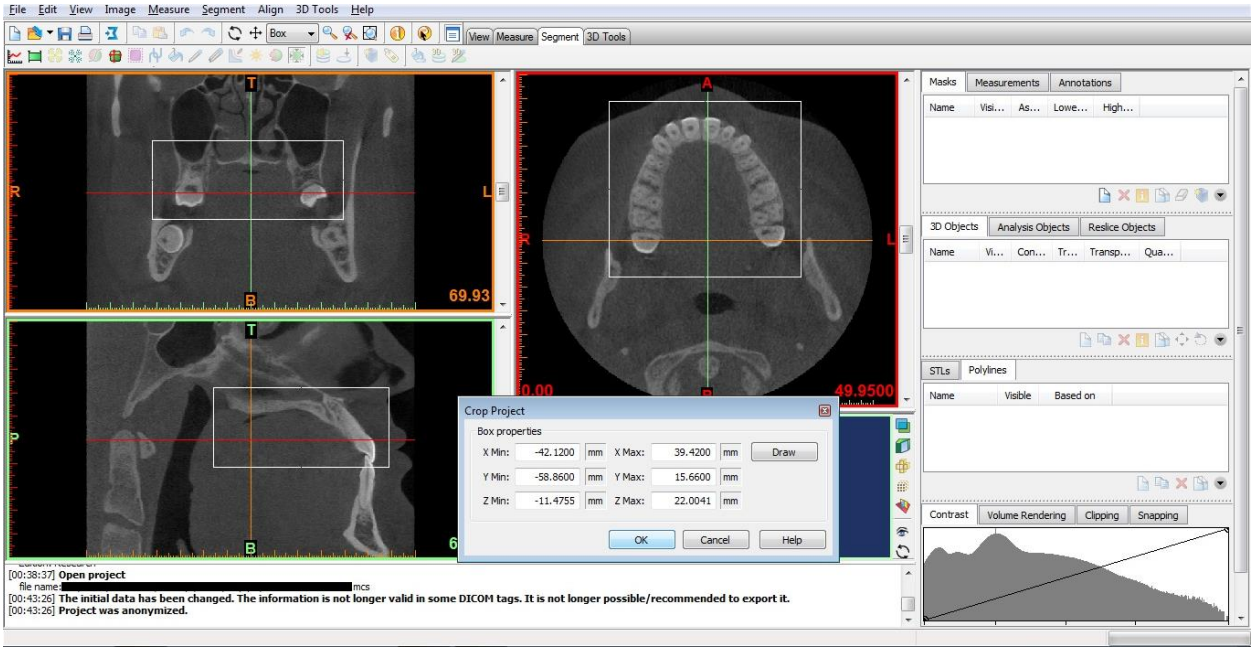

Figure IV-2: Crop tool in use demonstrating the bounding area of the image to be retained

The next step involves segmenting the teeth and bone out of the image. Segmenting involves highlighting areas of the image to store in a "mask" from which Mimics will generate a 3D structure. There are various ways to highlight areas to be added to a mask. The most easy and automated method is thresholding, which is a gray-value based method for Mimics to highlight areas of the image. Because threshold segmentation works off the gray values in the image, getting a clean selection of just a single tooth or multiple teeth requires a distinct gray value change between the tooth and the bone. Due to the lower resolution of the CBCT images compared to micro CT scans, the PDL space was not easily visualized and automatic threshold segmentation in Mimics proved to be unsuccessful for the teeth and bone.

CBCT image voxel sizes for the ten patients ranged between 0.20mm and 0.33mm. [Table 1] The average PDL thickness is around 0.2mm. Therefore, the resolution of the CBCTs was insufficient to be able to accurately and distinctly distinguish the PDL on the scans [

Figure IV-3]. This shortcoming with the CBCT scans created two issues: 1) the PDL cannot be segmented on its own and 2) segmenting the bone and teeth using thresholding was not possible due to a lack of a distinct gray value change between the two. As a result, the software was unable to distinguish between the teeth and bone because the gray values of the two were too similar. Thus, using predefined or custom thresholding within Mimics created masks that included both tooth

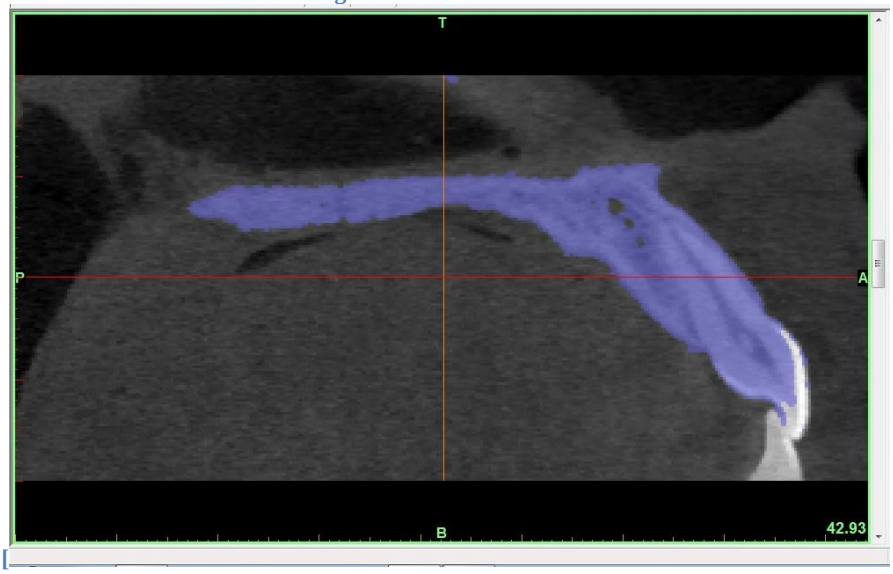

structure and bone structure [

Figure IV-4]. A different method of segmentation was required.

Figure IV-3: Sagittal slice of a central incisor demonstrating the difficulty in visualizing the periodontal ligament

Figure IV-5: Multi-slice Edit Tool – Highlighting a slice of a central incisor

Since the thresholding tool in Mimics was unable to segment the teeth and bone separately, a different method of segmentation was developed. After attempting numerous tools, such as the region growing or split tool in Mimics, it was determined that the best way to segment the teeth is by manually highlighting the tooth structure on each slice of the CBCT. If this sounds tedious, it is. However, the "multiple slice edit tool" does offer an efficiency advantage to the user. Instead of having to manually highlight *every* slice, the user only has to highlight some of the slices. For this reason, it was the best method for segmenting the teeth, as it provided the greatest accuracy in getting good anatomy of the teeth in a consistent manner. [

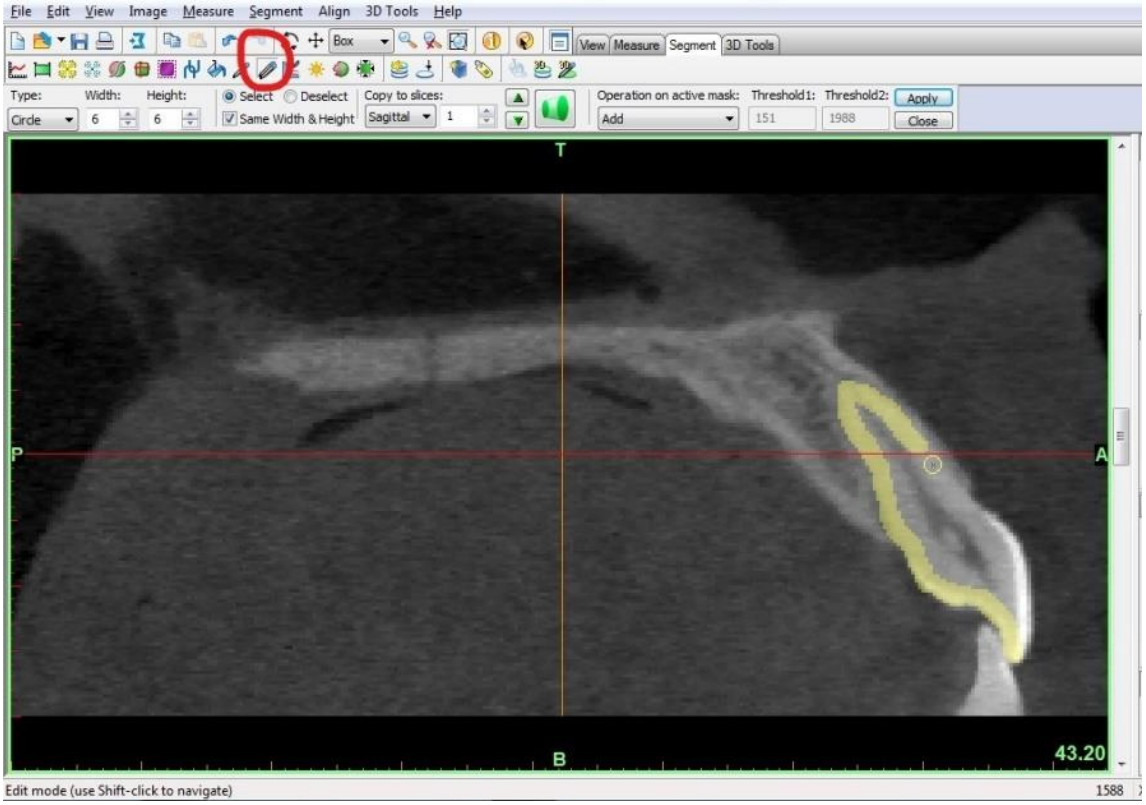

Figure IV-5]

The tool works by letting the user highlight only some slices of the CBCT, and then the computer will interpolate the proper highlighting for the remaining blank slices between those that the user highlighted based on the shape changes of the user's highlights. When all of the slices look good, they can be added to the segmentation mask for that tooth. While the tool is

still very manual in its implementation, being able to skip 2-4 slices of highlighting at a time makes the process more efficient. With a good quality mouse and as the user segments more teeth, the process becomes easier and more manageable.

With the teeth segmented, the next step is to segment the maxillary bone. Because the anatomy of the bone is even more complex than the teeth, the best method for segmenting the bone was to use thresholding in Mimics. The user is best served by starting with the "Compact Bone (CT, Adult)" predefined threshold set. Then, the upper and lower bounds of the threshold gray values can be adjusted as needed to capture as much of the bone as possible while avoiding the addition of soft tissue or noise into the mask. The custom adjustment is necessary because some images are exposed with different settings that alter what is captured for gray values within the predefined set. Be sure to check the "Fill Holes" box before applying the threshold. [

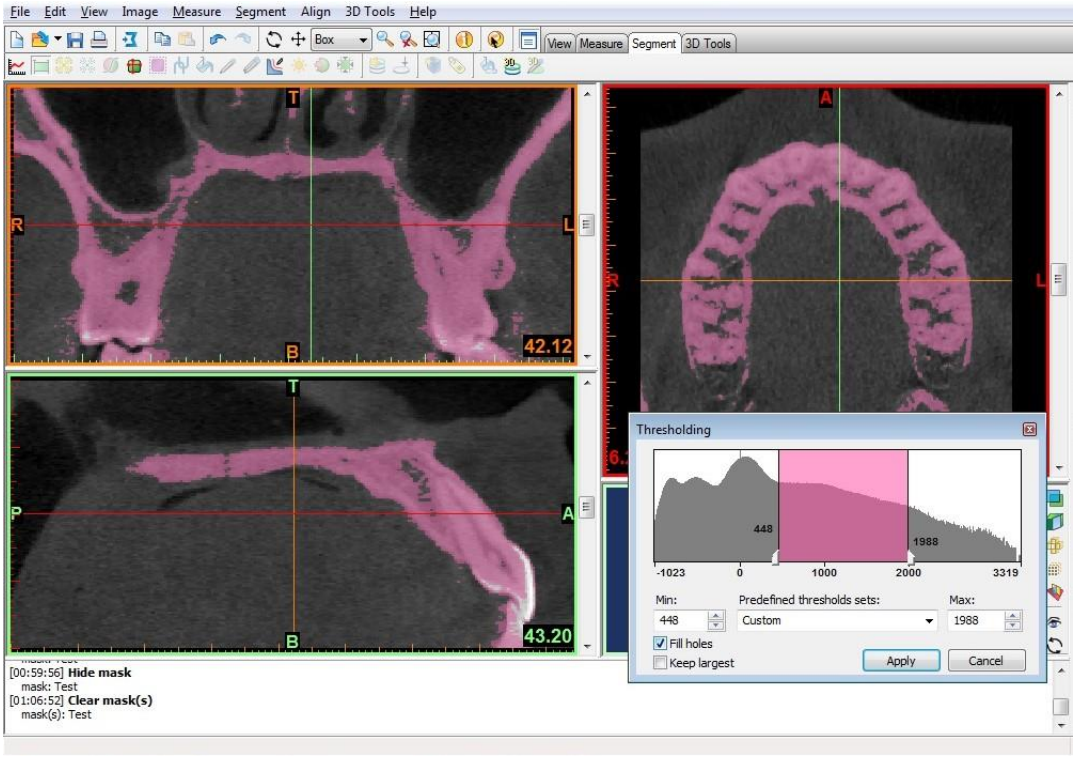

Figure IV-6: Bone thresholding – sliders in the inset window allow for customization of threshold; fill holes box checked

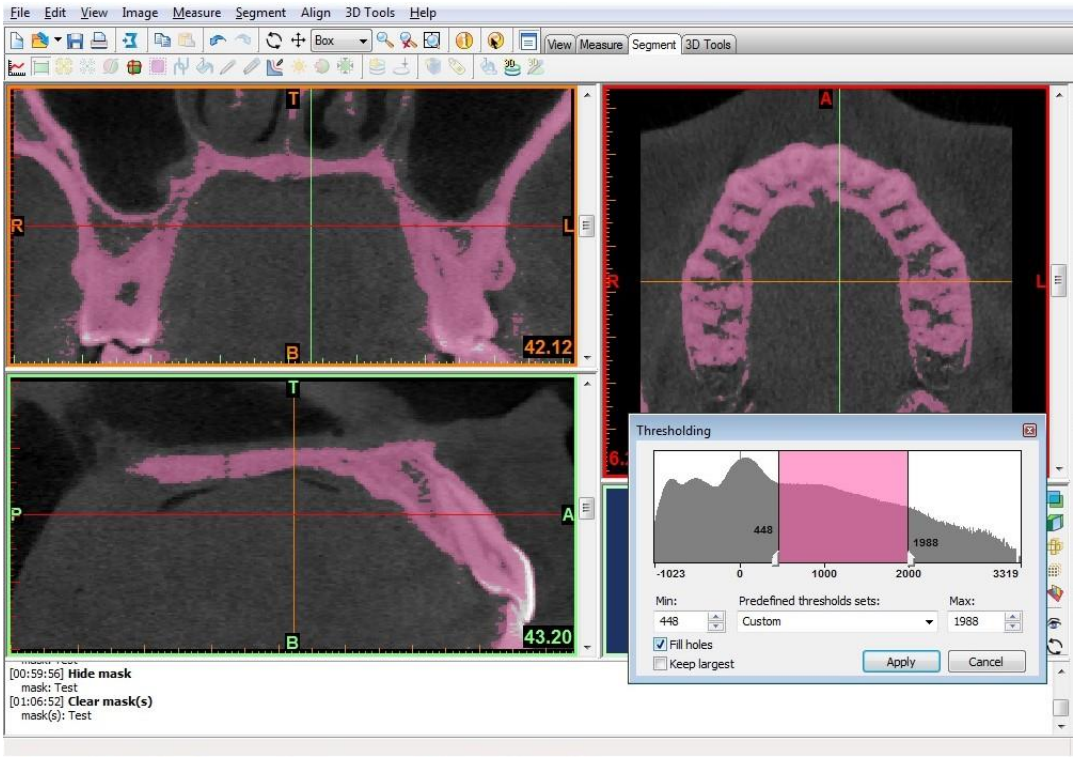

Figure IV-6]

At this point, a pretty good mask encompassing all of the bone should be visible on the screen. The teeth will be included in the mask; they will be removed at a later stage. The final processing step before finishing with the maxillary mask is to fill large holes in the cortical bone that are visible in the mask. The best method for accomplishing this is to use the "Dynamic Region Growing Tool." The user should be sure to select the maxillary bone mask as the target for the tool in addition to selecting the "multiple layer" box. The study found the best values for the "Min" and "Max" to be the default of 50 for the "Min" and 150 for "Max." Hold down the Ctrl key on the keyboard as you click with the mouse on the areas of cortical bone that are unhighlighted in the mask. [

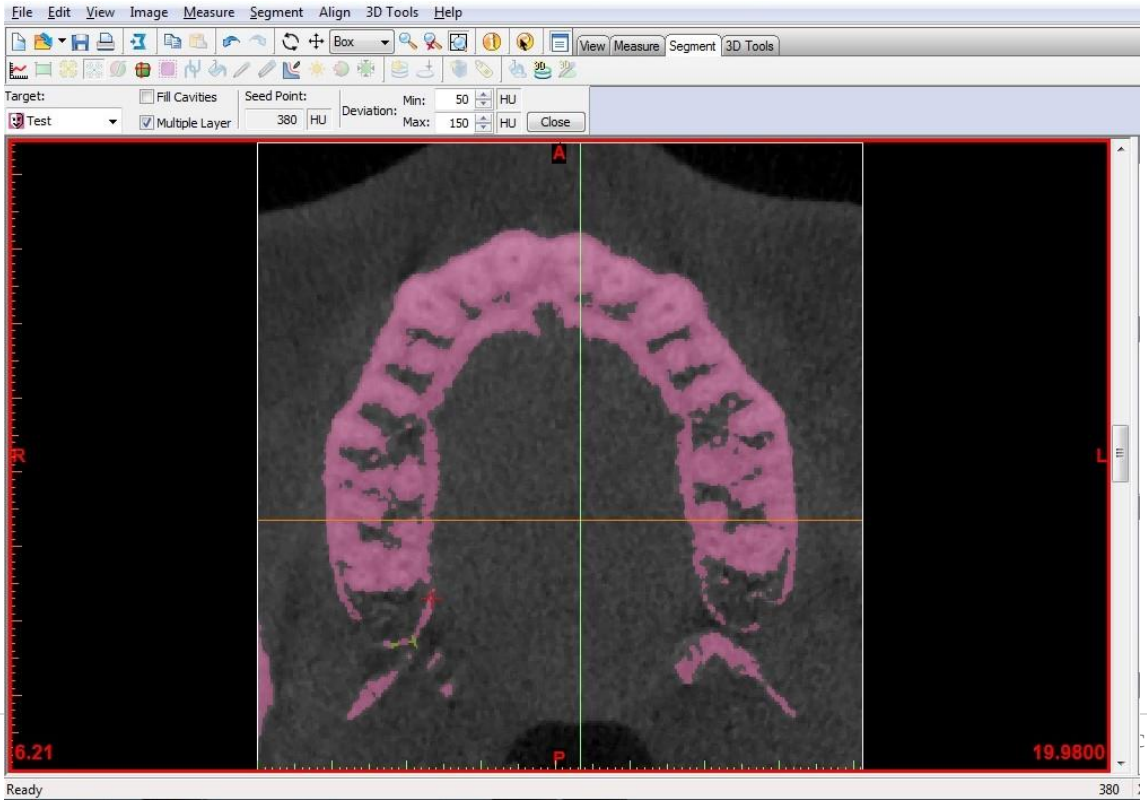

Figure IV-7: Region Growing Tool highlighting unselected cortical bone near the maxillary tuberosity

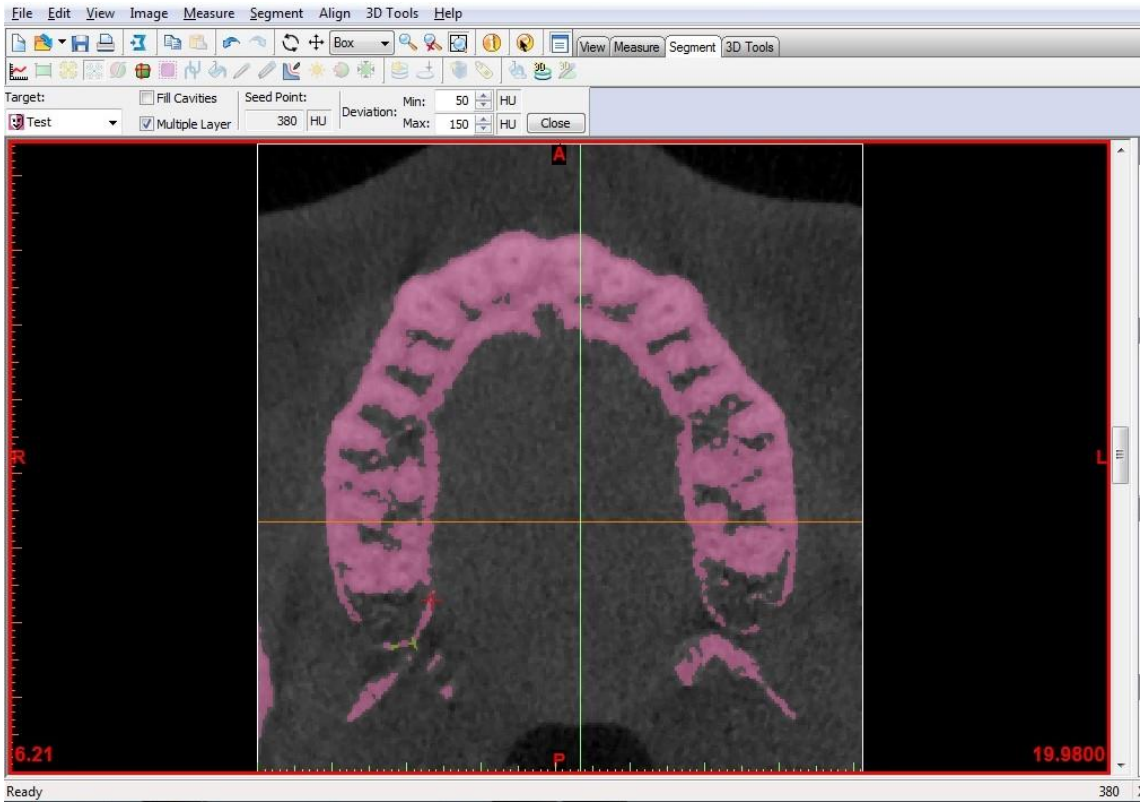

Figure IV-7] Small holes in the cortical bone 1mm or less are acceptable, as they can be removed easily in later stages. Once the selection is satisfactory, close the tool. One last refinement is required for the mask, which greatly helps clean it up. This refinement is the "Smooth Mask" function in Mimics. It not only fills small holes in the mask but it also removes extraneous voxels that are selected in the mask, which usually happens with the custom thresholding as the boundaries are stretched to include the maximum amount of bone. The study found that clicking the "Smooth Mask" button three times achieves the maximum amount of cleaning without losing anatomy. [

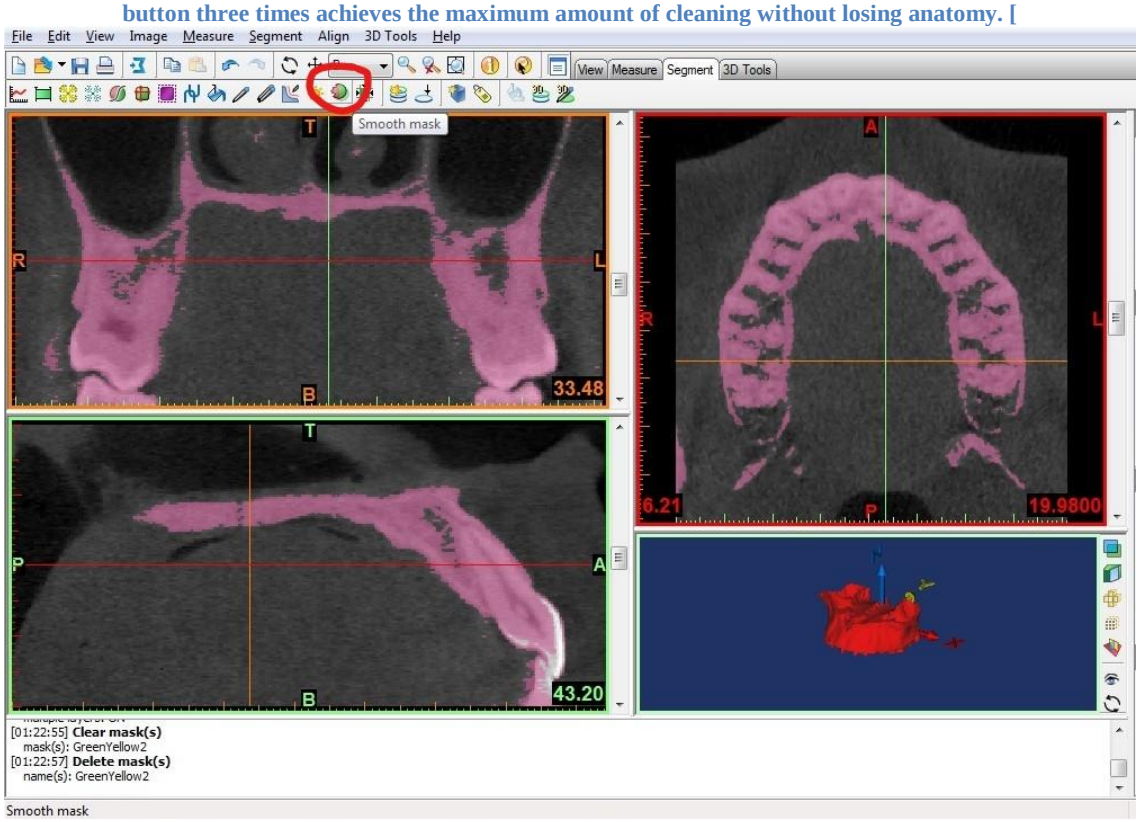

Figure IV-8] This tool can also be used on the individual tooth masks, but those are usually free from noise in the mask. If desired, one use of the smooth mask tool may help without removing anatomy.

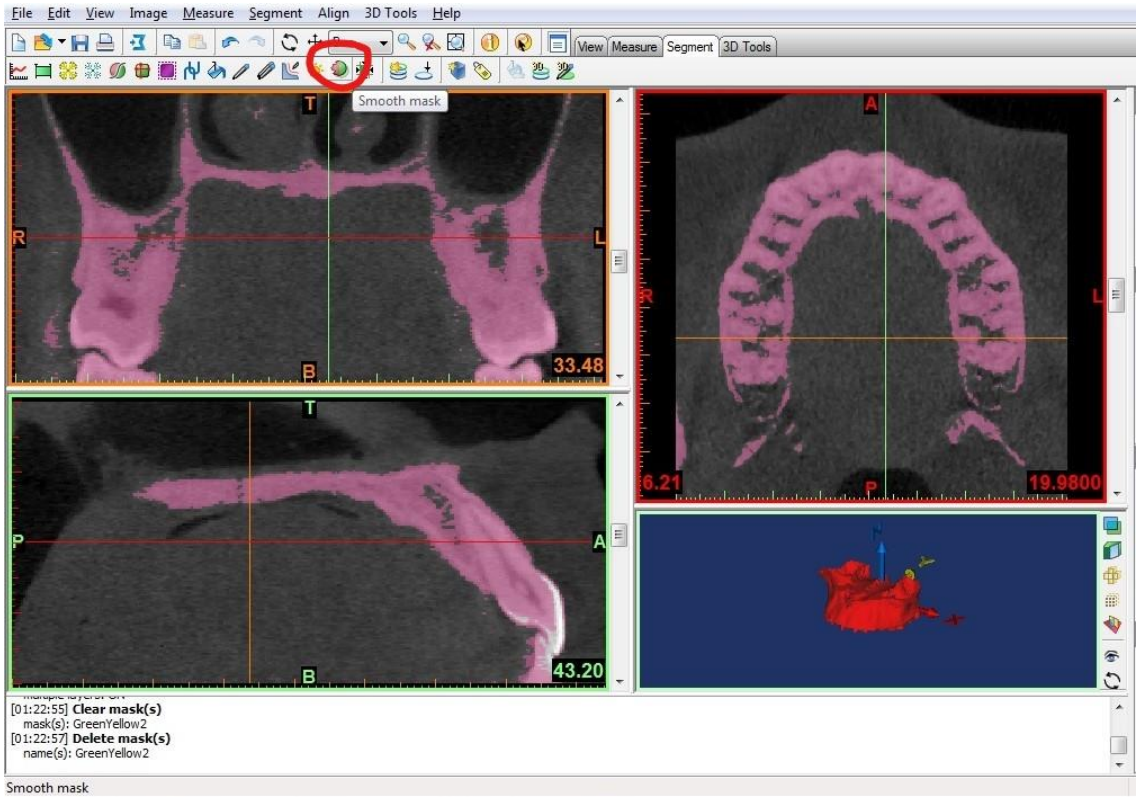

Figure IV-8: Smooth Mask Tool

Now that the masks are complete, the user should select a mask in the window pane, right click, and select "Calculate 3D…". A window will appear that lists all of the masks in the project with a quality option. Select all the masks from which the user wants to generate 3D structures, leave the quality as "optimal," and click calculate. [

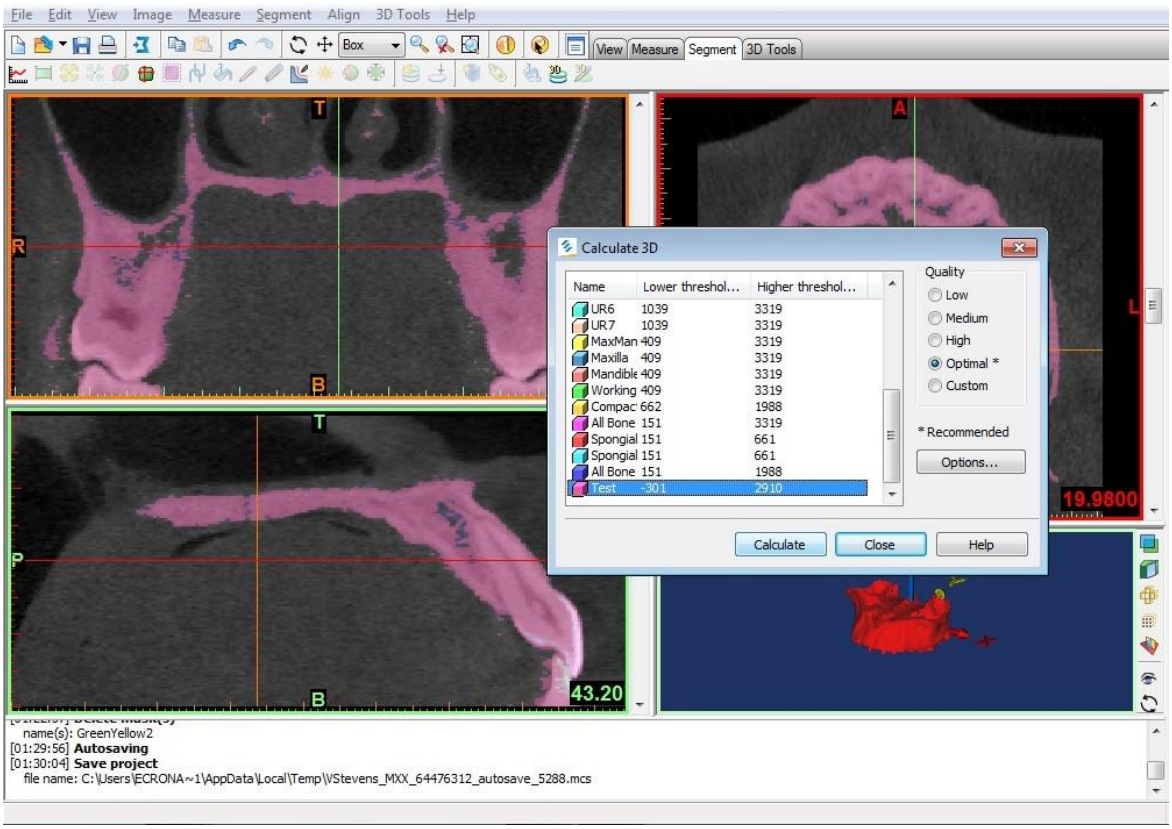

Figure IV-9] The 3D objects will appear in the 3D Objects pane to the right. The models will look extremely coarse and unrefined. The following steps will address this issue.

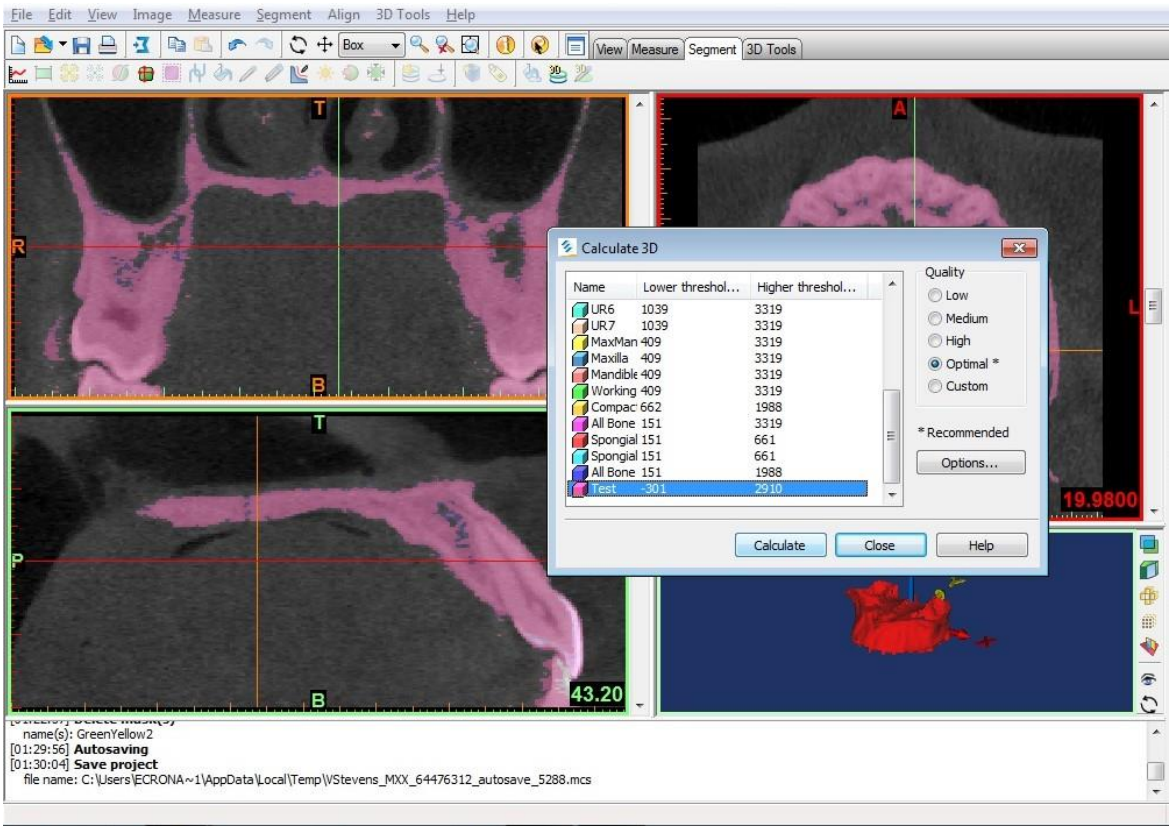

Figure IV-9: Calculate 3D window with options

On the top bar, select the "3D Tools" tab, and it will change the toolbar buttons below. Click the "Smooth Object" button. [

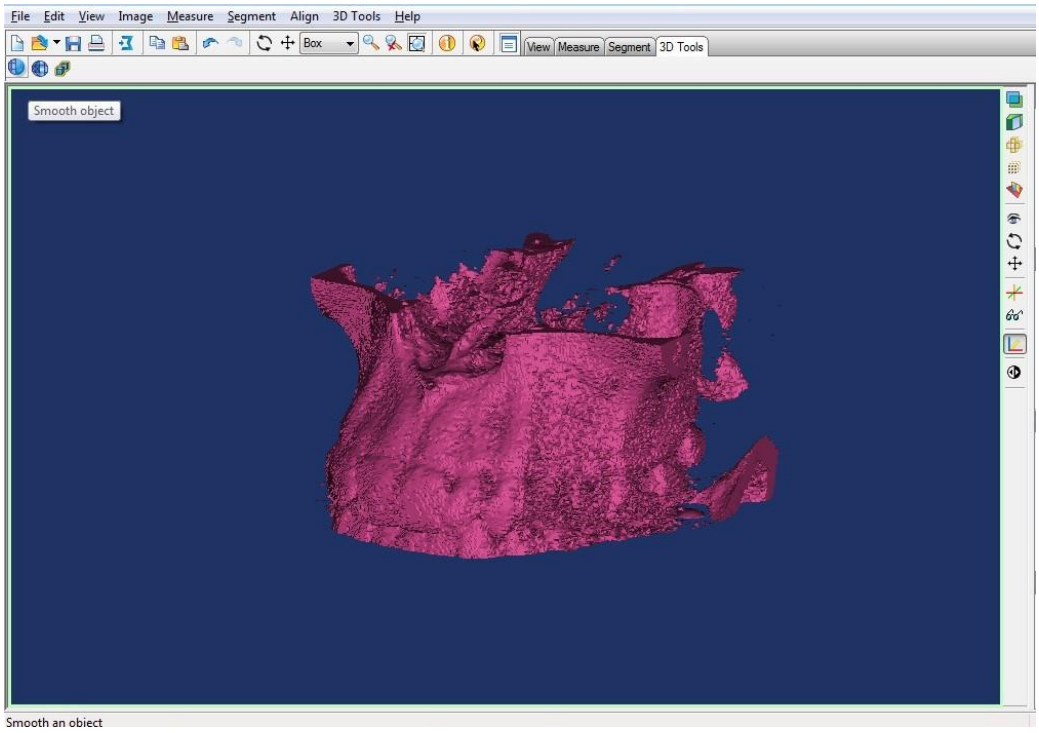

Figure IV-10] In the window that appears, set the smoothing factor to around 0.4 and iterations to 4. A smoother

3D object results. [

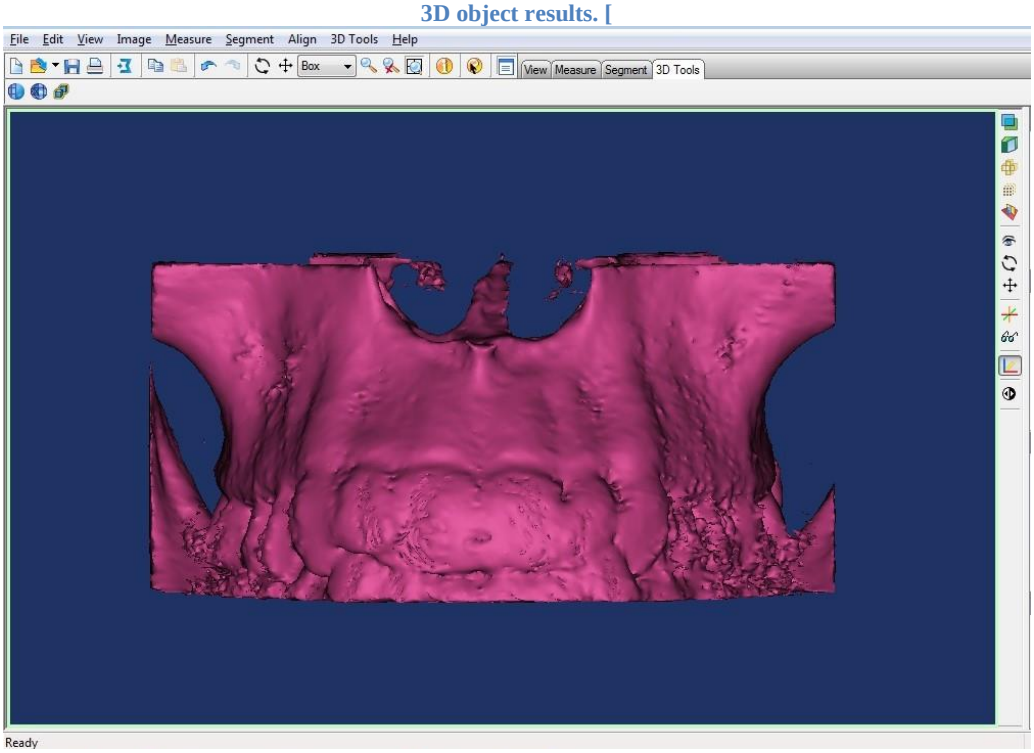

Figure IV-11] A second smoothing operation may be necessary. Lastly, the maxillary bone 3D object needs to be "wrapped" to help fill holes and smooth remaining surface imperfections. Click the wrap tool, select the objects to be wrapped, set smallest detail to 0.2mm and gap closing distance to 1mm, and click OK. [

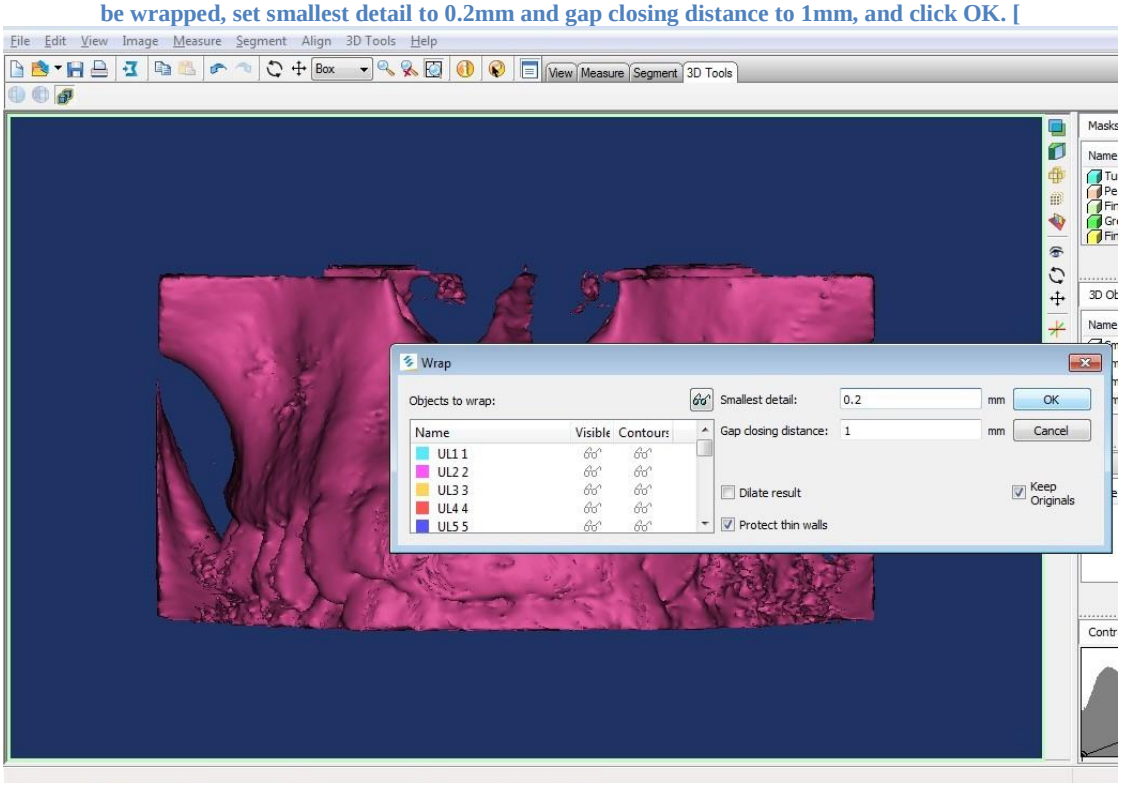

Figure IV-12]

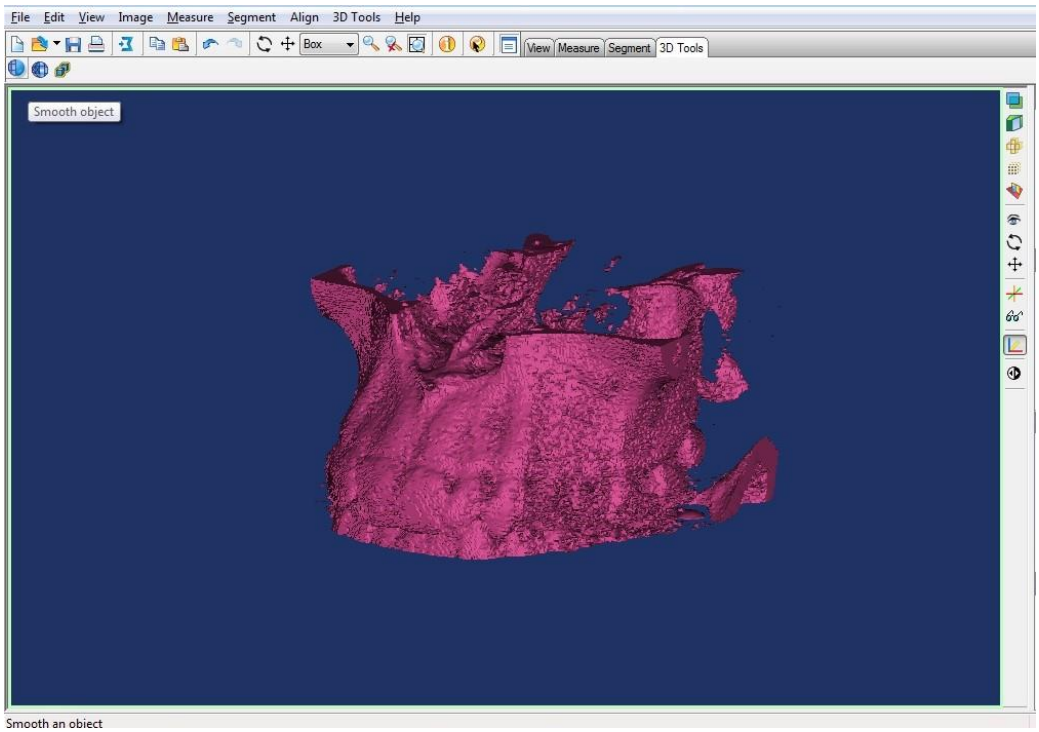

Figure IV-10: Object before smoothing

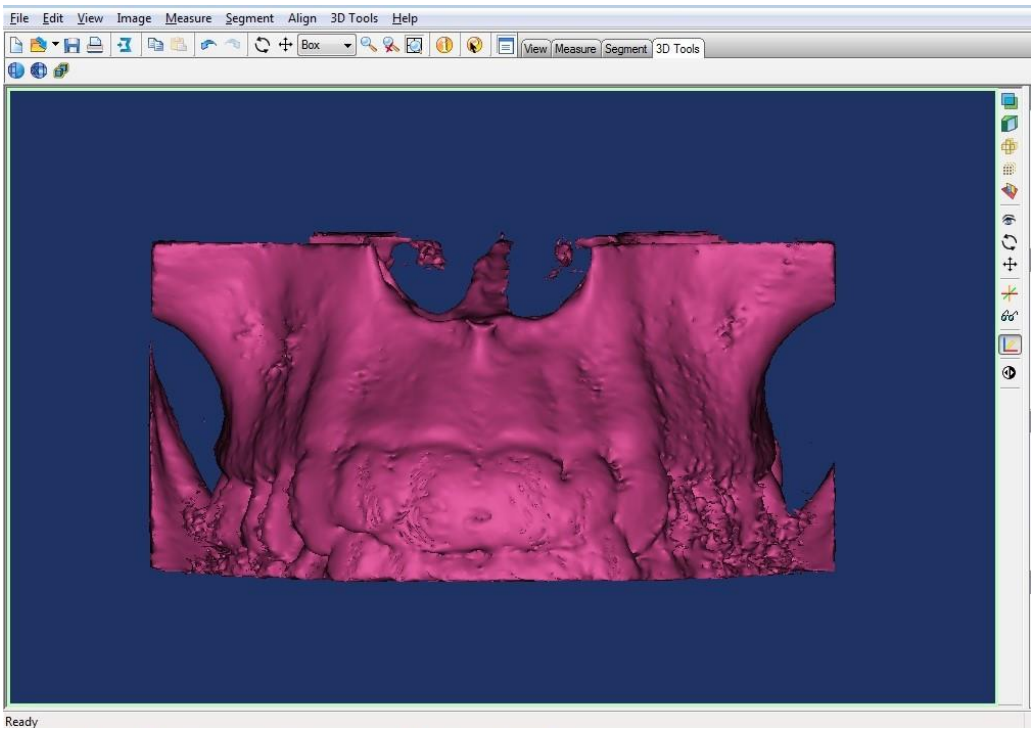

Figure IV-11: Object after smoothing

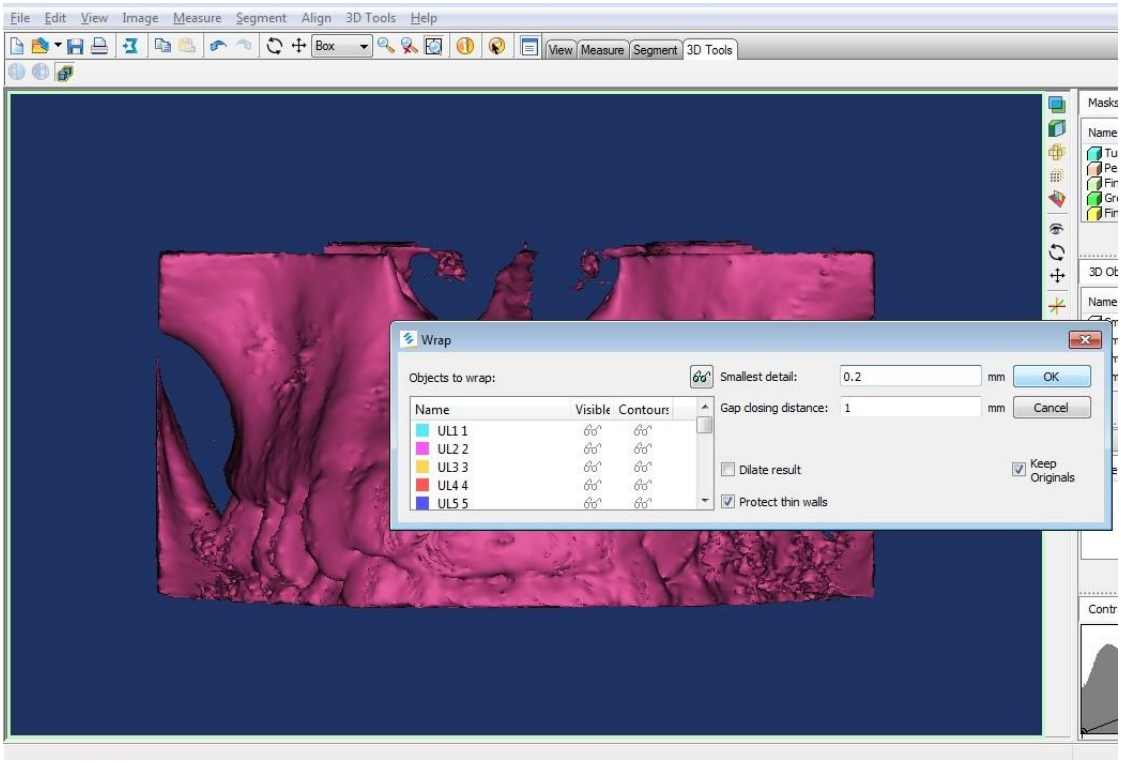

Figure IV-12: Wrap function within Mimics

2. Cleaning and Meshing:

Now that the 3D objects are complete, the user should select all of the objects desired, right click, and select copy. Open the 3matic software program. Click in the object tree and press Ctrl + V to paste the objects copied in Mimics into 3matic. They should appear in the object tree and in the work area of 3matic as a 3D structure.

The study determined that the goals of the cleaning and meshing stage are the following: that the models should be clean and representative of the patient's anatomy, that the models have coincident surfaces between the tooth, PDL, and bone, and that all model surfaces are relatively smooth and free of small surface topography that is insignificant for the overall model analysis, such as a projection of extra bone off the buccal cortical surface.

The study found that the first goal is important for getting representative and accurate models for each patient. The study also found that the second goal is critical for successful finite element analysis, as the surfaces must be tied together in the finite element analysis set up of the engineering software so that a load added to a tooth is propagated through the PDL to the bone. The engineering software will reject models whose surfaces are too far apart or intersect too much, which would make connecting the surfaces impossible and invalidate the FEA model.

The study found the third goal to be important because small, fine elements or projections of anatomy add unnecessary complication to the mesh of the final model by decreasing the size of the elements in complicated areas of fine anatomy thereby increasing the number of elements in the model. Smaller and more numerous elements increases the computing effort in the final finite element analysis. Therefore, if any of the 3D structures are still somewhat coarse, it was found that the first step is to perform general smoothing using the general smoothing tool in 3matic to help smooth the surface. Any remaining artifacts can be removed with the local smoothing tool. [

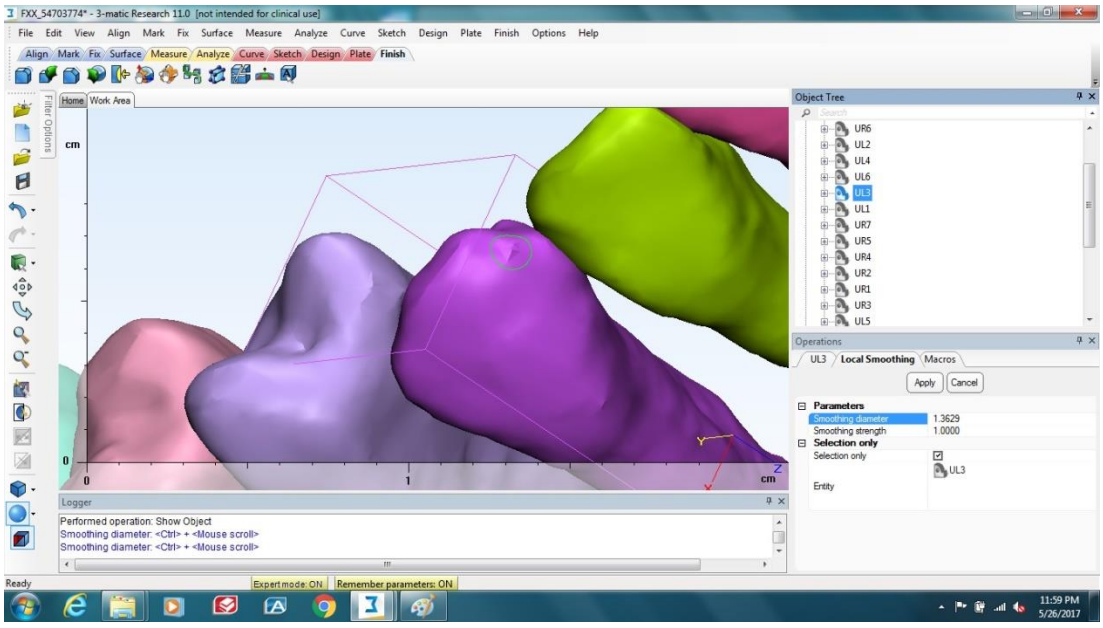

Figure IV-13: Local smoothing of a canine; green circle indicates area to be smoothed

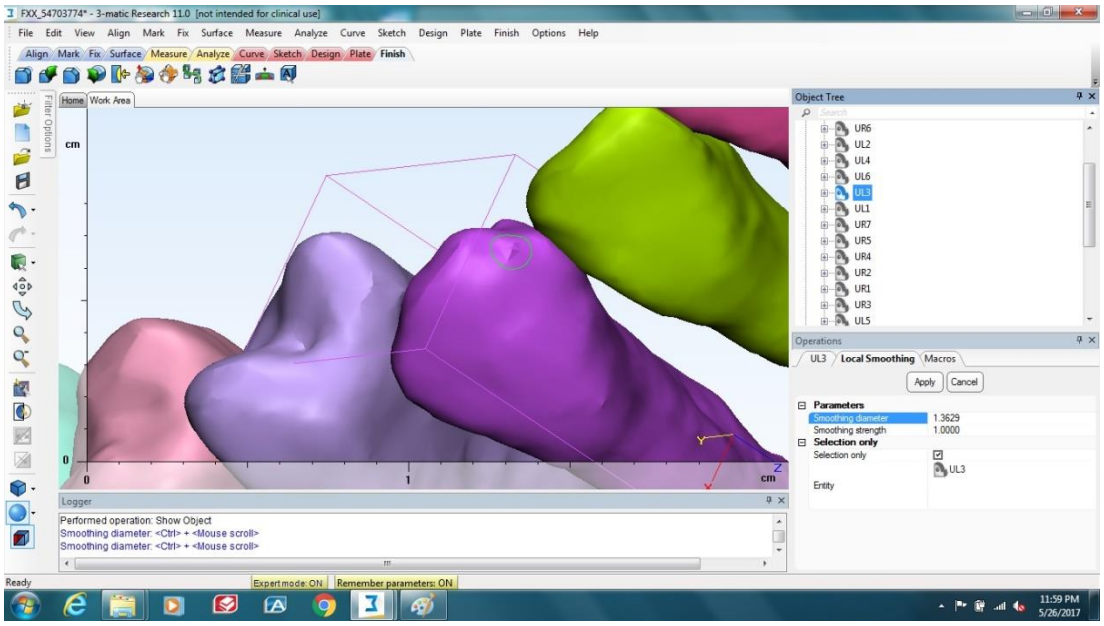

Figure IV-13] The user should complete any and all smoothing at this point. Once any of the following steps are performed, no changes to the root or crown surface can be performed, or it will cause interferences with surfaces in the FEA model.

Because the PDL was unable to be segmented in Mimics due to the lower resolution CBCT, the study found that it was necessary to grow the PDL from the root structure of the tooth. This required splitting the tooth into root and crown at the CEJ. The best tool for this was determined to be the curve tool in 3matic (Curve → Create Curve). Draw a curve around the CEJ and duplicate the tooth. Use the split by curve option (Curve → Split Surfaces by Curves)

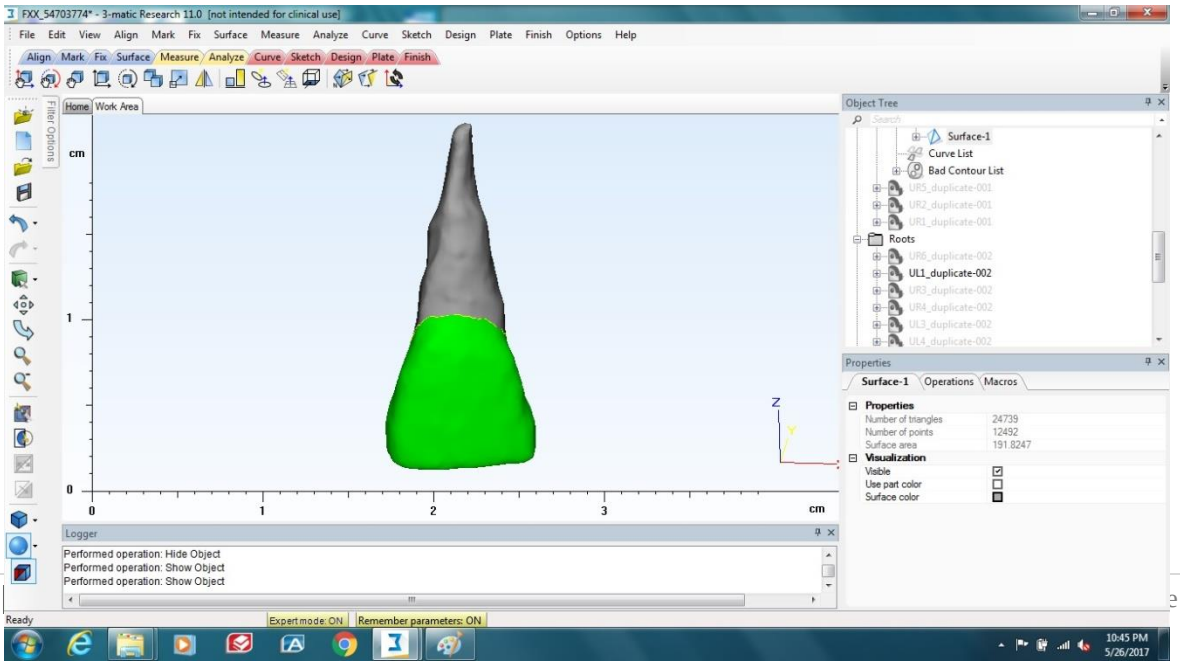

Figure IV-14: Separated crown and root surfaces; crown surface is a separate part and highlighted

on the duplicate tooth to split the tooth into root and crown surfaces. Separate the crown and root surfaces into their own parts. [Figure IV-14] Make duplicates of the crowns and roots for future use.

Because the thresholding in Mimics could not select just the bone, most of the following steps are intended to clean the maxilla and remove the tooth structure from the bone so that the remaining structure is just the maxillary bone. This study found that the best way to achieve this was to create an "enlarged crown" and a "heightened PDL" that can be subtracted from the pre-processed maxillary bone to fully remove all extra material not desired.

First, creation of the PDL must take place. The study found the best way to achieve this was to use the hollow tool to "grow" the PDL 0.2mm out from the root surface split in the previous step. The study found the best settings for the hollow tool to correspond to Table 2. Once grown, the PDL is nothing more than two surfaces parallel with each other spaced 0.2mm apart. [Figure IV-15] Thus, the object is not water-tight, which is a requirement for finite element analysis. The following steps resolve this.

Hollow Type:	Outside
Distance	0.2000
Smallest Detail:	0.0500
Reduce:	Checked
Cleanup at border:	Checked
Cleanup factor:	1.1000

Table 2: Hollow Tool Parameters

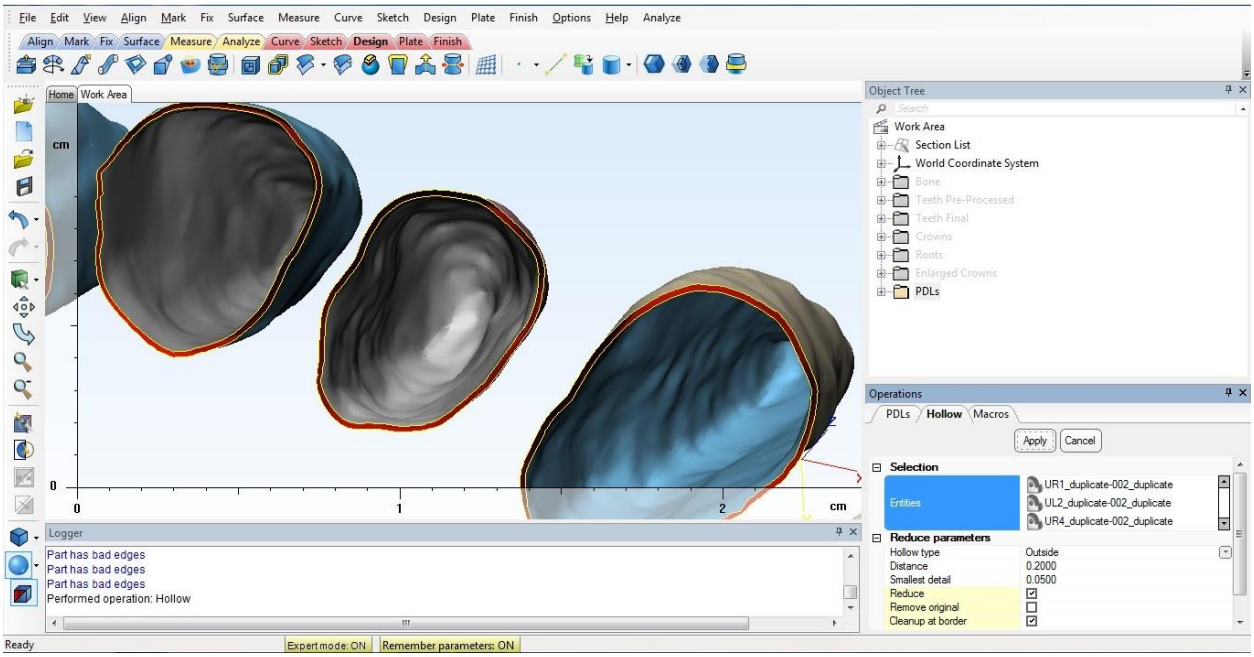

Figure IV-15: PDLs Hollowed

To patch the PDL into a water-tight object, the gap between the two surfaces must be filled. The study found that the best way to achieve this is to create a bridge (Fix → Create Bridge) between the two surfaces [Figure IV-16] and then fill the hole (Fix → Fill Hole Normal) that is now the remaining gap between the two surfaces after the bridge was created. [Figure IV-17]

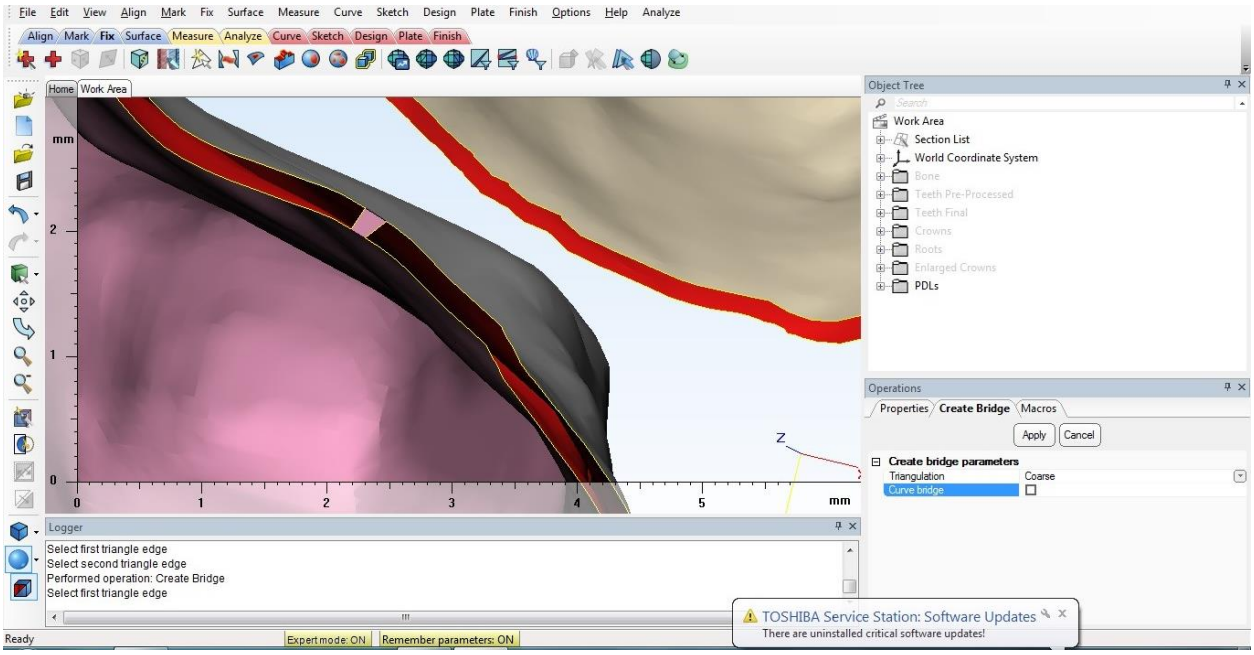

Figure IV-16: Bridge created between the two PDL surfaces

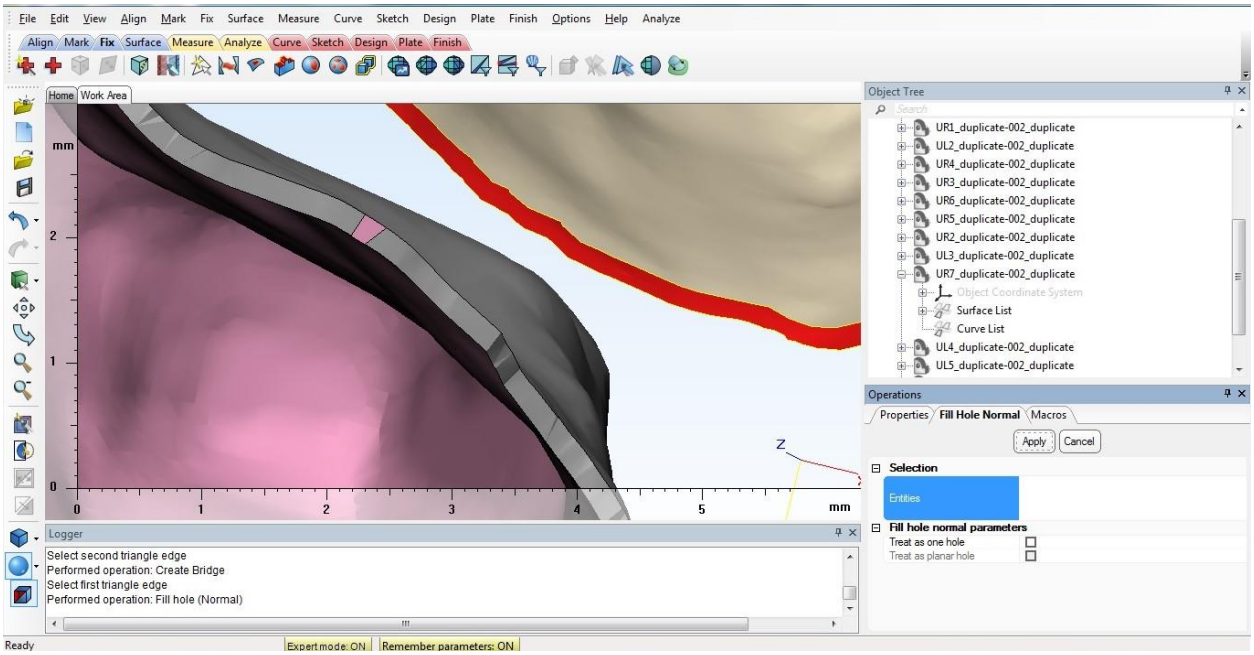

Figure IV-17: Filled hole around edge of PDL created by the bridge

The different coloration between the bridge and filled gap means that the two areas belong to different surfaces. These two pieces need to belong to the same surface before modifying the PDL further. To achieve this, the study found the best way to create a curve (Curve → Create Curve) around the bridged section. Split the bridge (Curve → Split Surfaces by Curves) and then join it with the rest of the PDL edge by selecting both surfaces, right clicking, and selecting merge. [Figure IV-18]

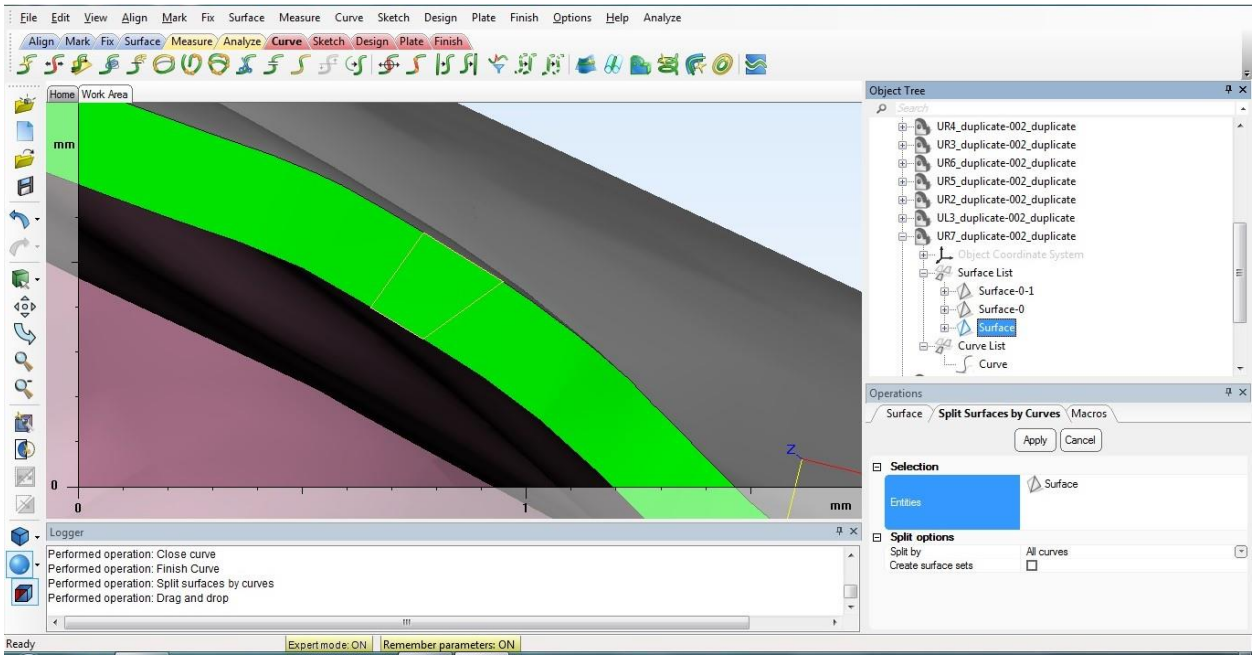

Figure IV-18: Combined surfaces

The user has to perform these steps for all of the PDLs. Once completed, duplicate the PDLs – one to keep as a final set and the other that will be the heightened PDL set modified for subtraction from the maxilla. The study found that to generate the heightened PDL, the user should first delete the inner surface of the PDL. Then use the fill hole tool (Fix → Fill Hole Normal) to fill the opening of the PDL surface. [Figure IV-19] Merge the new surface with the rim of the PDL and run the fix wizard (Fix → Fix Wizard) to make sure there are no errors in the model. Once complete, select the move surface tool (Design → Move Surface) and the top surface of the PDL. With the parameters in [Table 3], apply the move surface tool and the top of the PDL should grow by 3mm. [Figure IV-20]

Table 3: Move Surface Parameters

Method:	One direction for all surfaces
Direction:	May need adjustment to straighten segment
Distance:	3.0000
Solid:	Checked
Connection type:	Add side surface

After performing this modification to all PDLs, the enlarged crowns can be made. The first step in making the enlarged crowns is to fill the hole in the crowns (Fix → Fill Hole Normal) and run the fix wizard. Next is to use the local offset tool (Design → Local Offset) to help grow the outer surface of the crown without also growing the crown near the CEJ (Direction: external; Offset distance: 0.2500 (variable depending on needs); Diminishing Distance: 0.5000). [Figure IV-21]

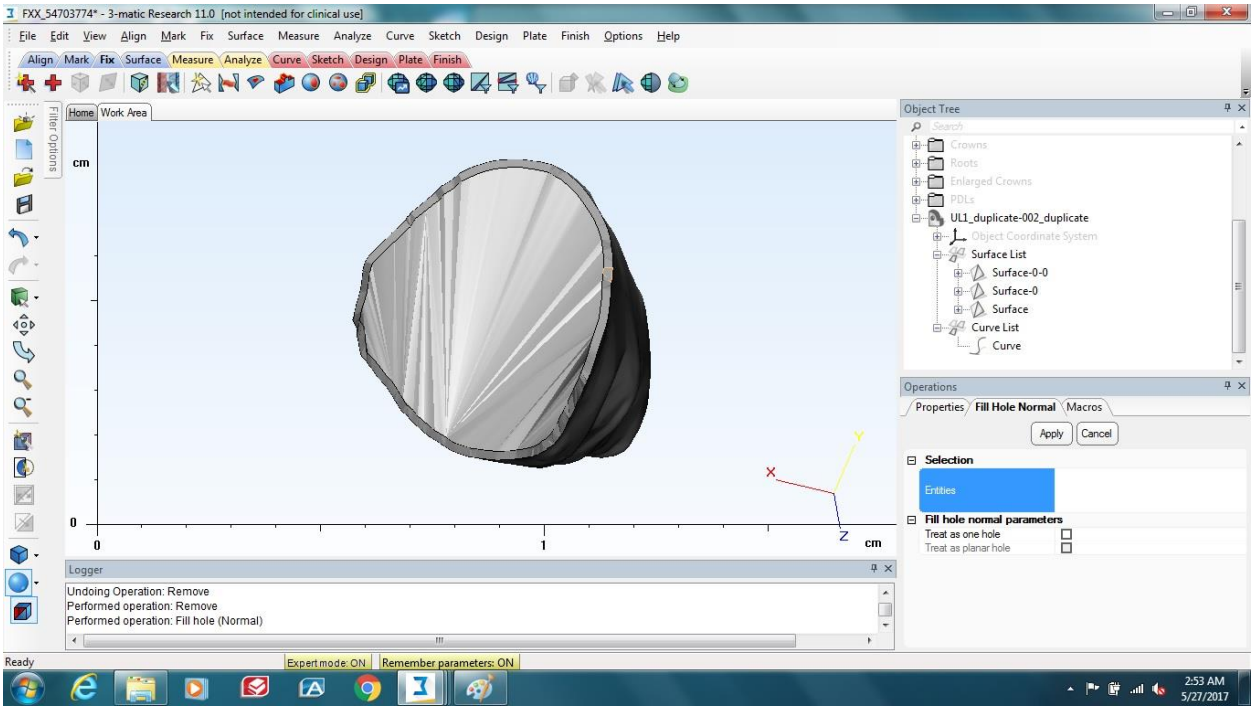

Figure IV-19: PDL Filled

With both the enlarged crowns and PDLs complete, the user can then subtract them from the maxillary bone using the Boolean subtraction tool (Design → Boolean Subtraction). The user can clean scraps left over after the subtraction and other small anatomical projections off the maxilla using the trim tool (Finish → Trim). The maxillary bone is complete at this point.

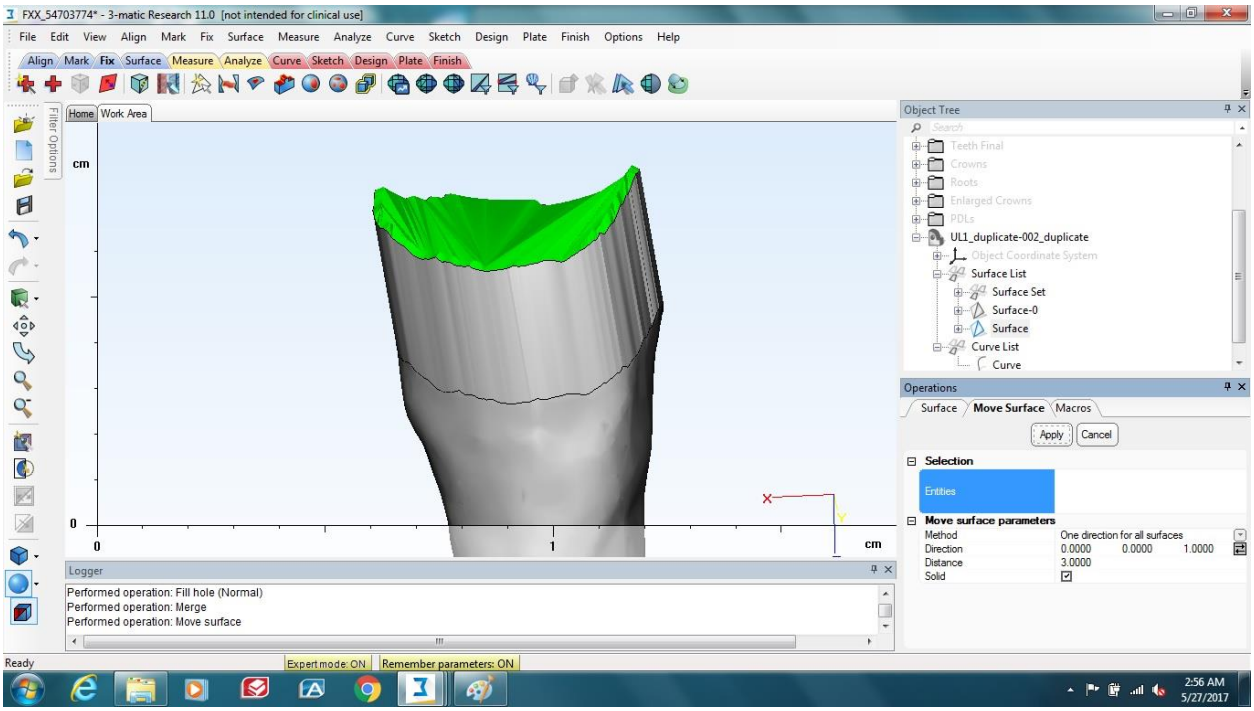

Figure IV-20: PDL heightened for maxillary subtraction

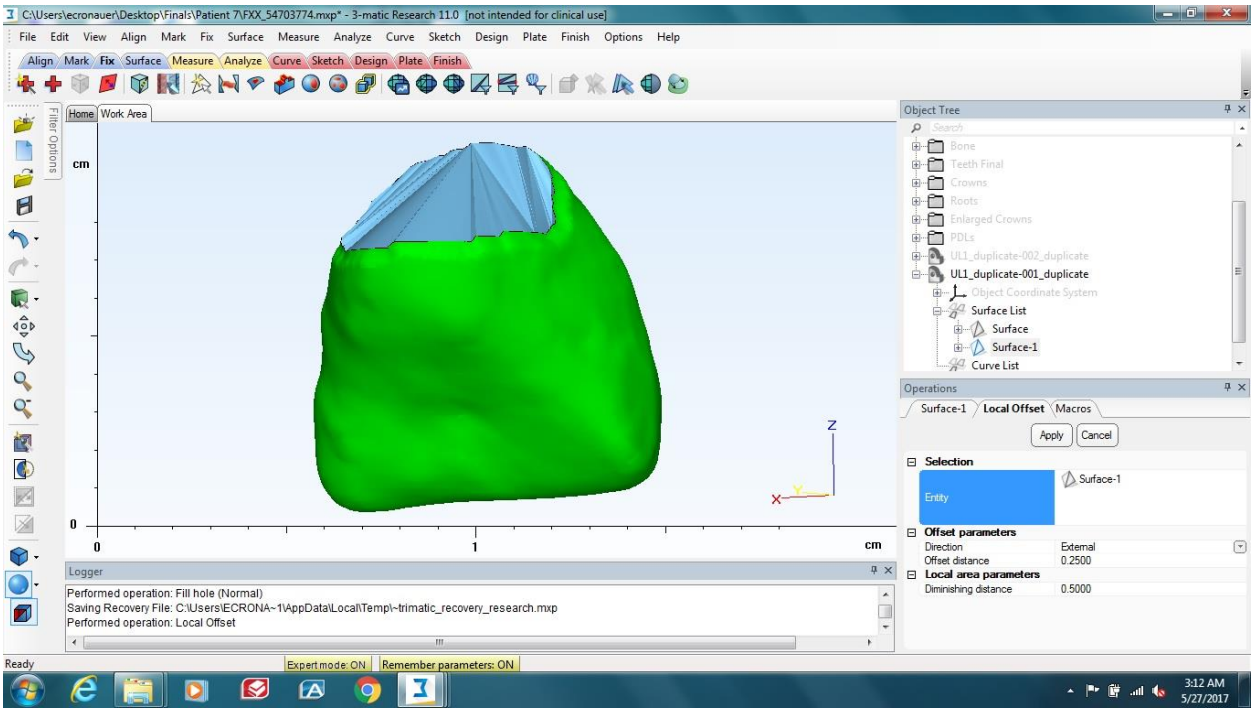

Figure IV-21: Enlarged crown for subtration from maxilla

The final structures to finalize are the PDLs that were duplicated previously. Duplicate the current PDL set to maintain a backup in case anything needs to be repaired or replaced. Use the smooth edge tool (Finish → Smooth Edge) to smooth the edges of the PDLs. Select the outer

edge of the lip, set the influence distance to 0.5000 and smooth detail to fine. The PDL edges become smooth and the coarseness that existed previously is gone. These are the final PDL structures. At this point, we have finished teeth, PDLs, and maxillary bone ready for remeshing and volume meshing.

The remeshing procedure is fairly straightforward. The study found that the first tool to use is the adaptive remesh tool (Remesh → Adaptive Remesh). Choose a method of judging triangle quality, set the threshold for quality, set the element growth to maximum, and lastly be sure to select the option to maintain surface geometry. After adaptively remeshing each object, the study found good use of the quality reducing triangles tool (Remesh → Quality Reducing Triangle) to further reduce the number of elements in each object without altering surface geometry.

Once these meshing stages are done, the surface meshing is complete. The final stage to meshing is creating a volume mesh (Remesh → Create Volume Mesh). In the tool options, this study determined that it is best to choose to mesh 10-node tetrahedral elements (tet10) with mid-side nodes. Enable the largest element growth rate and create the volume mesh. After completion of all volume meshes, export each object as either an Ansys or Abaqus file (File → Export → Ansys/Abaqus).

Return to Mimics, where the user is to import the maxillary bone solid volume mesh that was generated in 3matic. Right click on the object in the window and select Material Properties. A new window will open, which allows the input of a specific equation, various methods for stratifying material assignment, or even homogenous material assignment. Assign the modulus of elasticity and Poisson's ratio as desired. Save the object with the newly assigned material properties as an Ansys or Abaqus file for use next in the finite element pre-processing.

3. Finite Element Analysis Pre-processing

Pre-processing of the models into finite element software, such as Abaqus, follows a separate workflow. However, despite the different nature of these models compared to a typical engineering model, the workflow steps are the same and very well explained in the Abaqus documentation.

Abaqus pre-processing is set up in the software to be a stepwise procedure. The first step is to import all of the separate parts into Abaqus – individual teeth, PDLs, and bone. The second module in the software is the property module, where material properties are assigned homogenously to the teeth and with the Ogden model and parameters[29] to the PDLs. The maxillary bone was assigned material properties in Mimics, and therefore does not need assignment in Abaqus.

Following material property assignment, the next module in Abaqus is the assembly module. Parts are "duplicated" into instances that are then assembled into the tooth-PDL-maxilla assembly as it would be in a patient. Next steps are assigned to the model for when the analysis is carried out. These steps can be anything from changing the force to fixing teeth together.

Subsequently, the interaction module follows, which is where the coincident surfaces of the teeth, PDLs, and bone are tied together to simulate the physiologic attachment of these materials to each other. This study found that the best way to achieve this interaction assignment is through using the "Find contact pairs" tool, which examines the surfaces and how close the surface elements are to each other. The study found there is some tolerance built into this tool for contact pairs that are not perfectly touching or that are slightly intersecting, which is necessary as it is inevitable some elements are malpositioned slightly in the model. The tool has the ability to bring together slightly spaced elements and to resolve minor intersections.

The next step is the load module. Loads can be placed anywhere on the module, in any direction, and in any contact pattern and size. The study set a 2N load on the crowns of the central incisors along the horizontal plane of the model. Additionally in the load module, using the "create boundary condition" tool allows the user to set boundary conditions for the model. The tool allows for the selection of all the points on a plane, which the study found very useful for setting all of the points along the top of the maxilla to zero degrees of freedom to assure the model stays rigid in that area.

Abaqus has a mesh module that follows the load module, however, all of the solids in this study were previously meshed in 3matic. Therefore, the mesh module is not needed and the user can skip to the job module. The job module is where the user sets up one or more actions on the model. The job manager is where model analysis is started, progress is shown, and completion is noted.

Finally, the visualization module is where the user can see the results of the jobs that were performed, after which any post-processing can take place.

V. Discussion

The center of resistance is a concept that is frequently referred to in orthodontics. Biomechanics of tooth movement is based on this point, which causes translation of the tooth when a forced is placed through it or otherwise describes the movement that would occur if the force is placed elsewhere. For decades, orthodontic literature has done its best to locate and describe this point for clinicians in order to better plan treatment and more efficiently move teeth. The literature still does not agree on a set point, has a number of shortcomings, and does not even describe whether clinicians should expect the center of resistance to be consistent among patients. Add the fact that most of the studies look at a single tooth or a whole arch together, and it is easy to realize that clinicians need more research. This study wants to develop a workflow and toolset that can be followed in future studies and also develop models of patients that can be used in finite element analysis to determine the center of resistance for groups of teeth and the whole maxillary arch.

As evidenced by the number of steps outlined in the results workflow, creating finite element models is a complex task. An increasing number of studies are being conducted to model orthodontic questions in finite element models in an attempt to describe and predict tooth movements. Most studies up to this point deal with smaller scale models, such as a single tooth[2, 7] or a pair of teeth[8, 9]. A select few more complicated FEA studies have looked at more than one tooth,[10] but these studies have shortcomings from being modeled off non-patient sources. In most if not all of these studies, scans were obtained using high-dose radiation that provided micro computed tomography scans with high resolution, which is unrealistic for normal use in a patient environment and precludes it from regular use in future work.

In this study, we wanted to develop anatomical models that were derived from actual patient imaging. Because micro CT is an unrealistic mode of image acquisition for patients due

to its high radiation dose, this study desired to use more mainstream radiographic methods, such as cone beam computed tomography (CBCT) scans. These scans are becoming more frequently used as technology advances and radiation dose decreases. Many CBCT scans are now taken of patients as part of routine treatment. This study's intent was to use routine scans that were already acquired of patients to generate models of the maxillary bone, teeth, and periodontal ligaments for use in finite element analysis to determine the center of resistance of the entire arch and groups of teeth.

The workflow derived from this study is lengthy but thorough. The ten models derived from CBCTs as a result of the workflow are anatomically accurate and viable for finite element analysis. The intricacy of the steps to create these models is partially a result of the resolution of the CBCT images and partially a result of the manual manipulation some of the software requires to derive and clean the models. At this point with the current resolutions of CBCTs in the range of 0.2-0.33mm, the steps determined by this study are both acceptable and manageable. There is no difficulty in performing the steps, but much time was spent determining the right tools, settings, and order in which to perform them.

Compared to other studies, this one is very different. In no other literature does it describe in detail how models are made. Thus, there is variability in the literature in terms of what software is used, which tools are used, how the PDL is modeled, how the PDL and bone's material properties are set, and many other variables. This study attempts to answer those questions and provide a guide for future researchers to follow both to maintain consistency and to instead devote time to analysis and research rather than figuring a way to make a model.

To have a consistent workflow that can lead to immediate generation of models from CBCT images would be a significant advancement for finite element studies in orthodontics. More time could be devoted to making more models or to performing more in-depth analyses.

All of these things lead to determining the center of resistance for teeth and introduce the ability to compare it amongst many patients to evaluate consistency of those points.

Despite best efforts, there are some limitations to this study. First, because the PDL could not be visualized on the CBCT, it could not be segmented on its own and had to be generated from the root surface of the tooth at a uniform thickness of 0.2mm. Finite element studies have shown that uniform versus non-uniform modeling affects the outcome of the finite element analysis, and that non-uniform modeling is superior.[19, 24] Second, the number of steps to create an accurate model is very lengthly. This is a limitation in terms of how quickly models can be made, which limits the possibility of using this for personal treatment plans for patients on a case by case basis. Additionally, the software required to generate these models is very expensive and usually limited to the resources of an educational institution or a large business. Further, once the models are made, very powerful computing is necessary to run the finite element analysis. Thus, technology and availability are not quite there to make this a viable treatment planning tool.

Future research should be focused on using these models to perform finite element analyses on the maxillary teeth to determine the center of resistance for the arch and groups of teeth, especially those groups of teeth typically manipulated in orthodontics, such as the anterior segment in an extraction case. Once the center of resistance is determined for these models, additional models should be developed from additional CBCT images to add to the CR values found. With a sufficient data pool of CR locations, heat maps could be generated to indicate a general position of the center of resistance that could serve as an invaluable reference for clinicians.

VI. Conclusions

CBCT images can be used for generating finite element meshes. Segmentation procedures need to be modified and performed semi-manually to successfully segment the tooth, PDL, and bone from CBCT radiographs.

A specific sequence of steps with certain tools is necessary to develop final models for use in finite element analysis without incurring errors along the way or at the time of analysis.

The workflow and toolset suggested by this study will be invaluable for future researchers trying to use CBCT images for finite element analysis.

VII. References

1. Smith RJ, Burstone CJ. Mechanics of tooth movement, American Journal of Orthodontics, Volume 85, Issue 4, April 1984, Pages 294-307

2. Tanne K, Nagataki T, Inoue Y, Sakuda M, Burstone CJ. Patterns of initial tooth displacements associated with various root lengths and alveolar bone heights. American Journal of Orthodontics and Dentofacial Orthopedics. 1991 Jul;100(1):66-71.

3. Christiansen RL, Burstone CJ. Centers of rotation within the periodontal space. American Journal of Orthodontics. 1969 Apr;55(4):353-369

4. Burstone CJ, Pryputniewicz RJ. Holographic determination of centers of rotation produced by orthodontic forces. American Journal of Orthodontics. 1980 Apr;77(4):396-409.

5. Dermaut LR, Kleutghen JP, De Clerck HJ. Experimental determination of the center of resistance of the upper first molar in a macerated, dry human skull submitted to horizontal headgear traction. American Journal of Orthodontics and Dentofacial Orthopedics. 1986 Jul;90(1):29-36.

6. Tanne K, Sakuda M, Burstone CJ. Three-dimensional finite element analysis for stress in the periodontal tissue by orthodontic forces. American Journal of Orthodontics and Dentofacial Orthopedics. 1987 Dec;92(6):499-505.

7. Meyer BN, Chen J, Katona TR. Does the center of resistance depend on the direction of tooth movement? American Journal of Orthodontics and Dentofacial Orthopedics. 2010 Mar;137(3):354-61.

8. Cattaneo PM, Dalstra M, Melsen B. Moment-to-force ratio, center of rotation, and force level: a finite element study predicting their interdependency for simulated orthodontic loading regimens. American Journal of Orthodontics and Dentofacial Orthopedics. 2008 May;133(5):681-9.

9. Cattaneo PM, Dalstra M, Melsen B. The finite element method: a tool to study orthodontic tooth movement. Journal of Dental Research. 2005 May;84(5):428-33.

10. Kojima Y, Fukui H. A finite element simulation of initial movement, orthodontic movement, and the centre of resistance of the maxillary teeth connected with an archwire. European Journal of Orthodontics. 2014 Jun;36(3):255-61.

11. Reimann S, Keilig L, Jäger A, Bourauel C. Biomechanical finite-element investigation of the position of the centre of resistance of the upper incisors. European Journal of Orthodontics. 2007 Jun;29(3):219-24.

12. Tominaga JY, Chiang PC, Ozaki H, Tanaka M, Koga Y, Bourauel C, Yoshida N. Effect of play between bracket and archwire on anterior tooth movement in sliding mechanics: A three-dimensional finite element study. Journal of Dental Biomechanics. 2012;3:1758736012461269.

13. Viecilli RF, Budiman A, Burstone CJ. Axes of resistance for tooth movement: Does the center of resistance exist in 3-dimensional space? American Journal of Orthodontics and Dentofacial Orthopedics. 2013 Feb;143(2):163-72.

14. Ammar HH, Ngan P, Crout RJ, Mucino VH, Mukdadi OM. Three-dimensional modeling and finite element analysis in treatment planning for orthodontic tooth movement. American Journal of Orthodontics and Dentofacial Orthopedics. 2011 Jan;139(1):e59-71.

15. Yoshida N, Koga Y, Mimaki N, Kobayashi K. In vivo determination of the centres of resistance of maxillary anterior teeth subjected to retraction forces. European Journal Orthodontics. 2001 Oct;23(5):529-34.

16. Sia S, Koga Y, Yoshida N. Determining the center of resistance of maxillary anterior teeth subjected to retraction forces in sliding mechanics. An in vivo study. Angle Orthodontist. 2007 Nov;77(6):999-1003.

17. Cai Y, Yang X, He B, Yao J. Finite element method analysis of the periodontal ligament in mandibular canine movement with transparent tooth correction treatment. BMC Oral Health. 2015 Sep 4;15:106.

18. Jeong GM, Sung SJ, Lee KJ, Chun YS, Mo SS. Finite-element investigation of the center of resistance of the maxillary dentition. Korean Journal of Orthodontics. 2009 Apr;39(2):83-94.

19. Hohmann A, Kober C, Young P, Dorow C, Geiger M, Boryor A, Sander FM, Sander C, Sander FG. Influence of different modeling strategies for the periodontal ligament on finite element simulation results. American Journal of Orthodontics and Dentofacial Orthopedics. 2011 Jun;139(6):775-83.

20. Qian H, Chen J, Katona TR. The influence of PDL principal fibers in a 3-dimensional analysis of orthodontic tooth movement. American Journal of Orthodontics and Dentofacial Orthopedics. 2001 Sep;120(3):272-9.

21. McCormack SW, Witzel U, Watson PJ, Fagan MJ, Gröning F. The Biomechanical Function of Periodontal Ligament Fibres in Orthodontic Tooth Movement. Agarwal S, ed. *PLoS ONE*. 2014;9(7):e102387. doi:10.1371/journal.pone.0102387.

22. Dong-Xu L, Hong-Ning W, Chun-Ling W, Hong L, Ping S, Xiao Y. Modulus of elasticity of human periodontal ligament by optical measurement and numerical simulation. Angle Orthodontist. 2011 Mar;81(2):229-36.

23. Nanci, A. Ten Cate's Oral Histology. Elsevier; 2013: 220.

24. Toms SR, Eberhardt AW. A nonlinear finite element analysis of the periodontal ligament under orthodontic tooth loading. American Journal of Orthodontics and Dentofacial Orthopedics. 2003 Jun;123(6):657-65.

25. Toms SR, Lemons JE, Bartolucci AA, Eberhardt AW. Nonlinear stress-strain behavior of periodontal ligament under orthodontic loading. American Journal of Orthodontics and Dentofacial Orthopedics. 2002 Aug;122(2):174-9.

26. Pietrzak G, Curnier A, Botsis J, Scherrer S, Wiskott A, Belser U. A nonlinear elastic model of the periodontal ligament and its numerical calibration for the study of tooth mobility. Comput Methods Biomech Biomed Engin. 2002 Apr;5(2):91-100.

27. Nelson SJ, Ash MM. Wheeler's Dental Anatomy, Physiology, and Occlusion. 9th ed. St. Louis, MO: Saunders/Elsevier; 2010:172.

28. Figueiredo de Magalhães M, Neto Ferreira RA, Grossi PA, de Andrade RM. Measurement of thermophysical properties of human dentin: effect of open porosity. J Dent. 2008 Aug;36(8):588-94.

29. Huang H, Tang W, Yan B, Wu B, Cao D. Mechanical responses of the periodontal ligament based on an exponential hyperelastic model: a combined experimental and finite element method. Comput Methods Biomech Biomed Engin. 2016;19(2):188-98.

VIII. Appendix

A. Patient 1 – 18.8 year old male

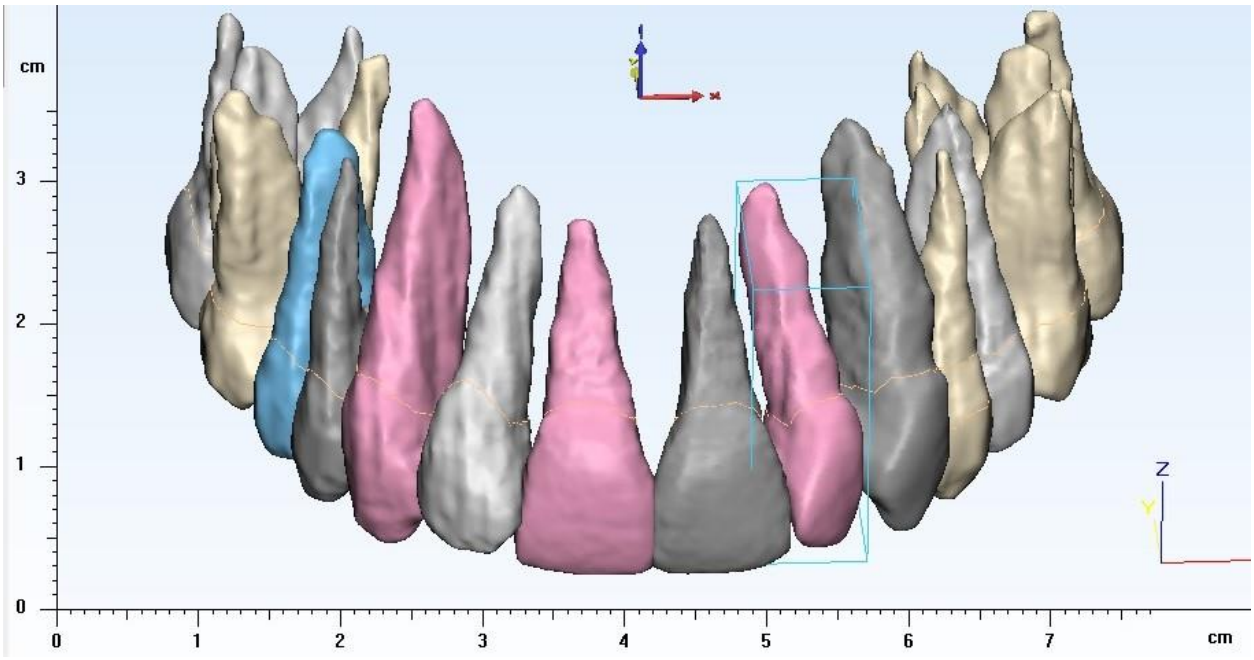

Figure VIII-1: Teeth

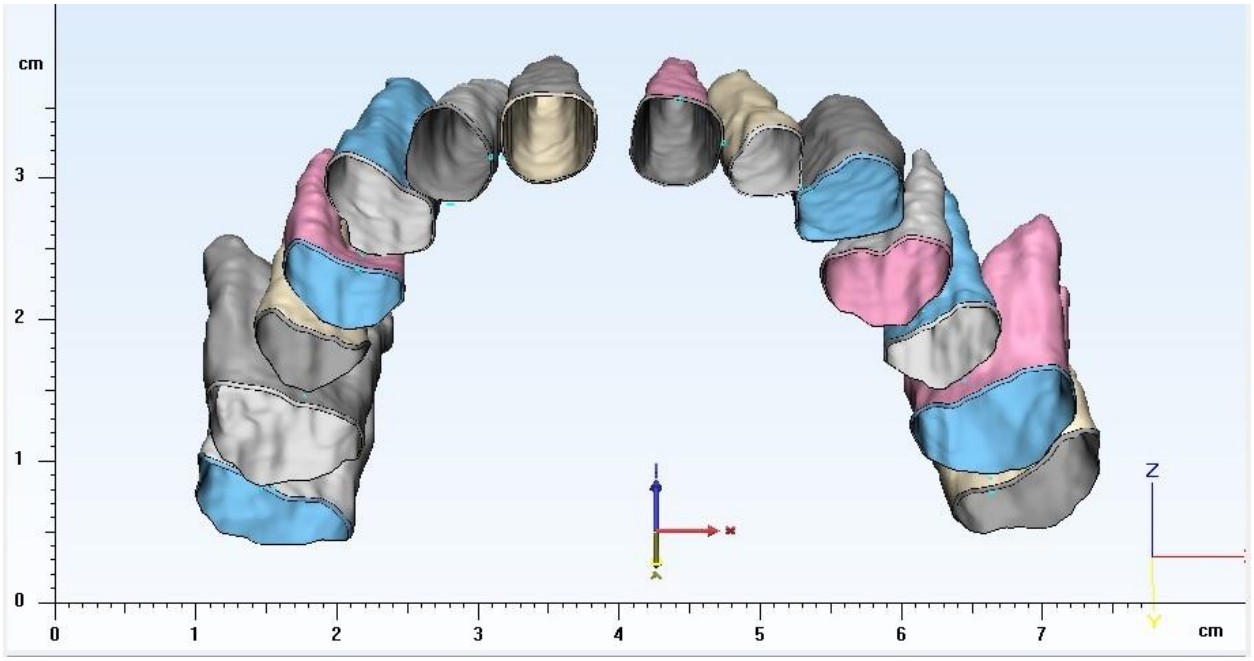

Figure VIII-2: Periodontal Ligaments

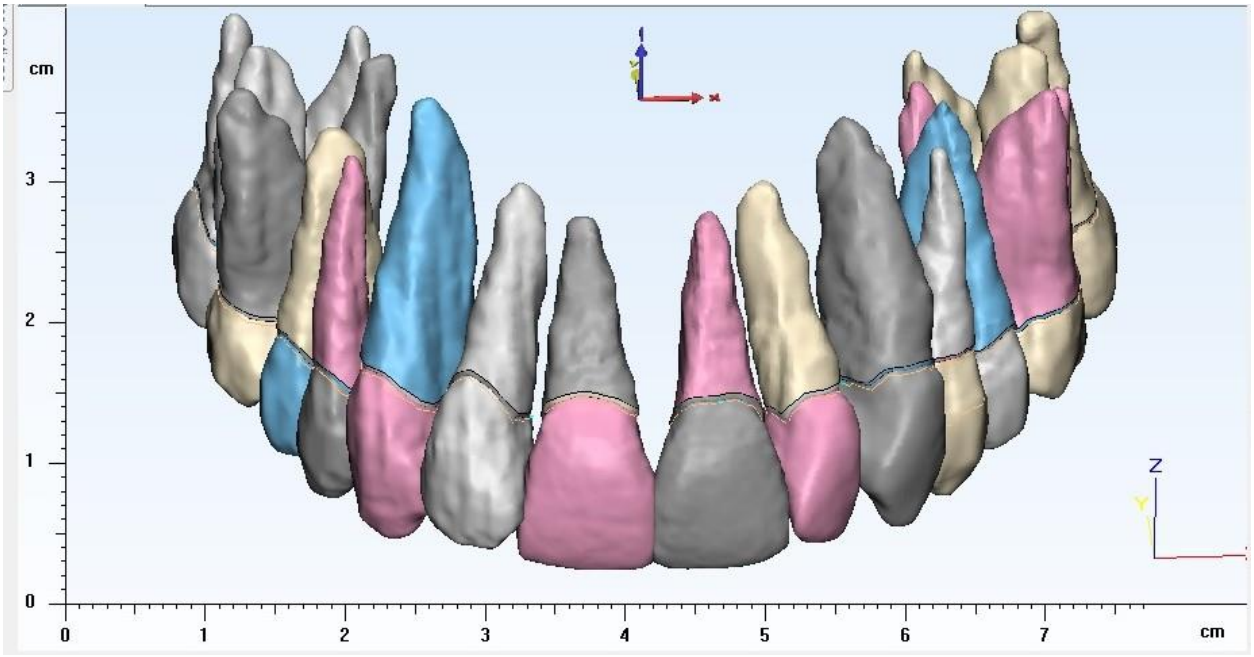

Figure VIII-3: Teeth and periodontal ligaments

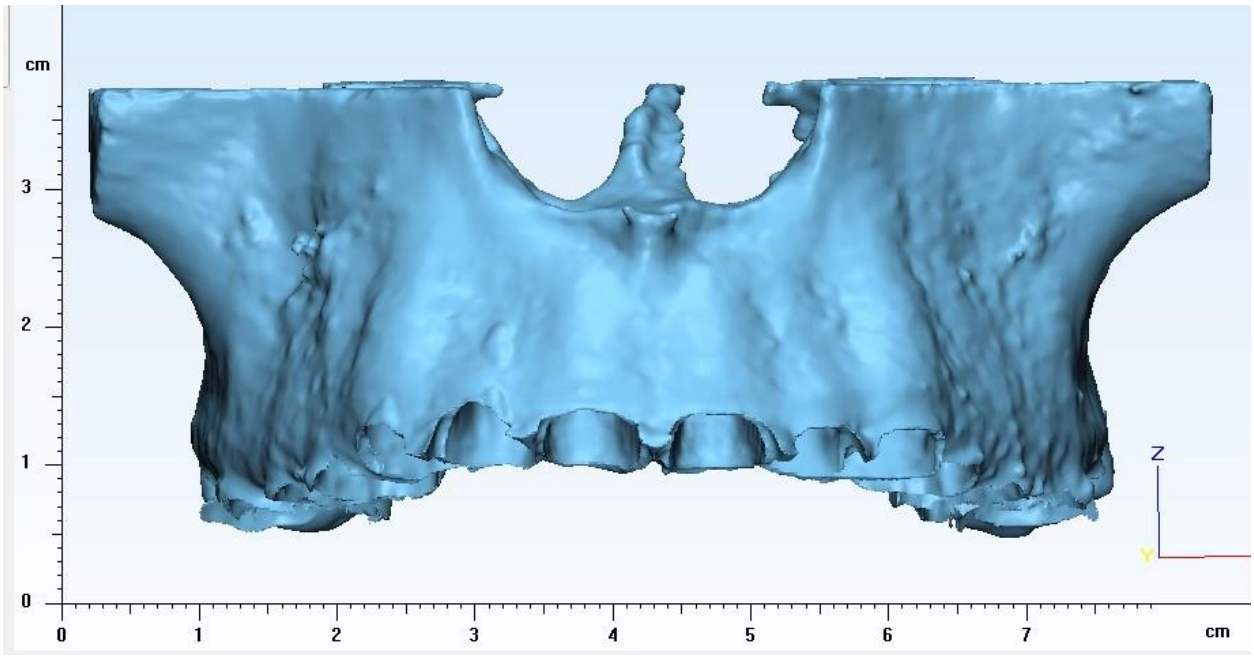

Figure VIII-4: Maxillary Bone

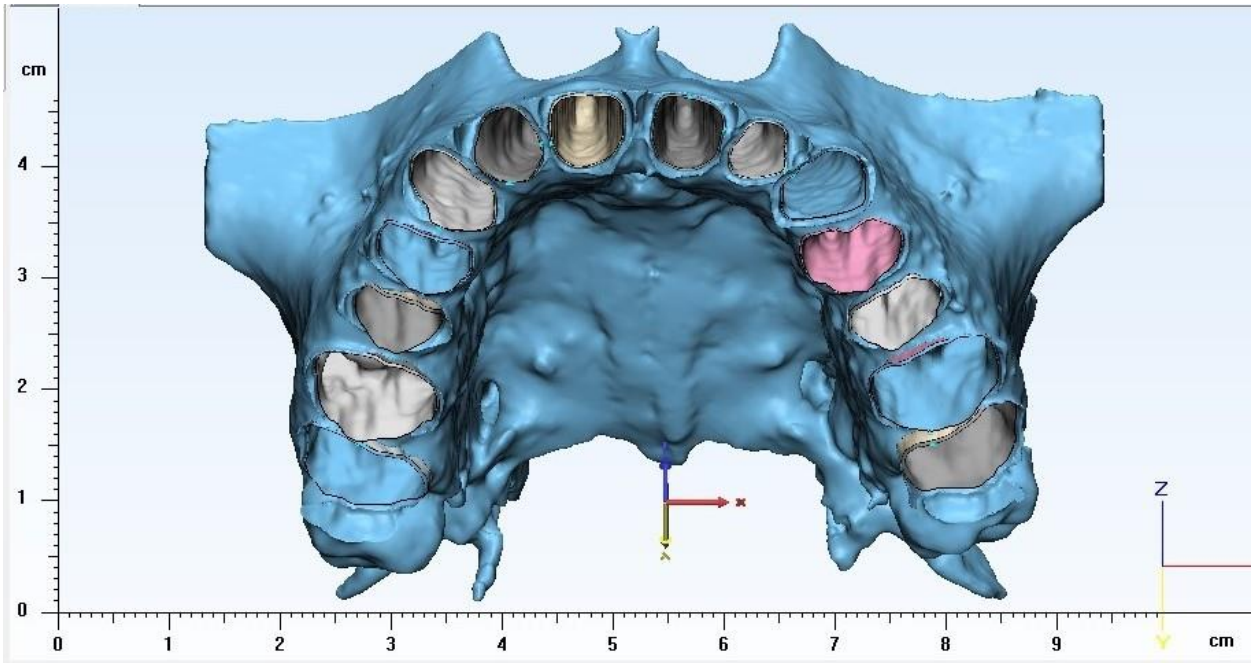

Figure VIII-5: Maxillary Bone with Periodontal Ligaments

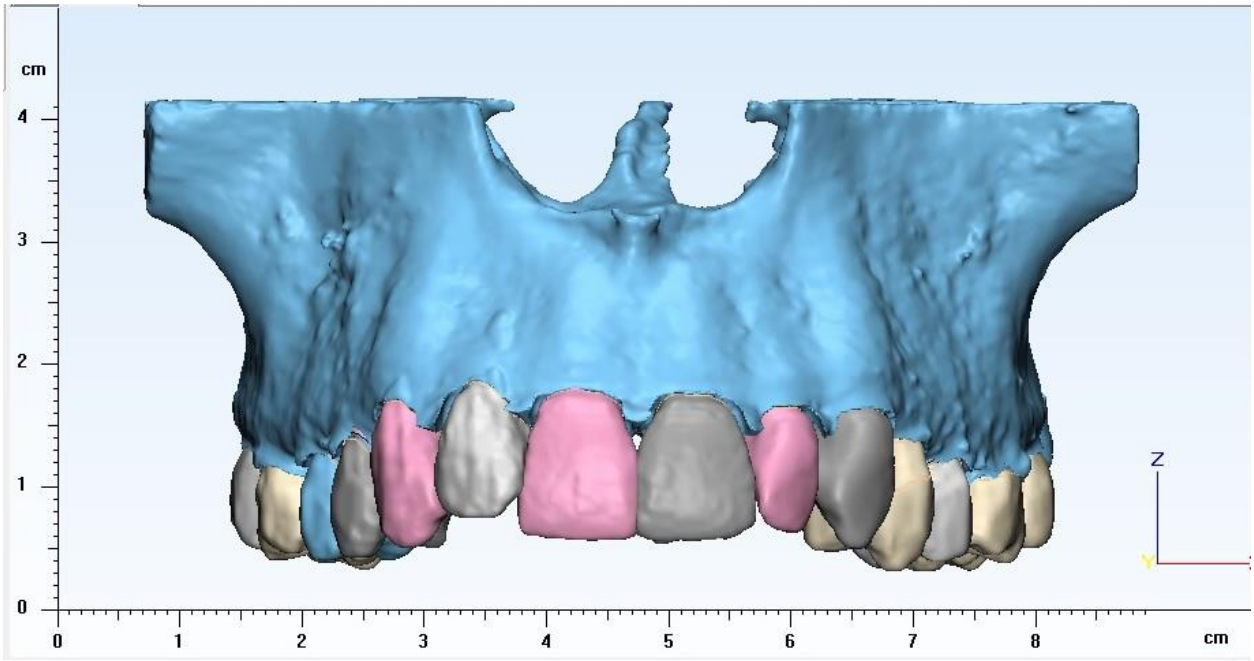

Figure VIII-6: Teeth, Periodontal Ligaments, and Bone together

B. Patient 2 – 18.4 year old female

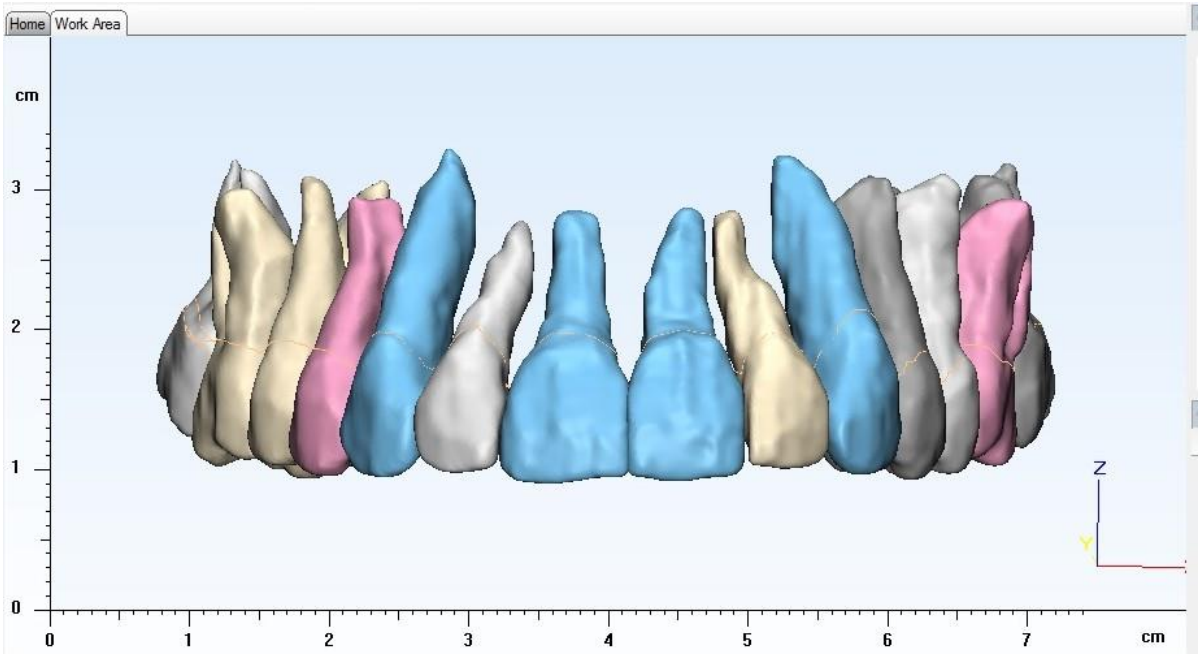

Figure VIII-7: Teeth

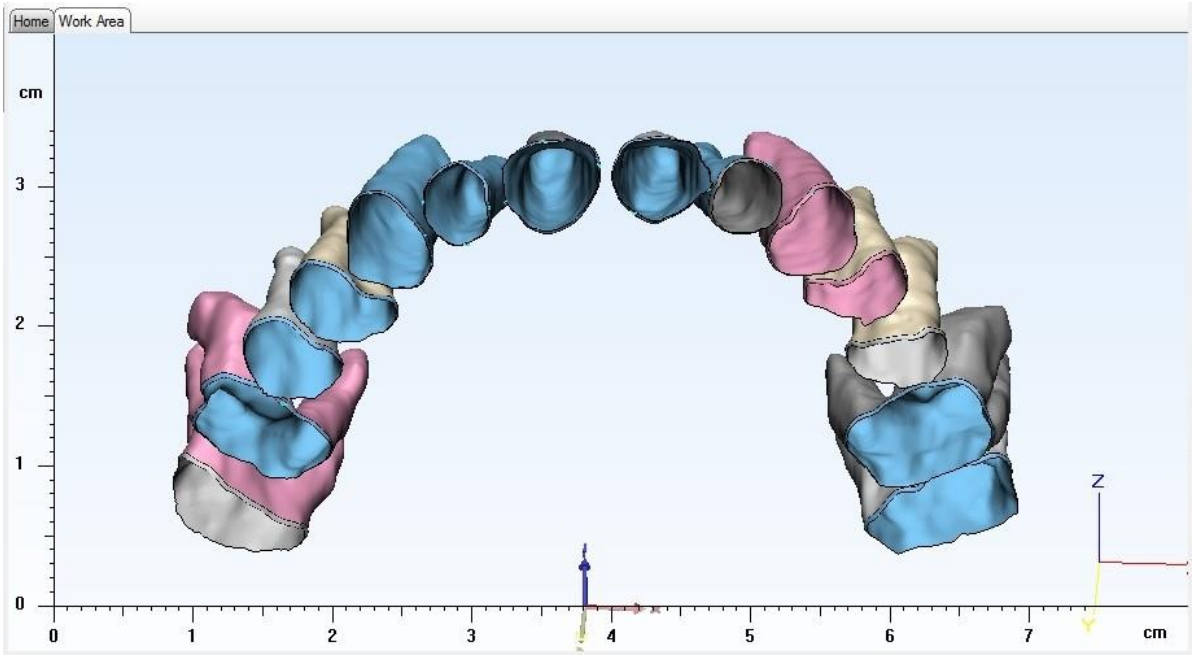

Figure VIII-8: Periodontal Ligaments

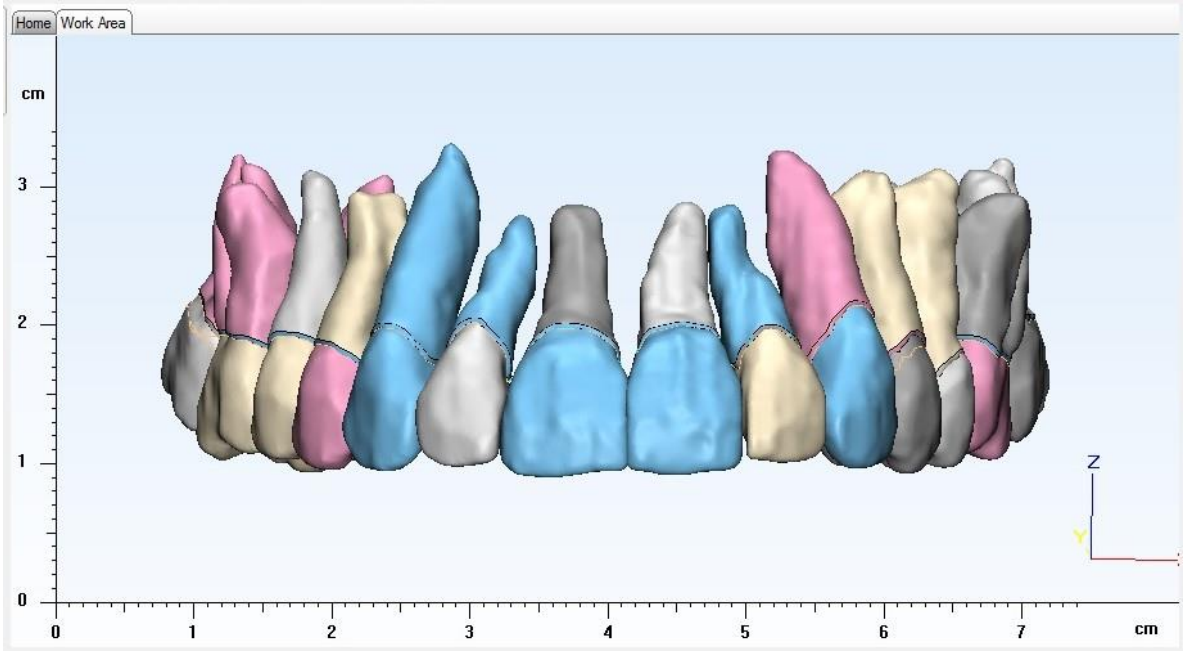

Figure VIII-9: Teeth and periodontal ligaments

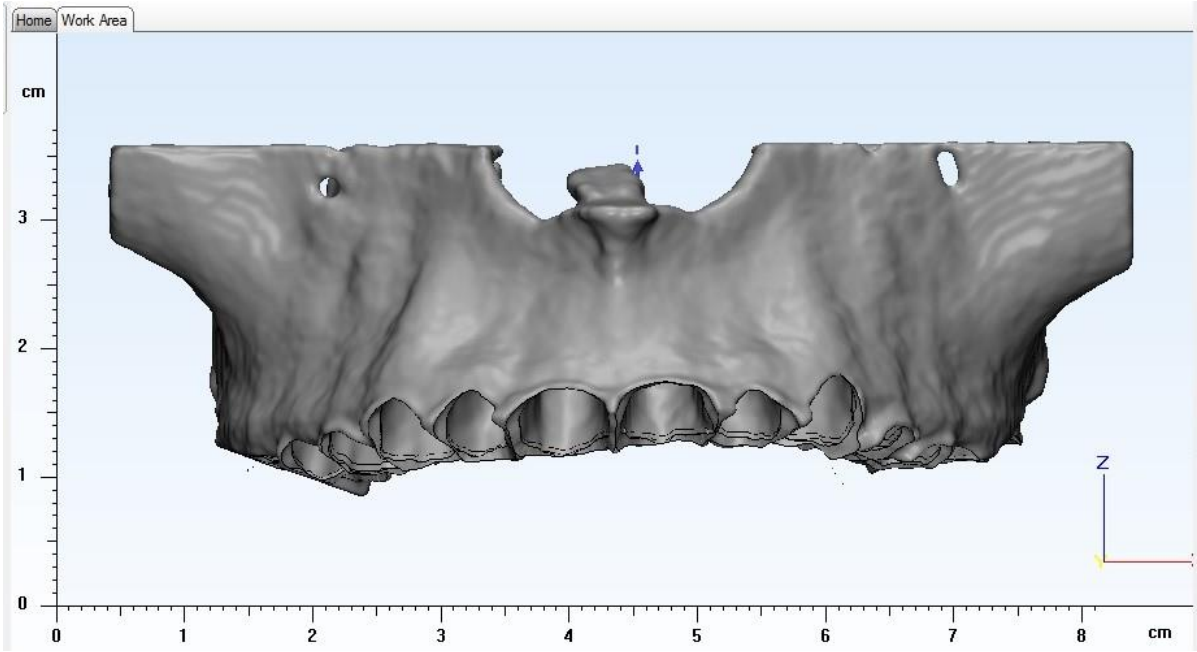

Figure VIII-10: Maxillary Bone

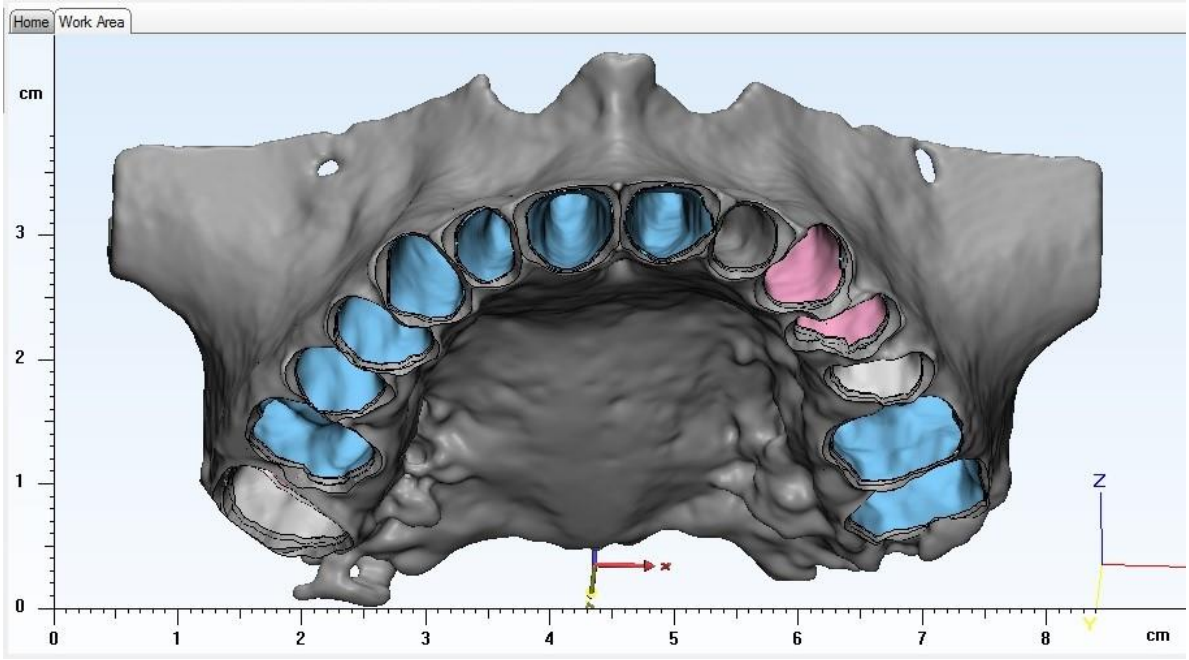

Figure VIII-11: Maxillary Bone with Periodontal Ligaments

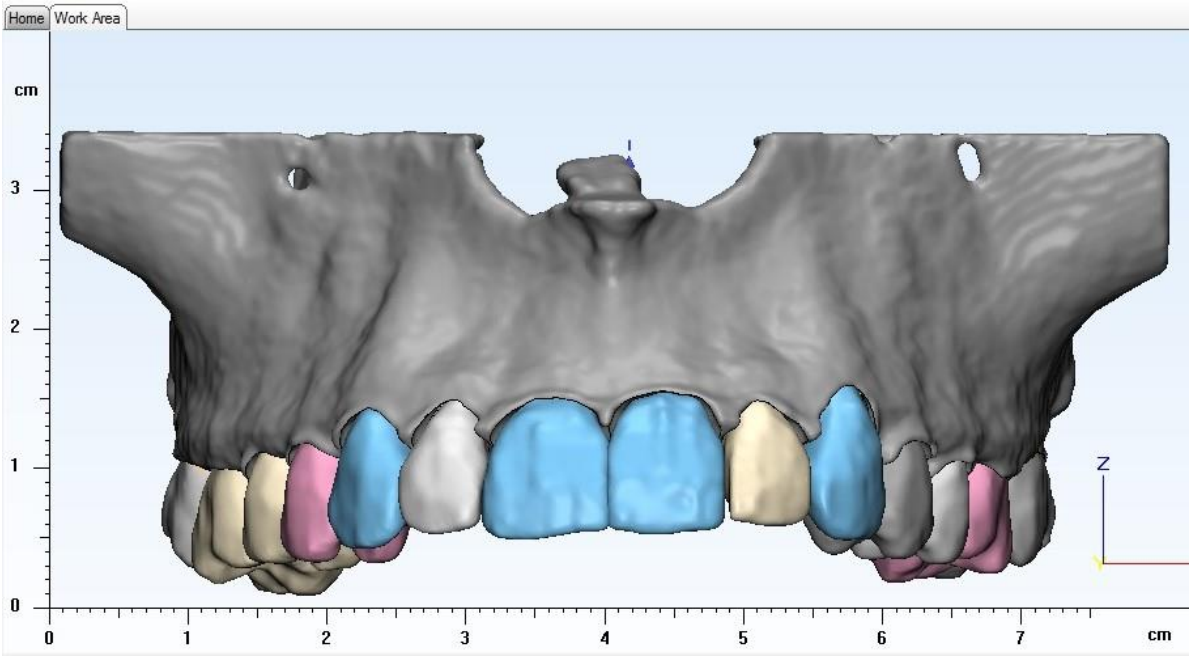

Figure VIII-12: Teeth, Periodontal Ligaments, and Bone together

C. Patient 3 – 15.9 year old female

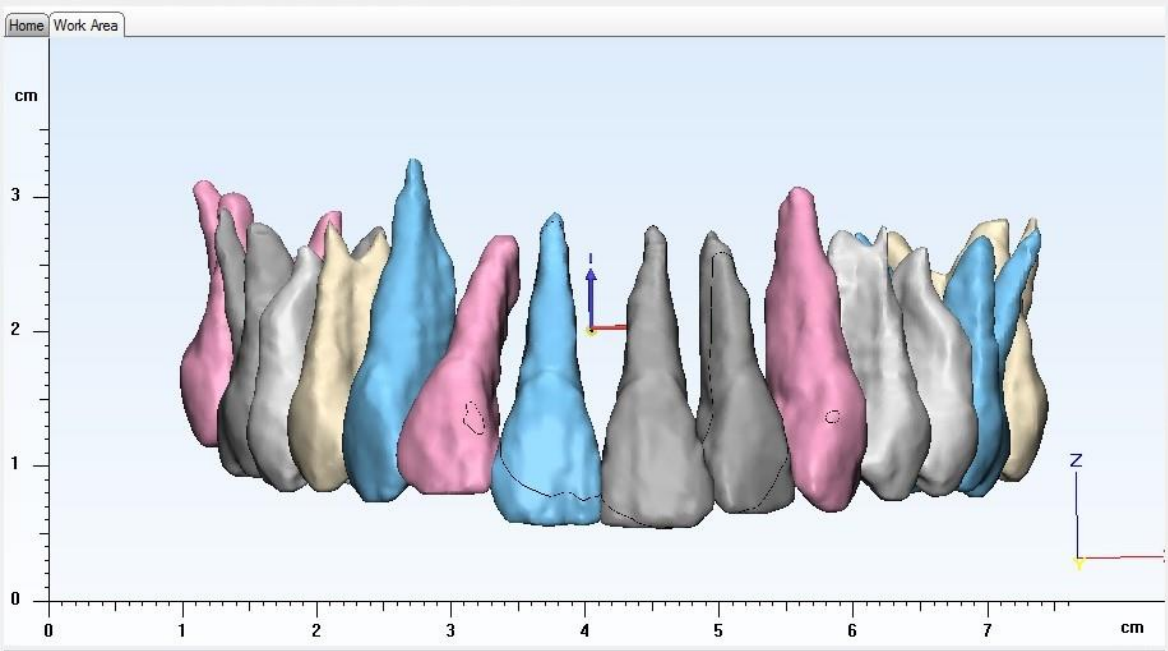

Figure VIII-13: Teeth

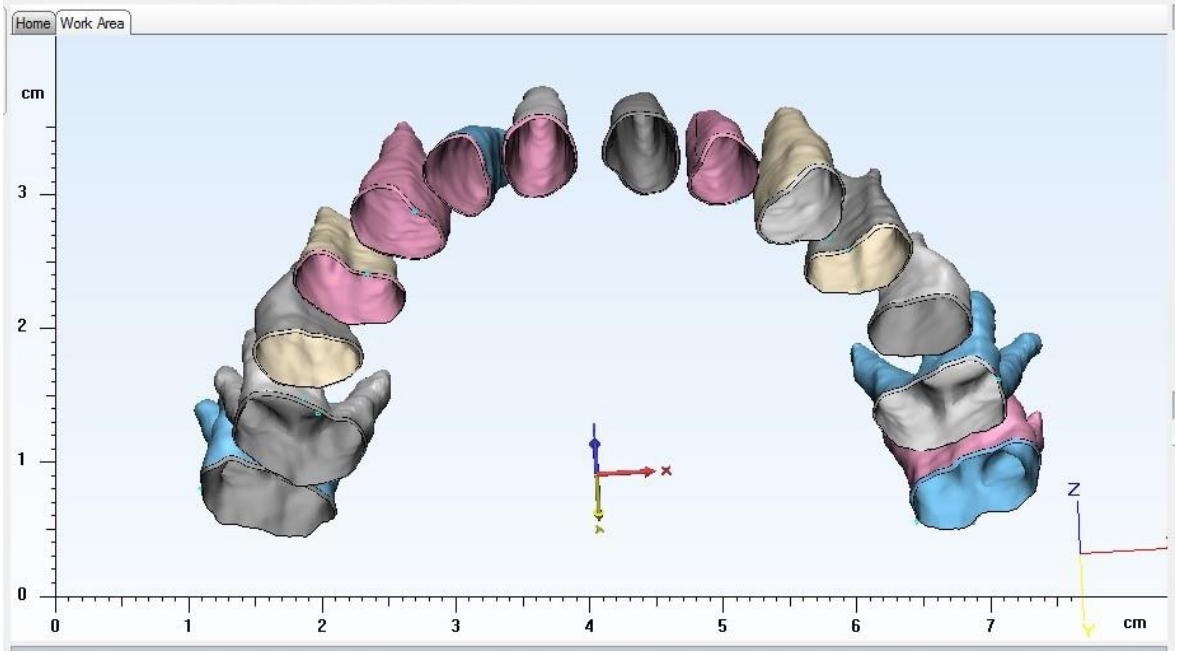

Figure VIII-14: Periodontal Ligaments

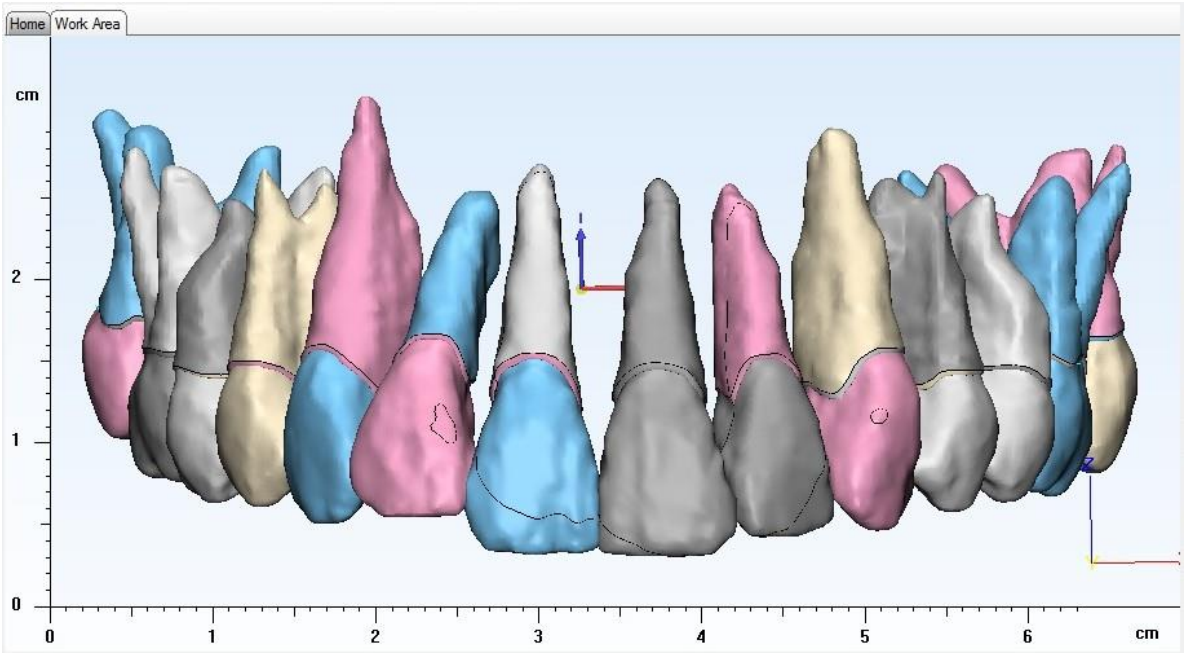

Figure VIII-15: Teeth and periodontal ligaments

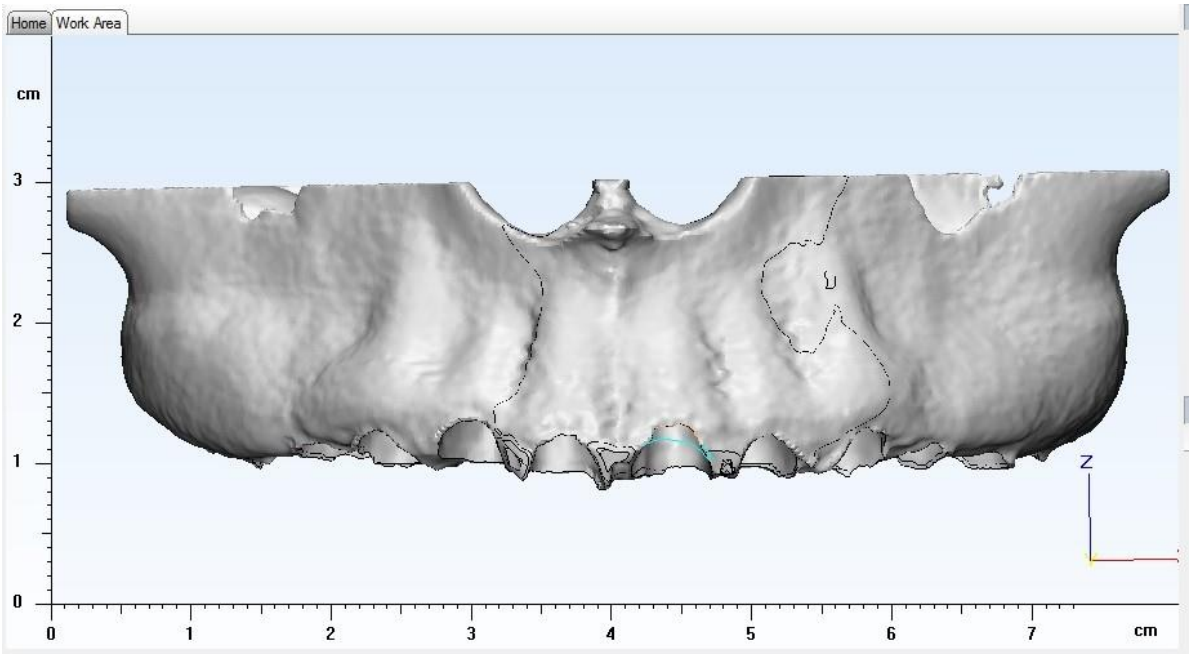

Figure VIII-16: Maxillary Bone

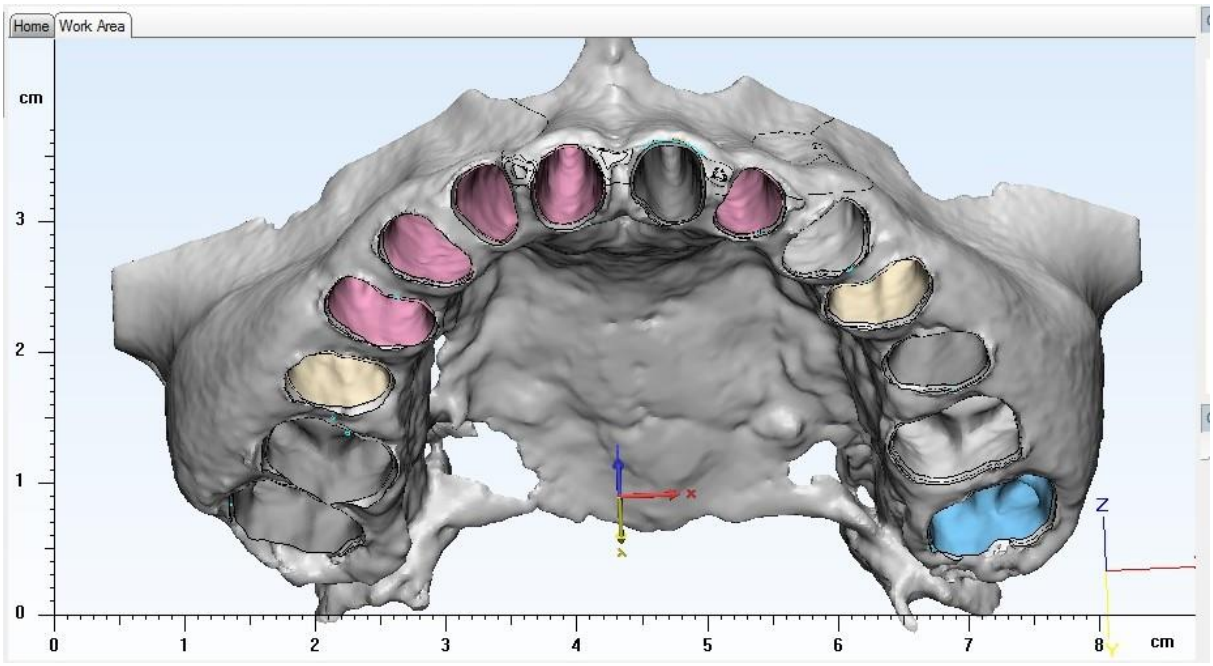

Figure VIII-17: Maxillary Bone with Periodontal Ligaments

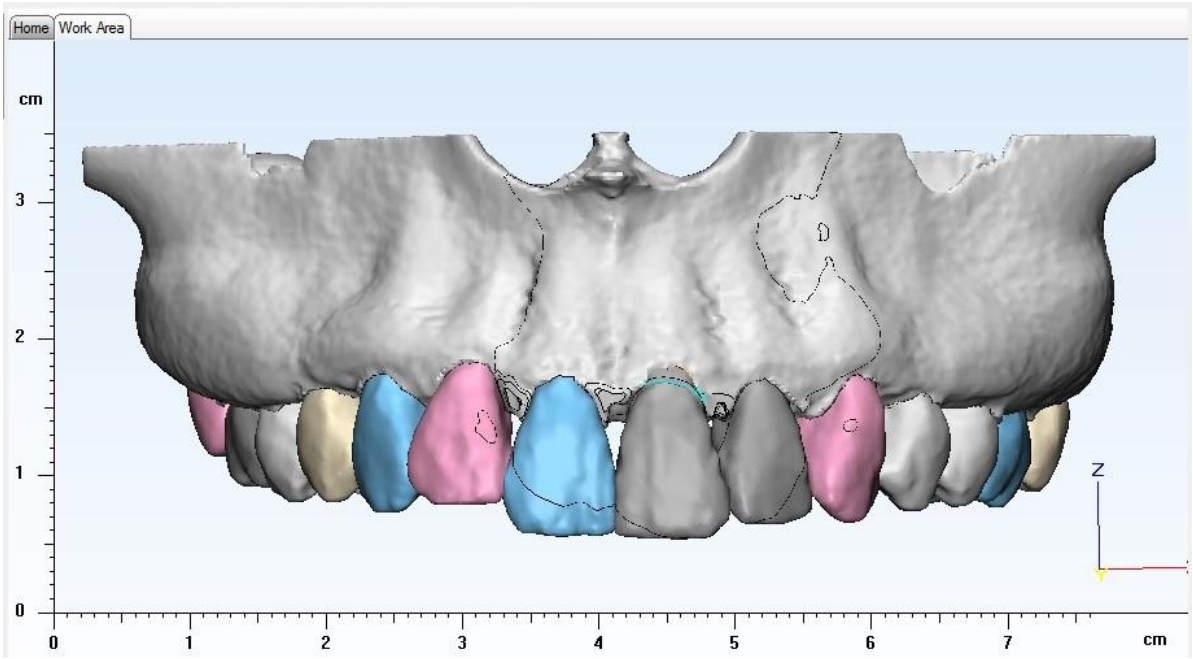

Figure VIII-18: Teeth, Periodontal Ligaments, and Bone together

D. Patient 4 – 49.9 year old male

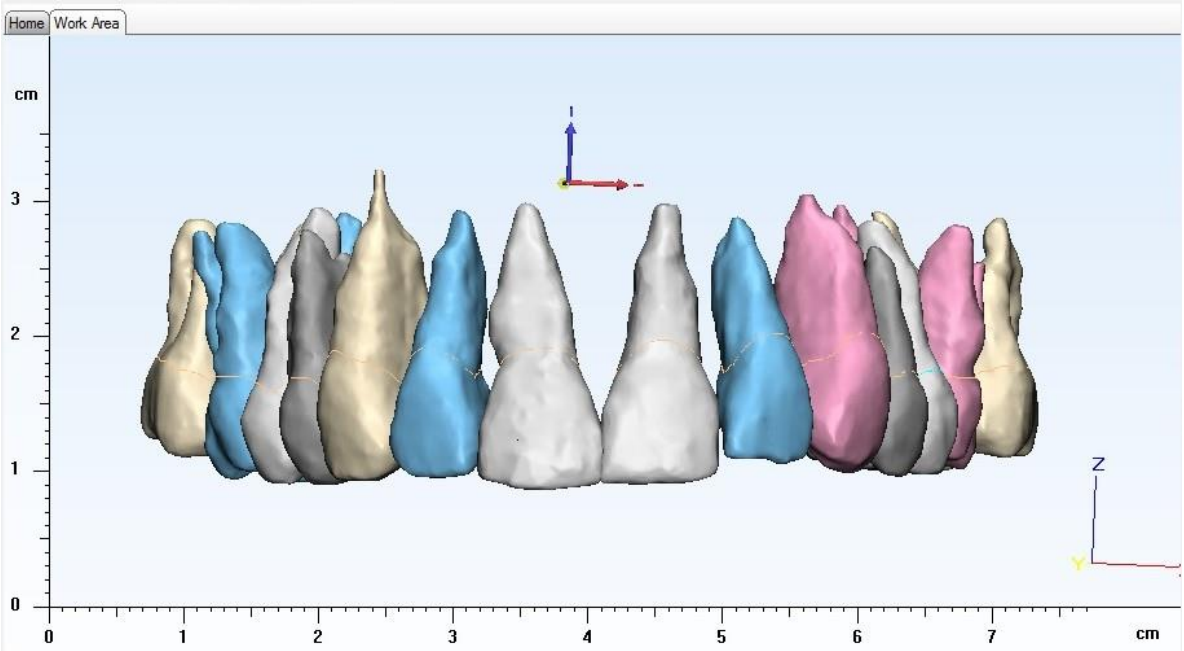

Figure VIII-19: Teeth

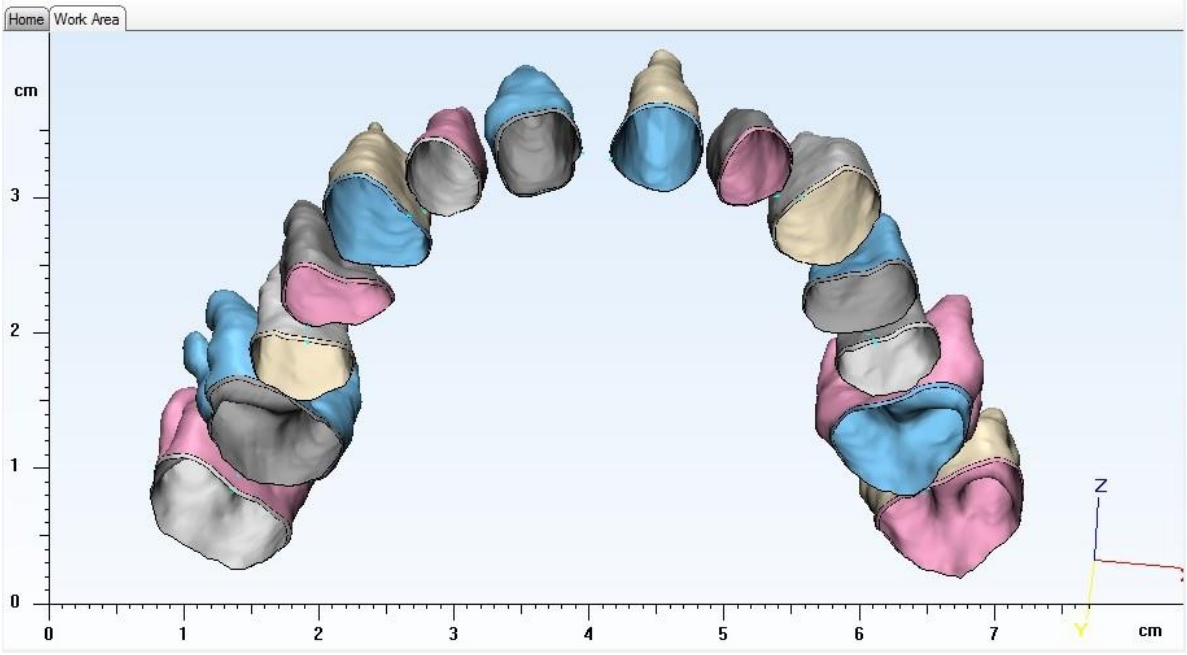

Figure VIII-20: Periodontal Ligaments

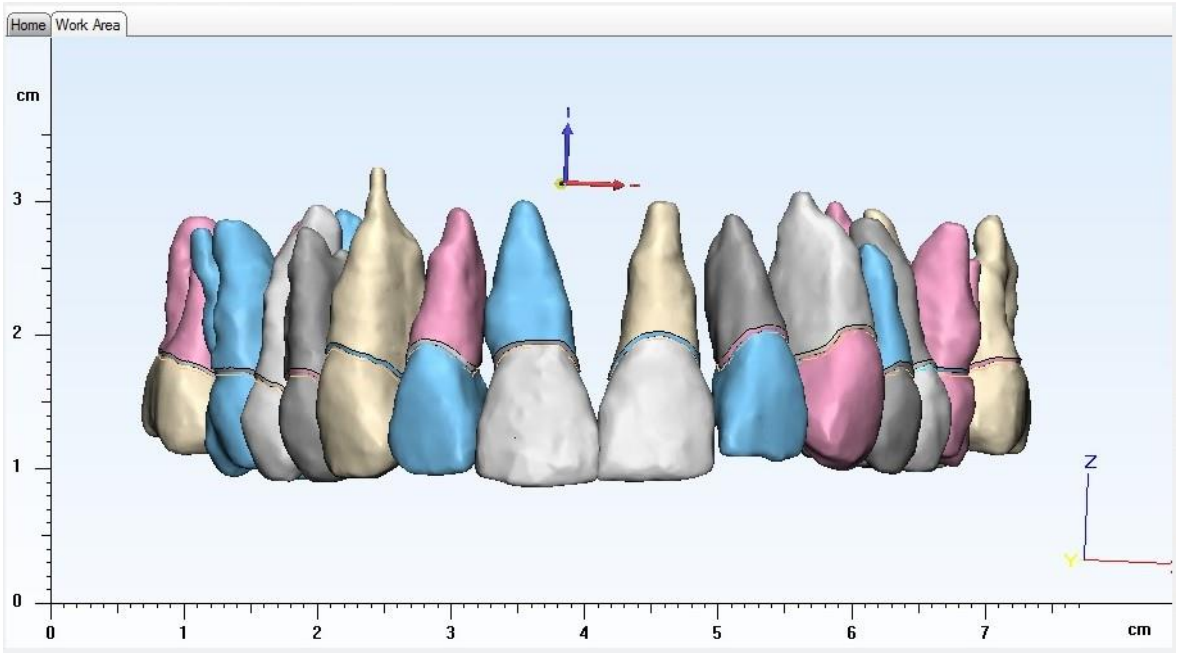

Figure VIII-21: Teeth and periodontal ligaments

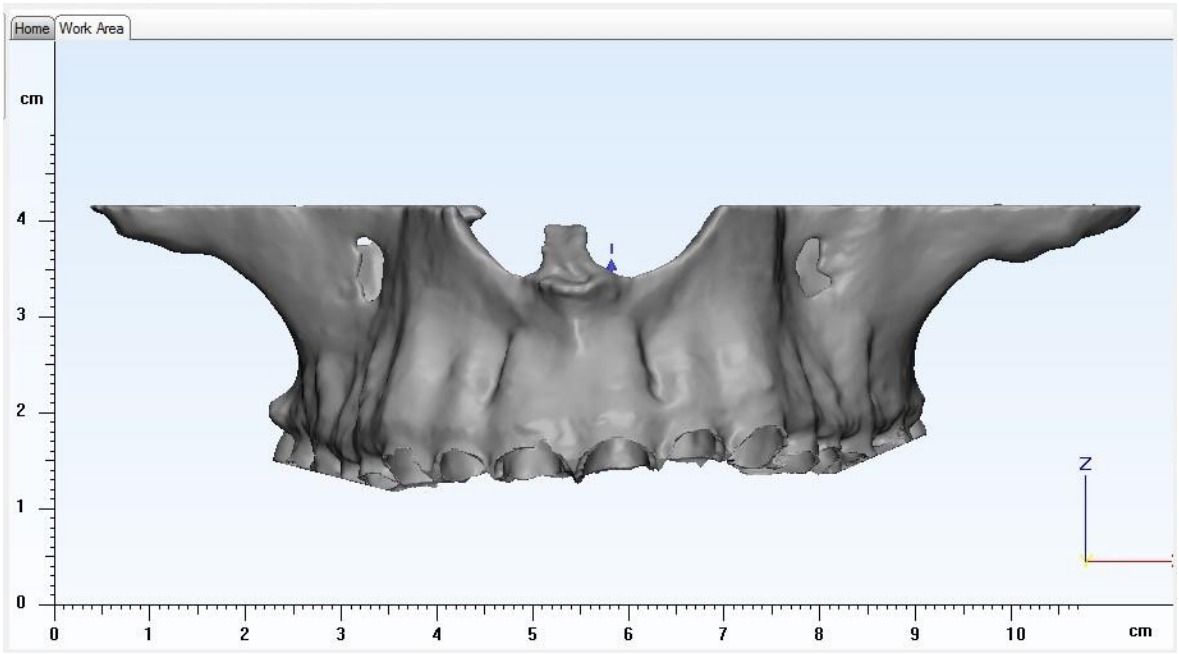

Figure VIII-22: Maxillary Bone

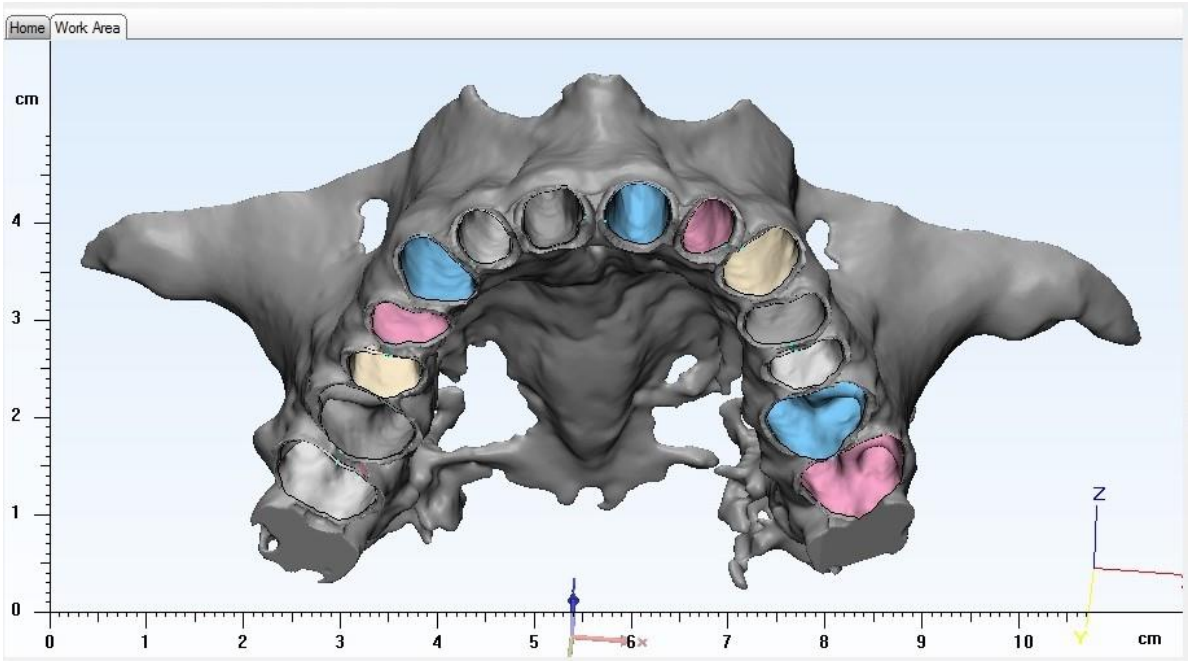

Figure VIII-23: Maxillary Bone with Periodontal Ligaments

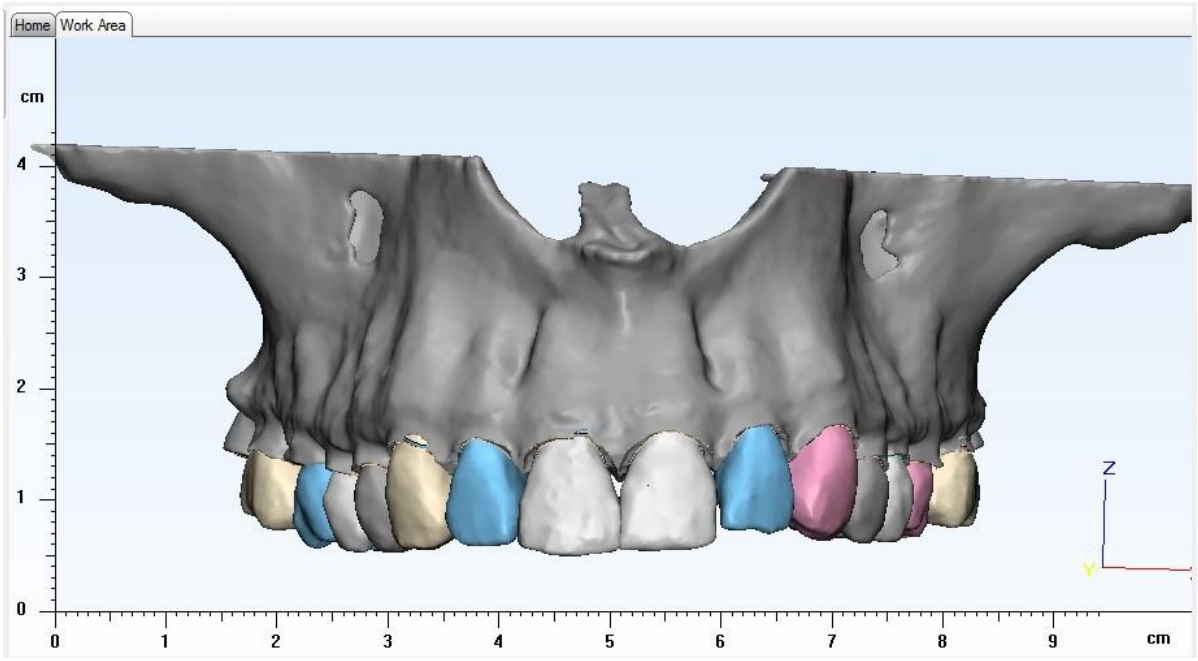

Figure VIII-24: Teeth, Periodontal Ligaments, and Bone together

E. Patient 5 – 22.9 year old male

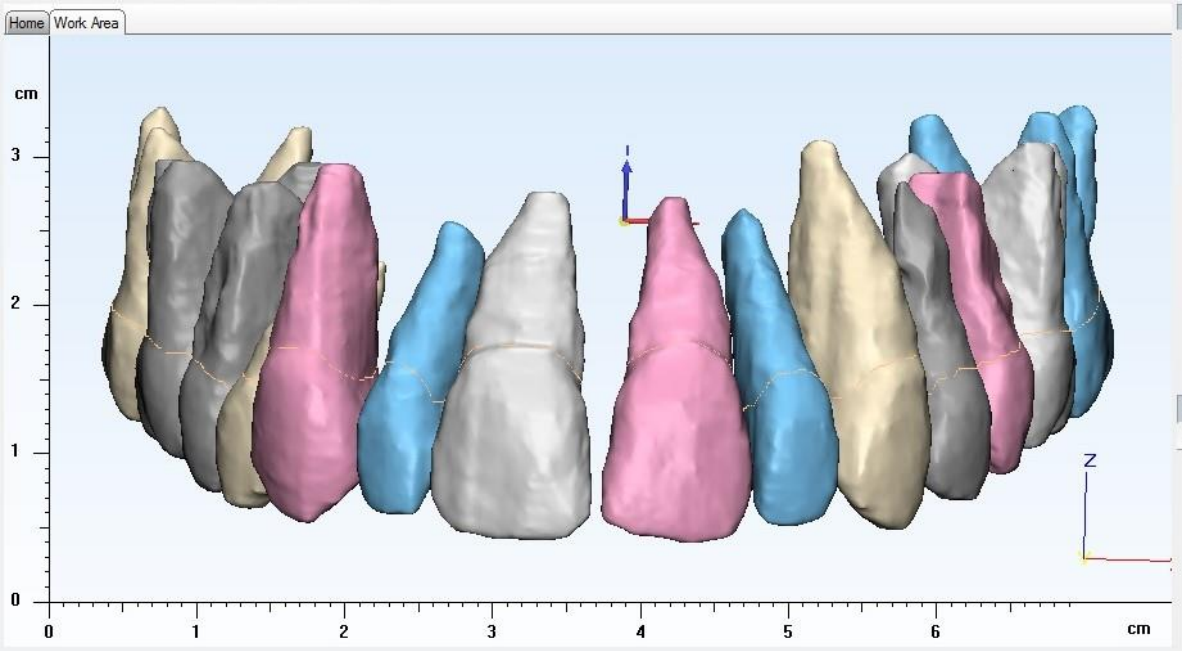

Figure VIII-25: Teeth

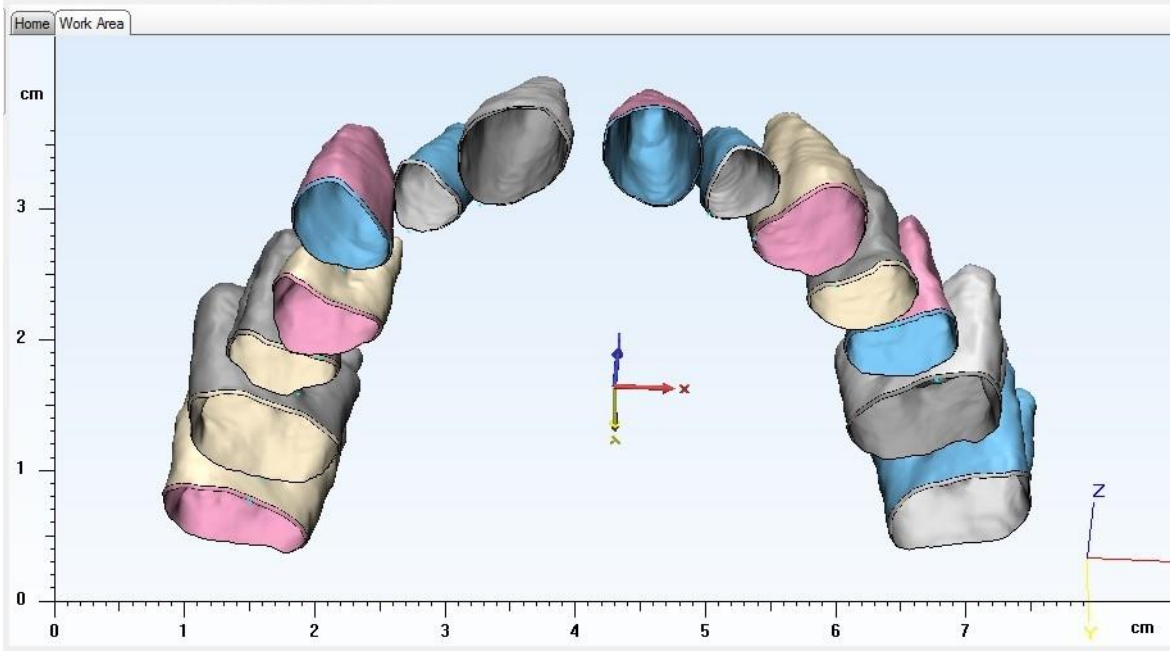

Figure VIII-26: Periodontal Ligaments

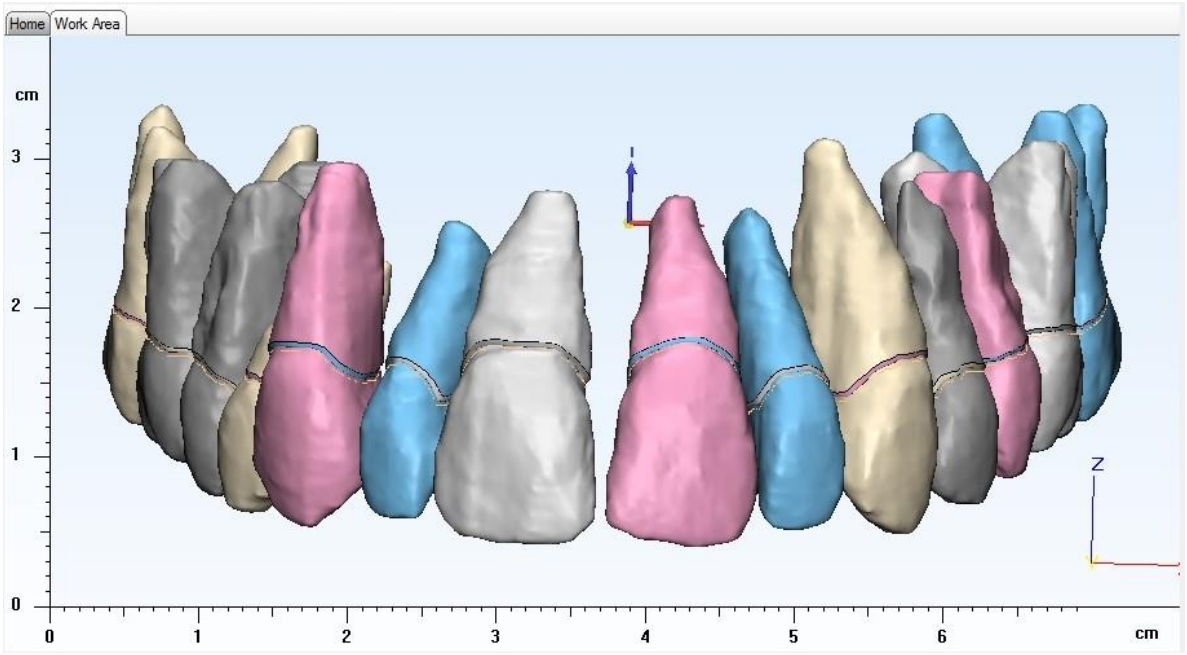

Figure VIII-27: Teeth and periodontal ligaments

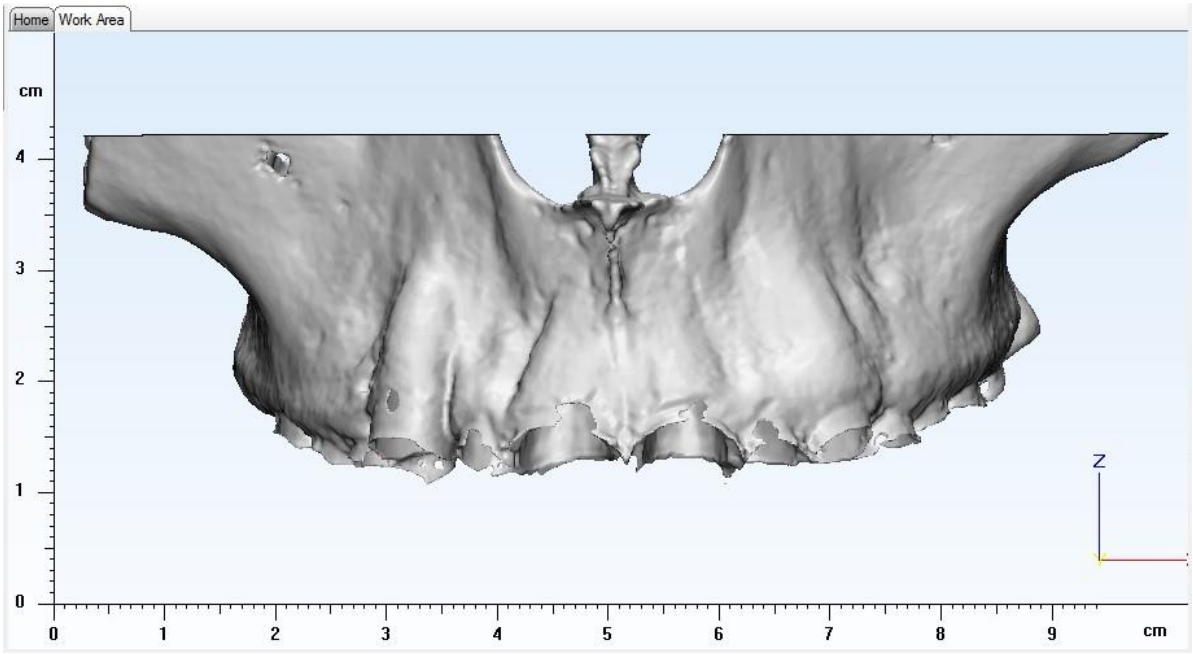

Figure VIII-28: Maxillary Bone

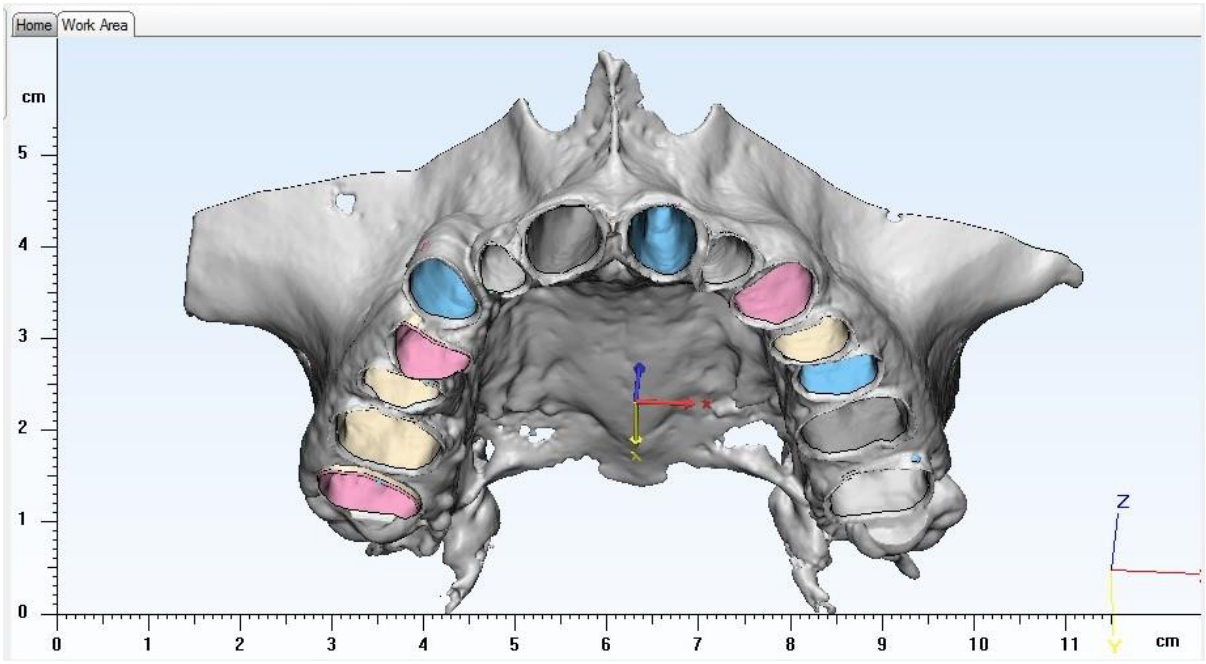

Figure VIII-29: Maxillary Bone with Periodontal Ligaments

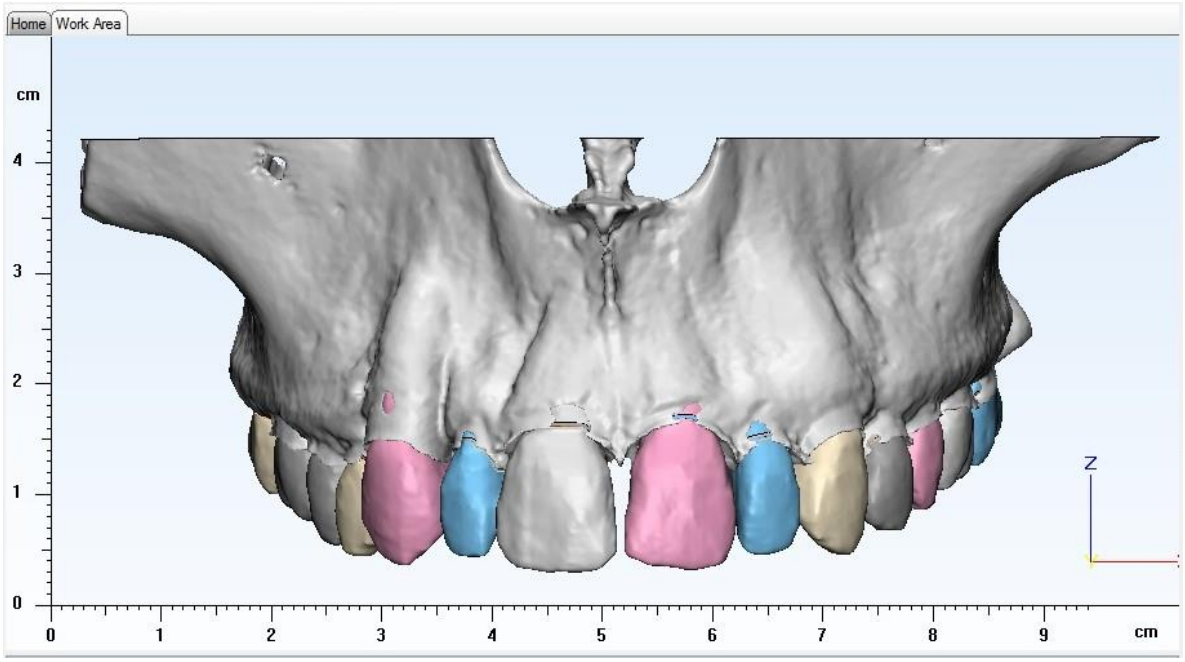

Figure VIII-30: Teeth, Periodontal Ligaments, and Bone together

F. Patient 6 – 16.9 year old male

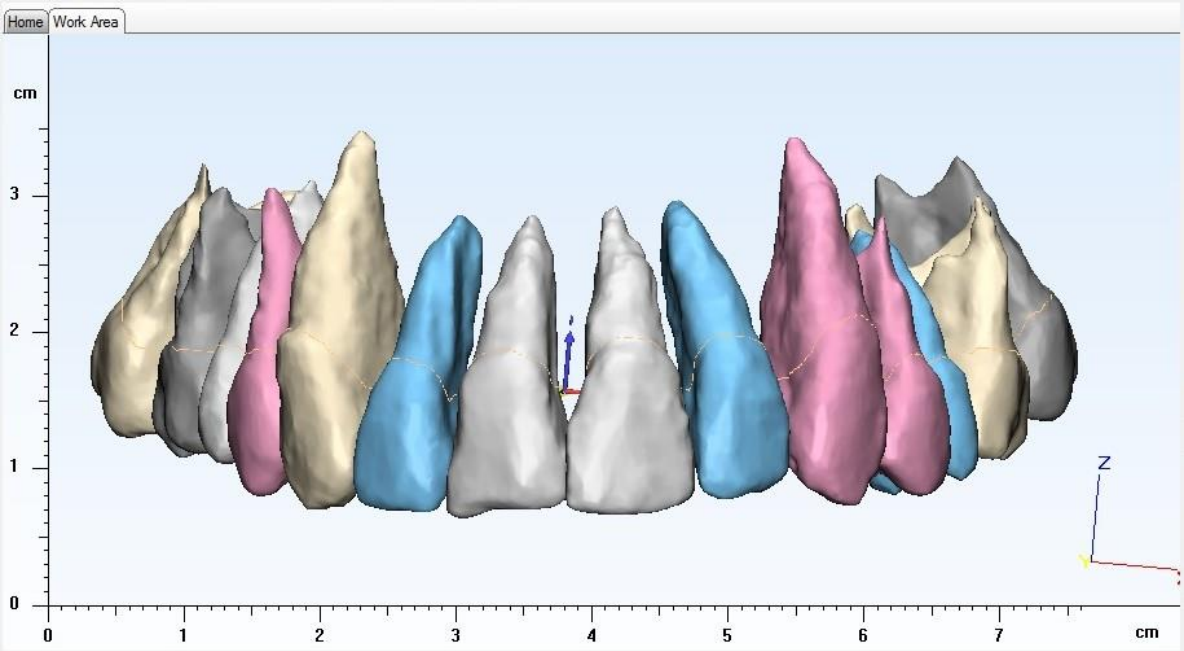

Figure VIII-31: Teeth

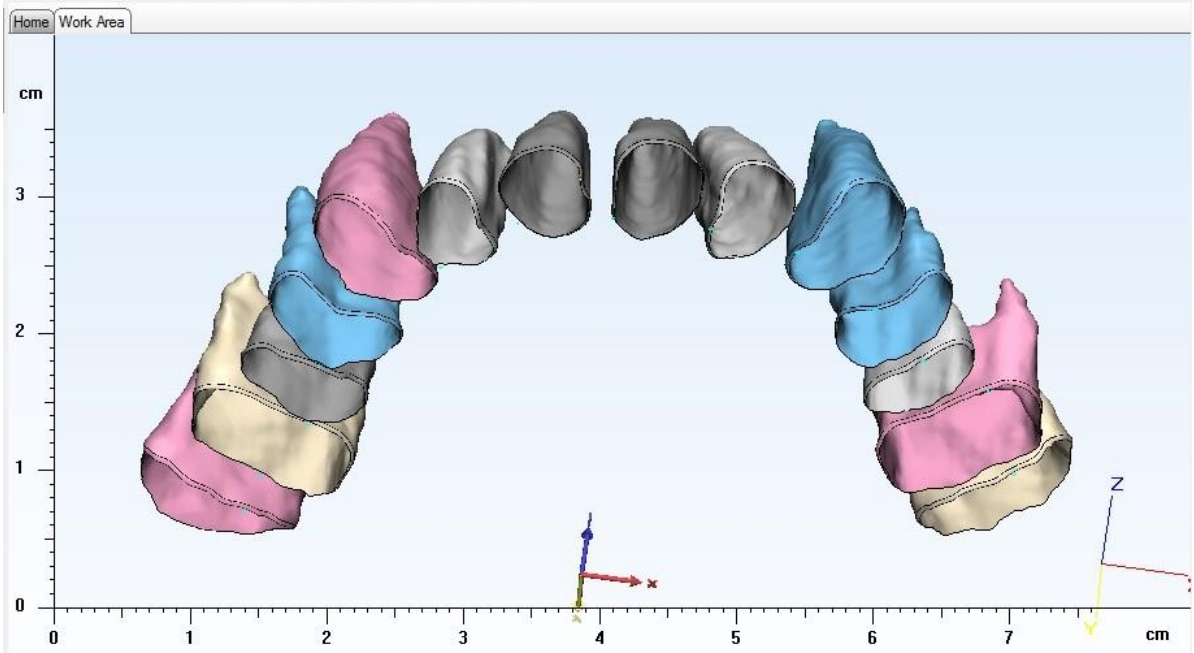

Figure VIII-32: Periodontal Ligaments

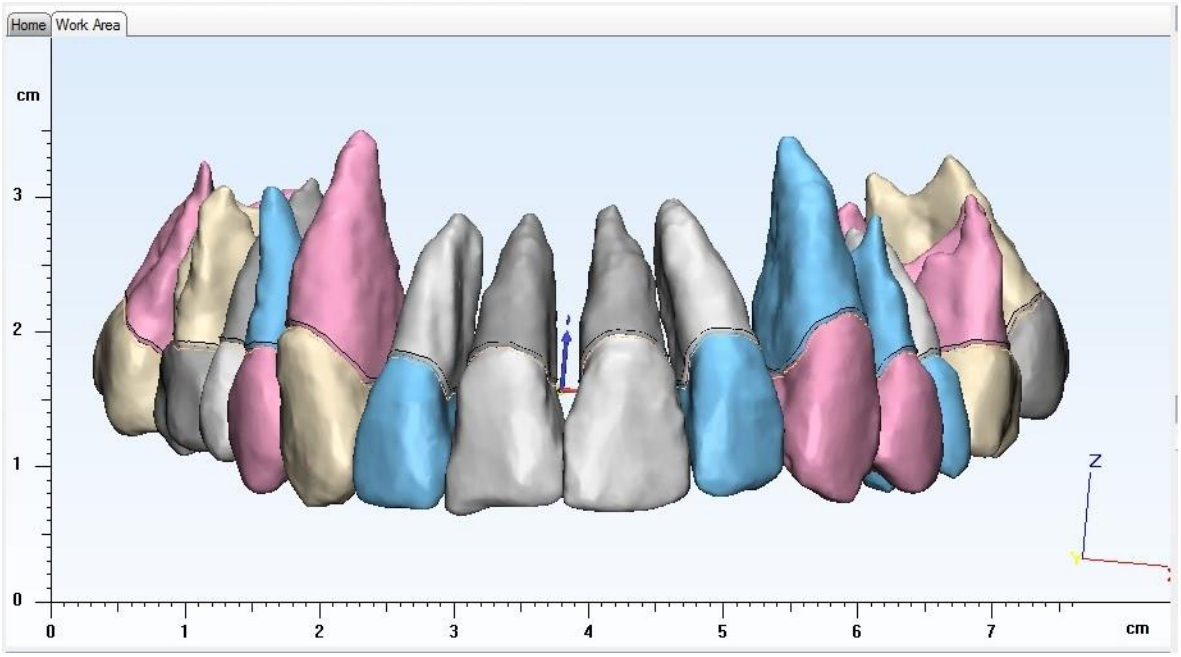

Figure VIII-33: Teeth and periodontal ligaments

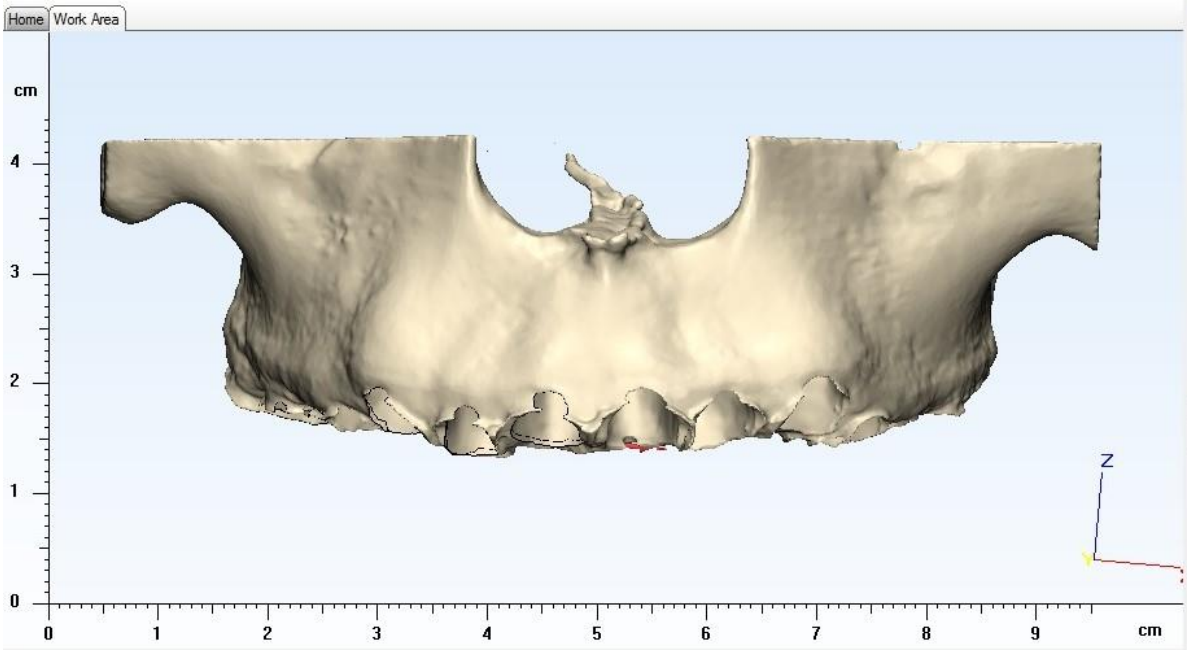

Figure VIII-34: Maxillary Bone

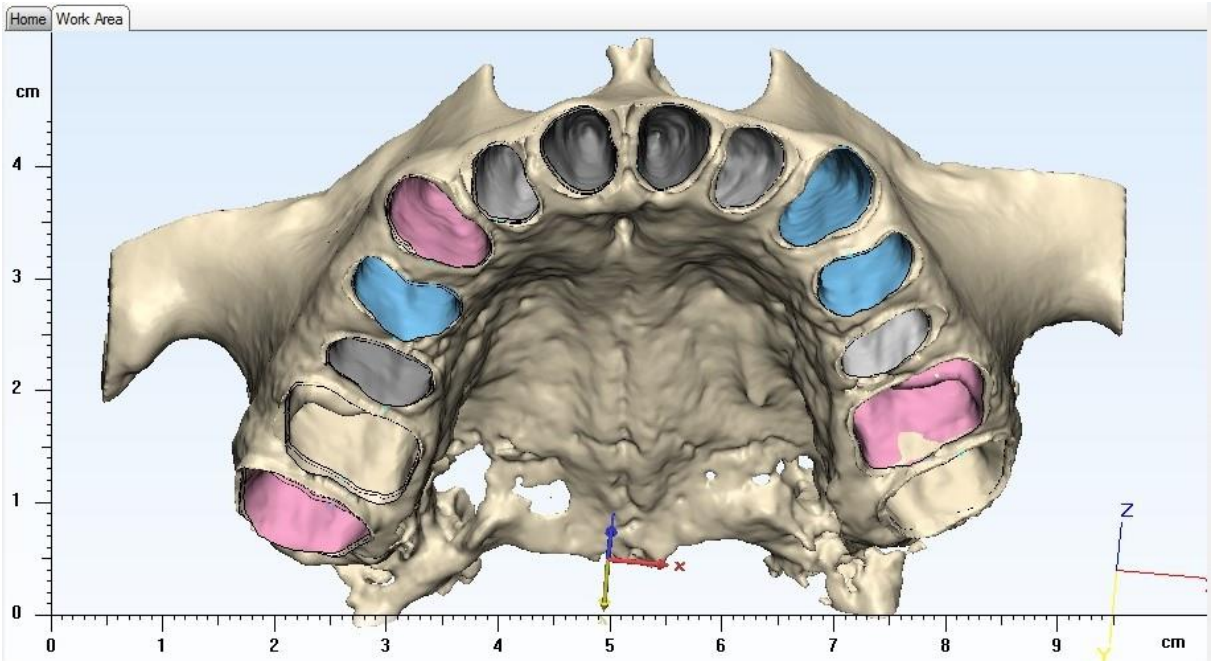

Figure VIII-35: Maxillary Bone with Periodontal Ligaments

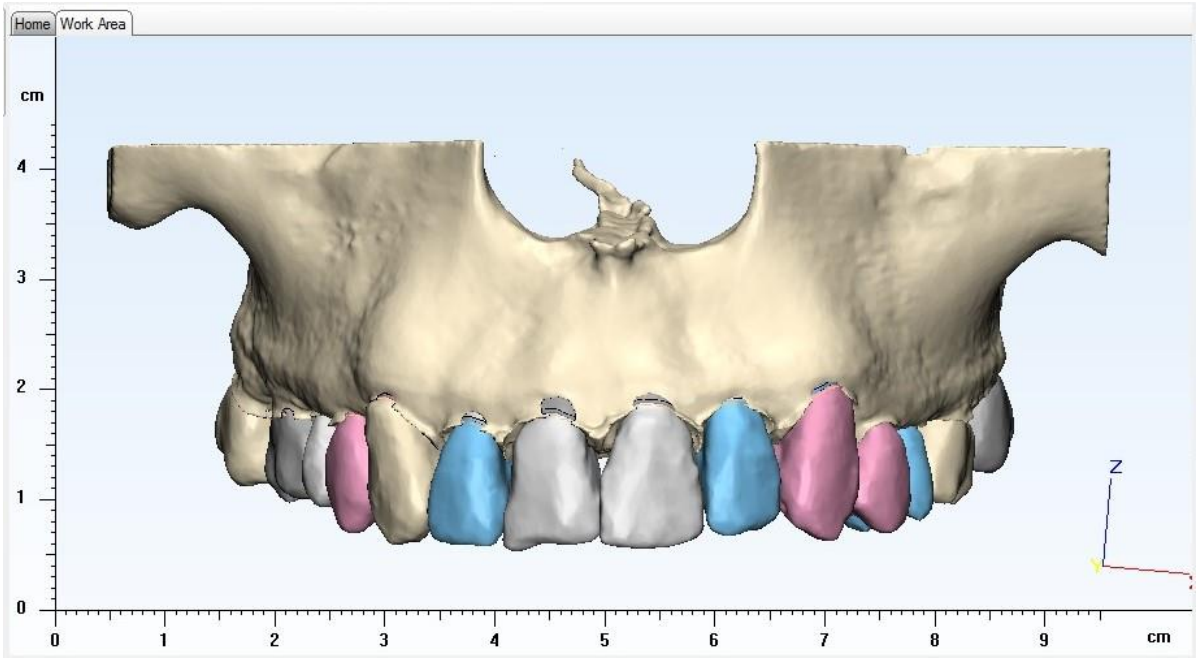

Figure VIII-36: Teeth, Periodontal Ligaments, and Bone together

G. Patient 7 – 61.2 year old female

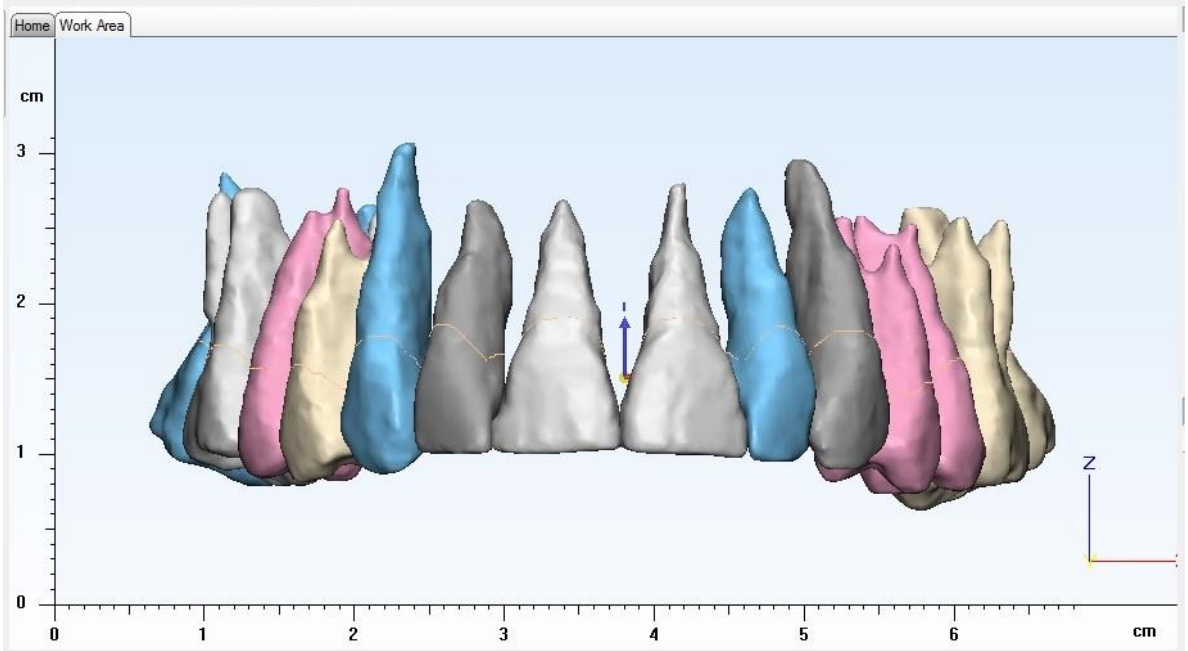

Figure VIII-37: Teeth

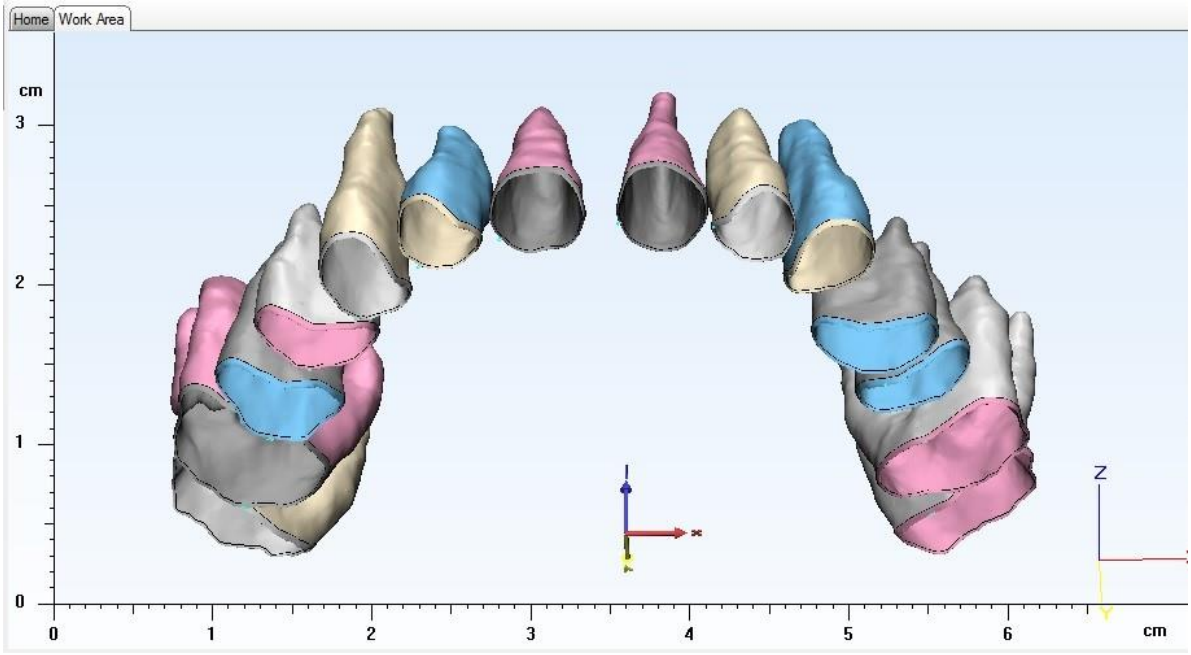

Figure VIII-38: Periodontal Ligaments

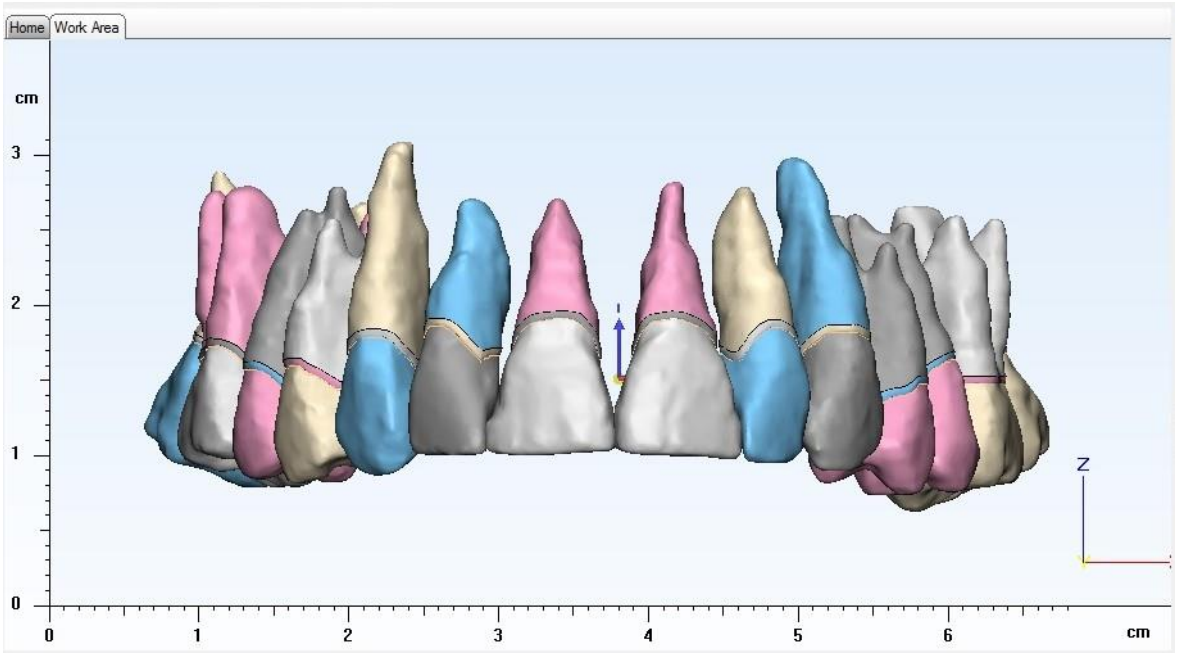

Figure VIII-39: Teeth and periodontal ligaments

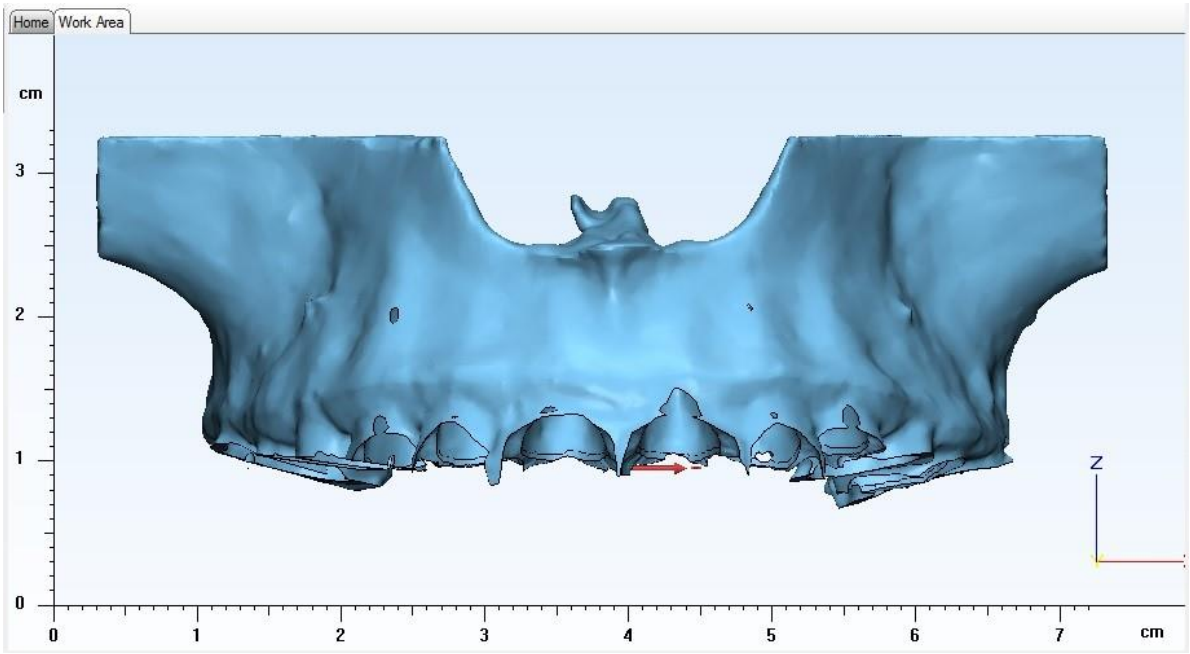

Figure VIII-40: Maxillary Bone

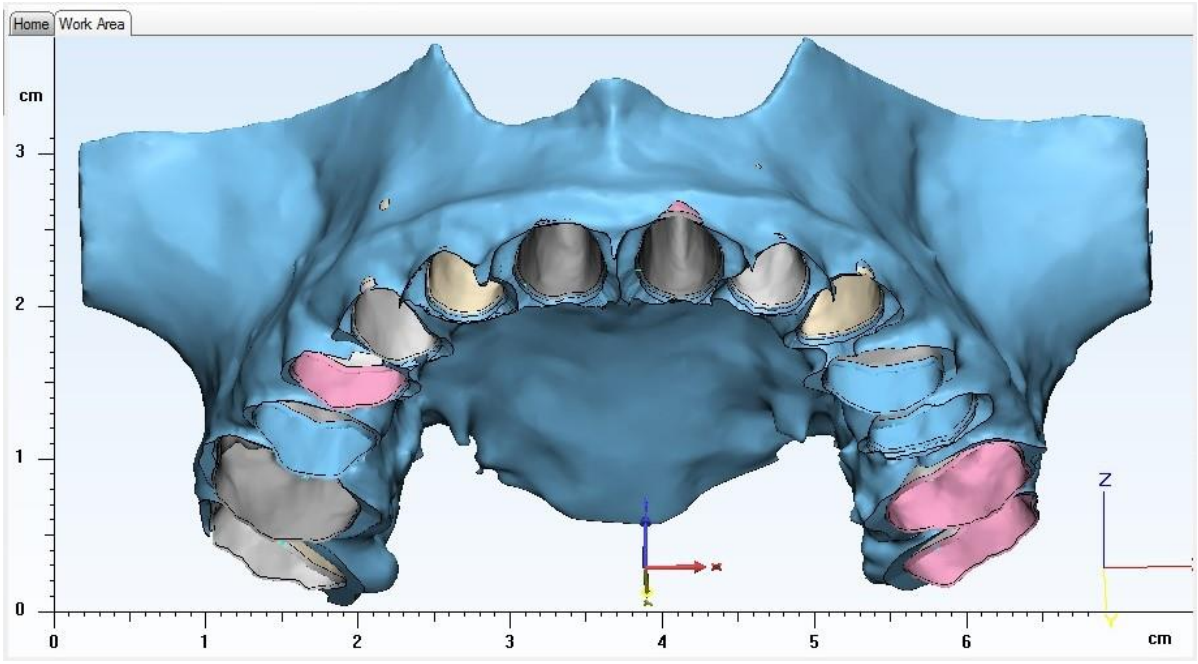

Figure VIII-41: Maxillary Bone with Periodontal Ligaments

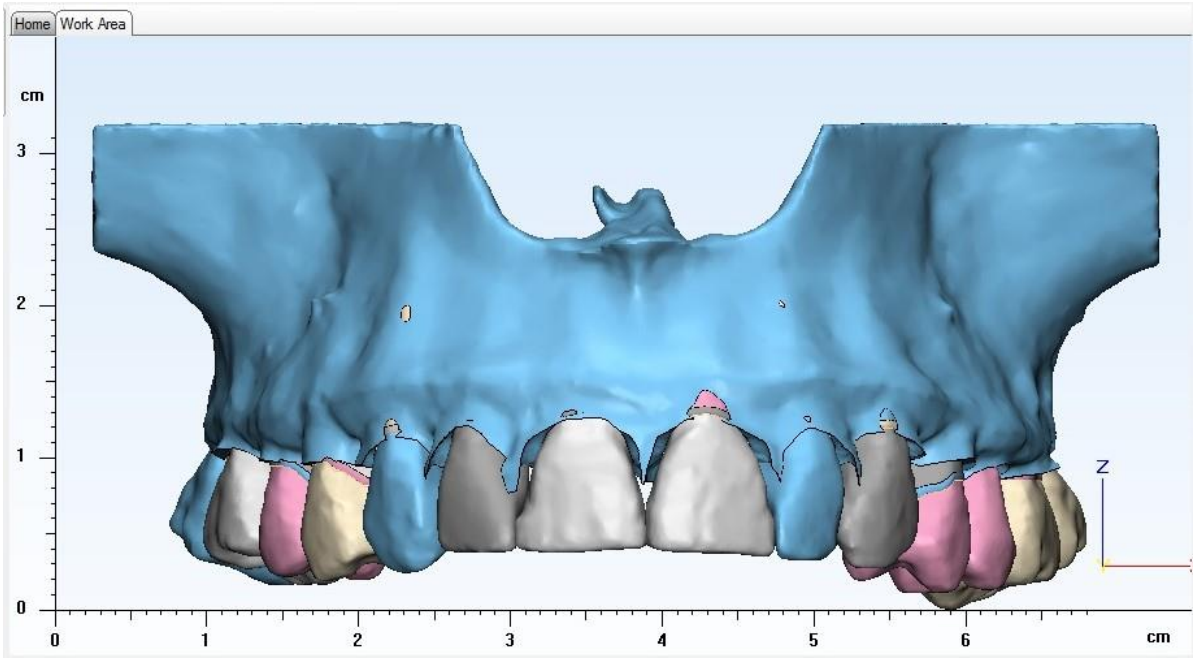

Figure VIII-42: Teeth, Periodontal Ligaments, and Bone together

H. Patient 8 – 11.6 year old female

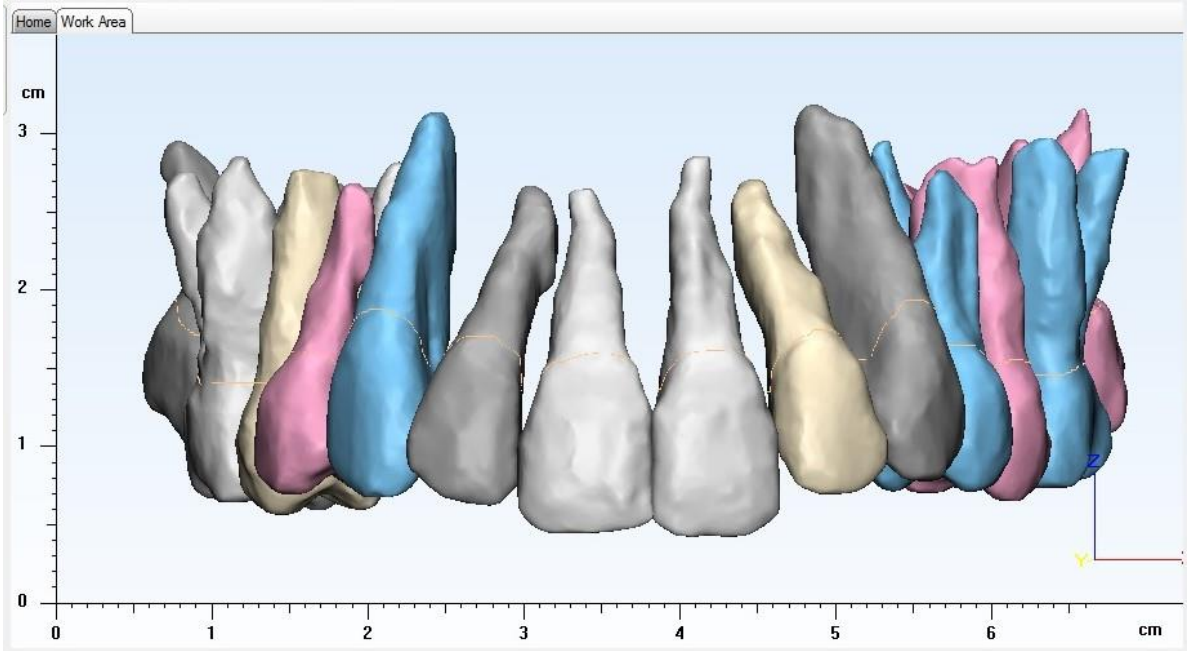

Figure VIII-43: Teeth

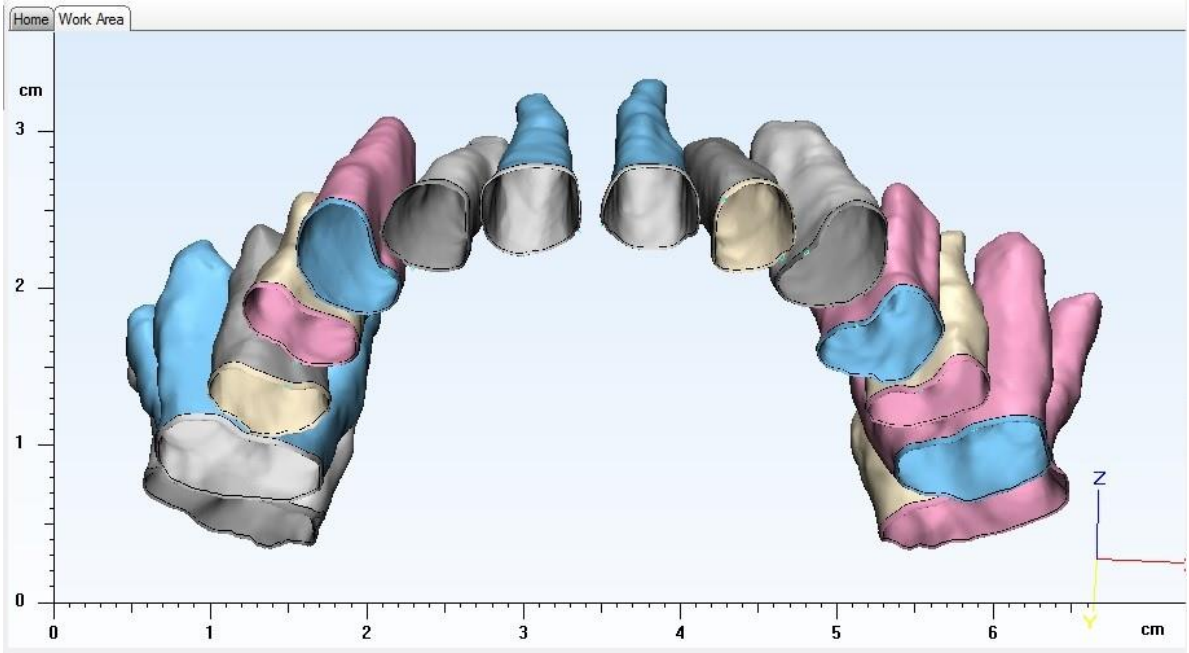

Figure VIII-44: Periodontal Ligaments

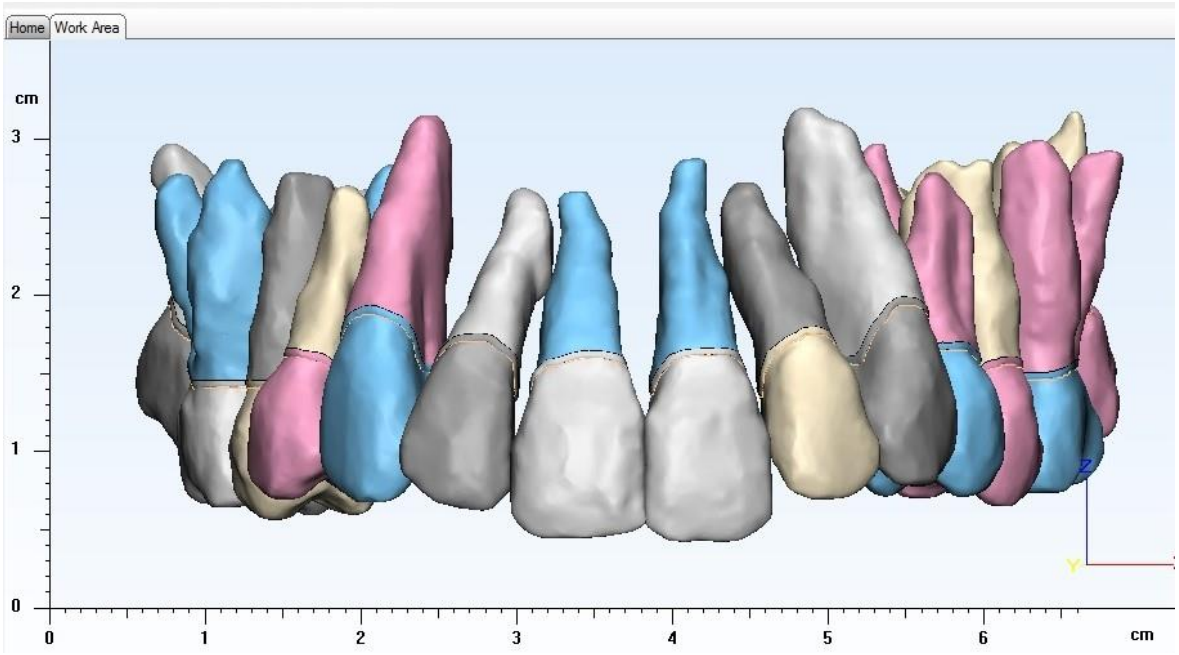

Figure VIII-45: Teeth and periodontal ligaments

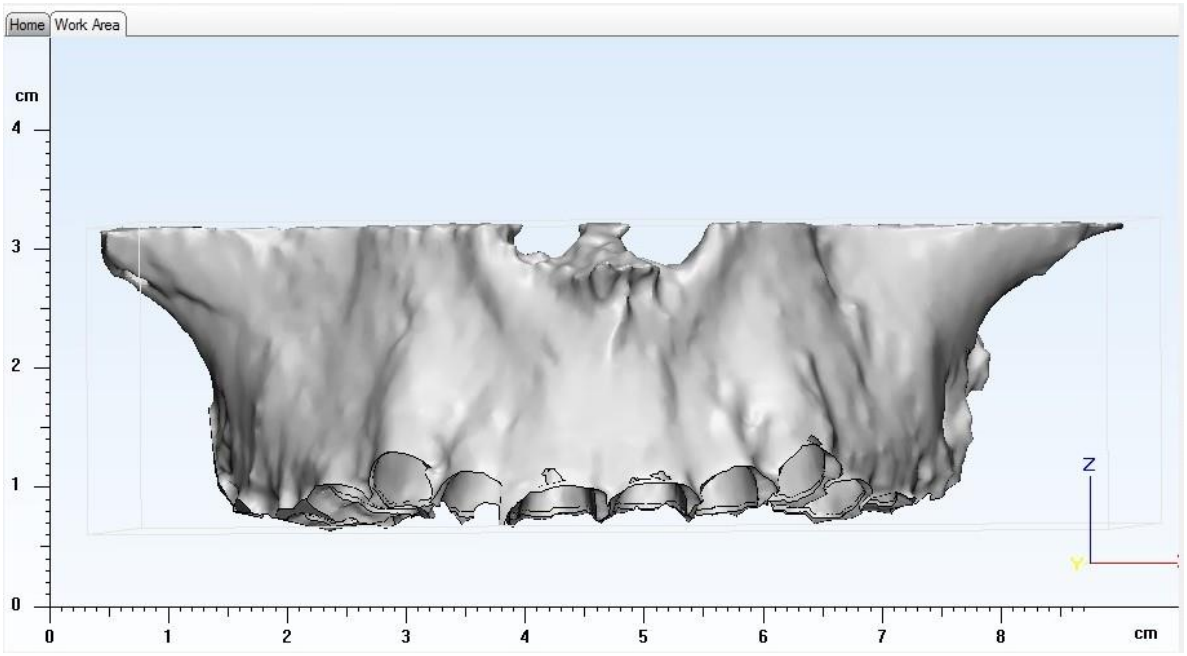

Figure VIII-46: Maxillary Bone

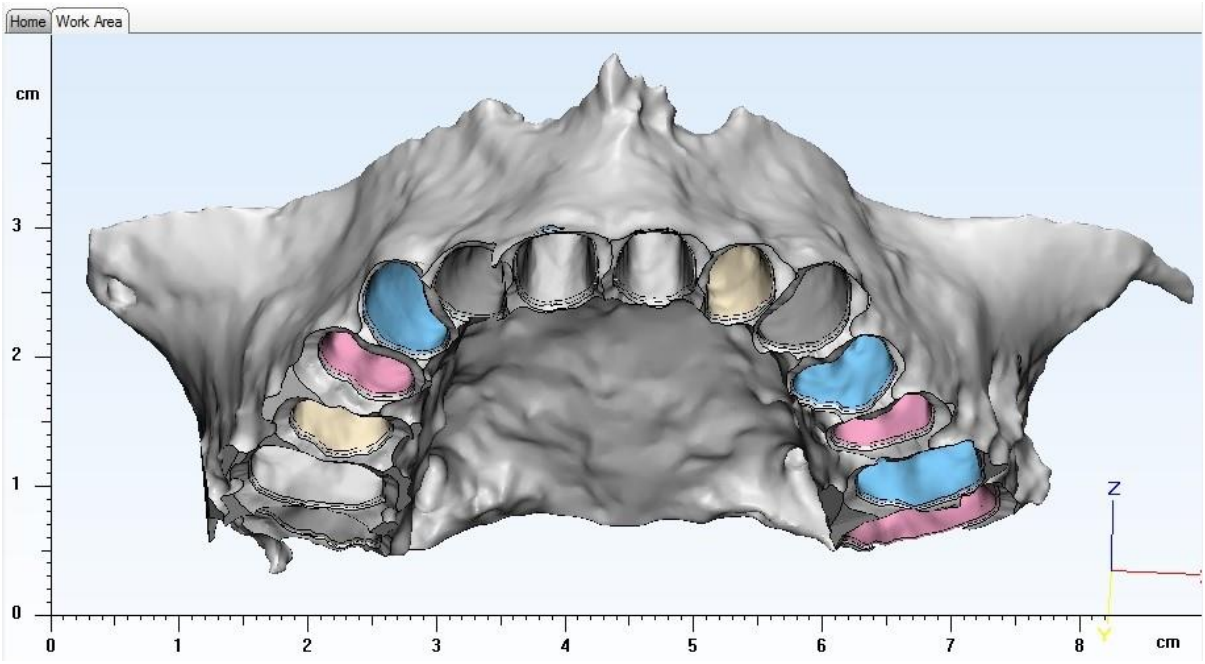

Figure VIII-47: Maxillary Bone with Periodontal Ligaments

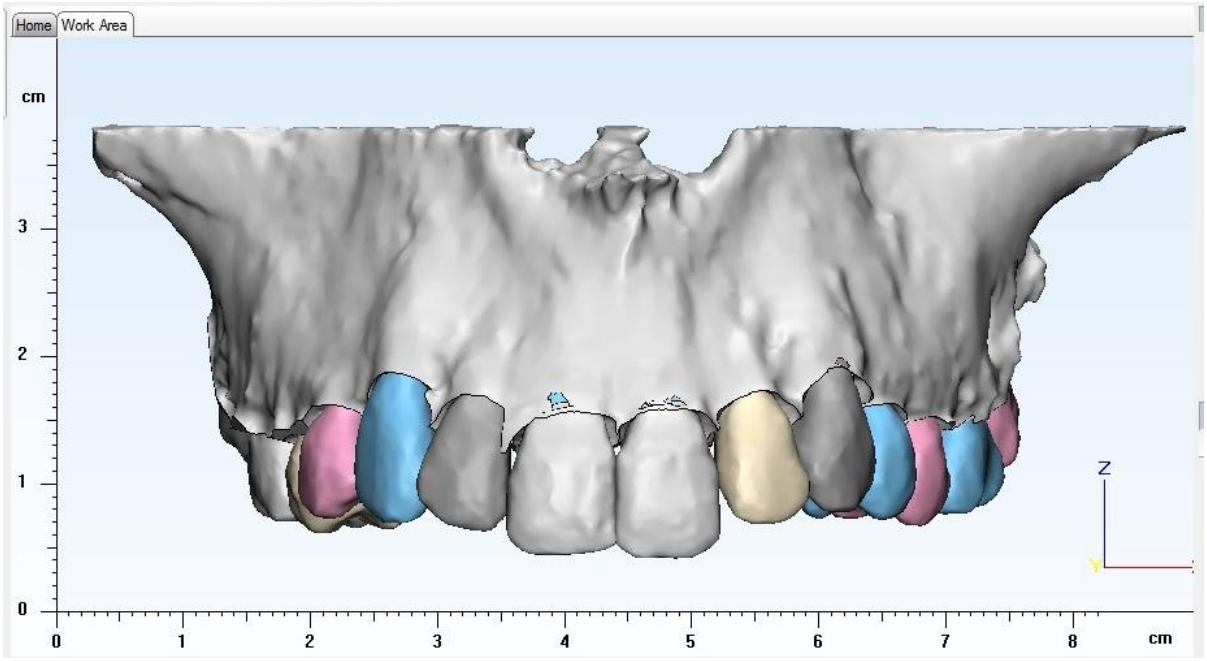

Figure VIII-48: Teeth, Periodontal Ligaments, and Bone together

I. Patient 9 – 60.9 year old male

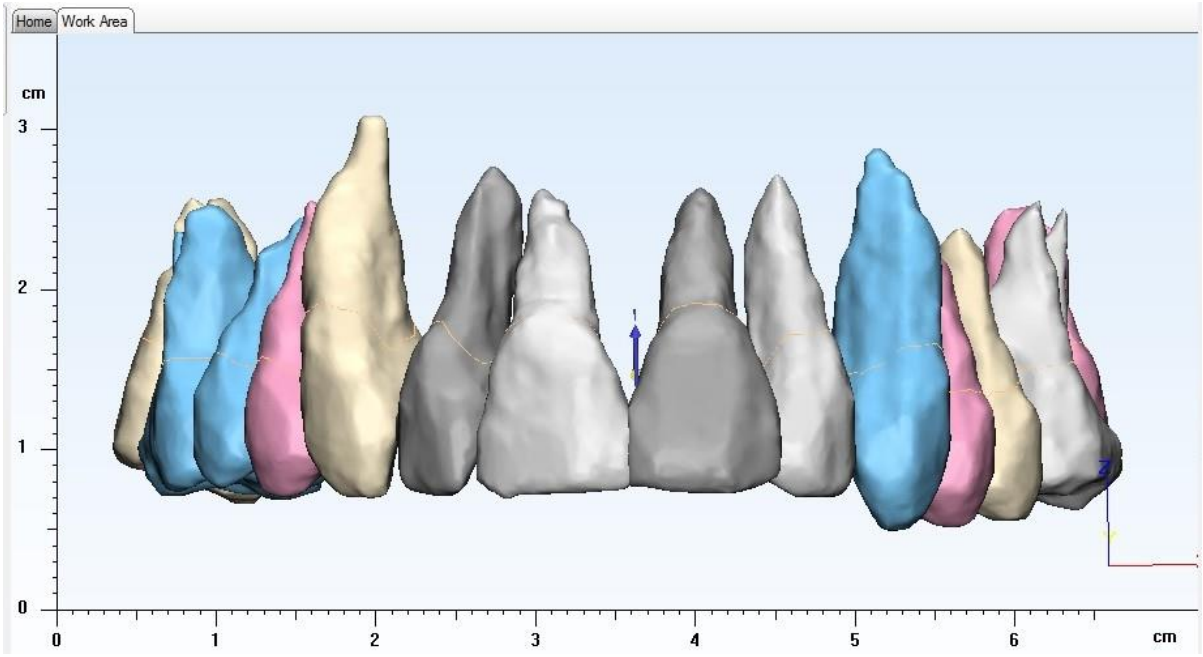

Figure VIII-49: Teeth

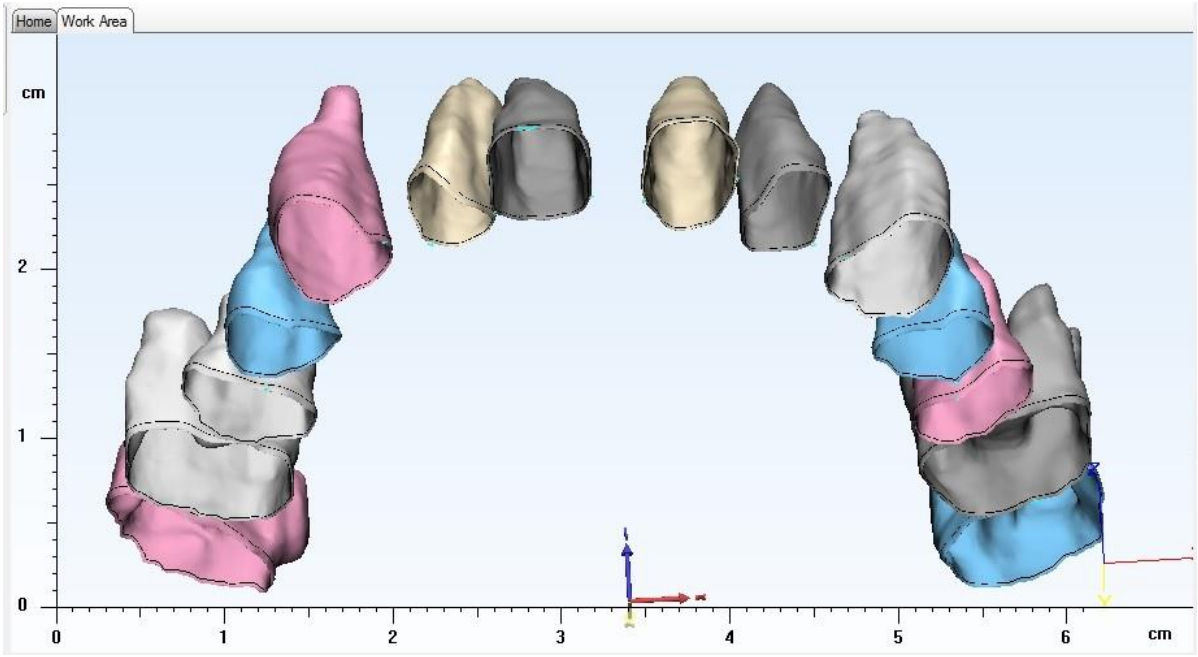

Figure VIII-50: Periodontal Ligaments

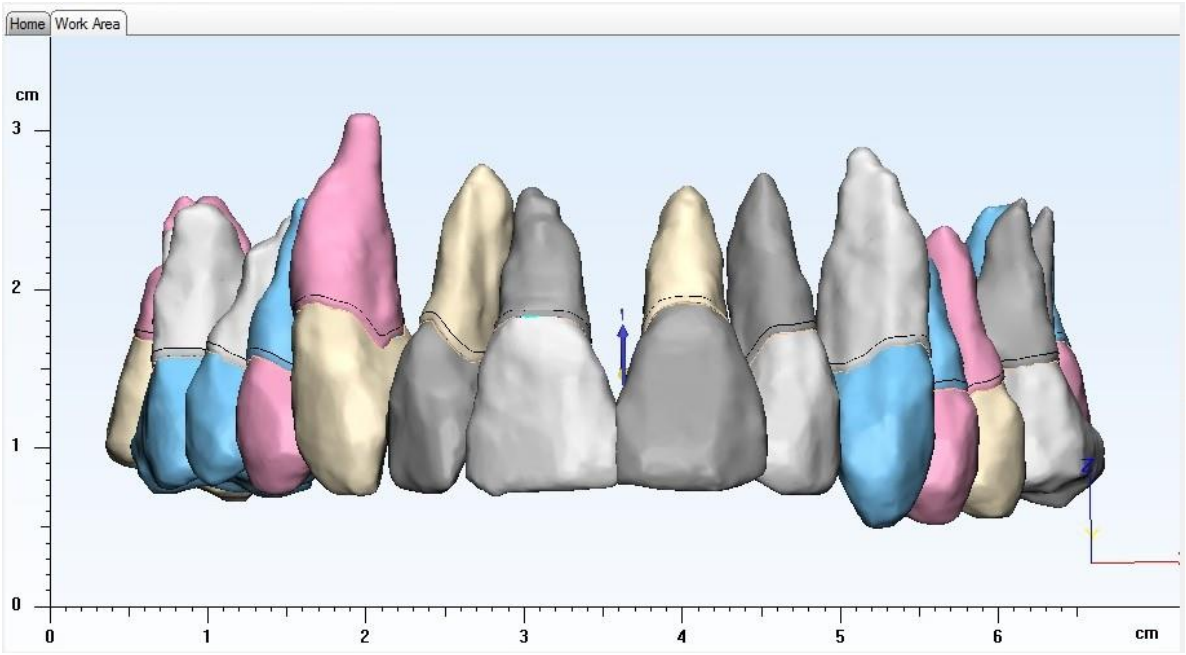

Figure VIII-51: Teeth and periodontal ligaments

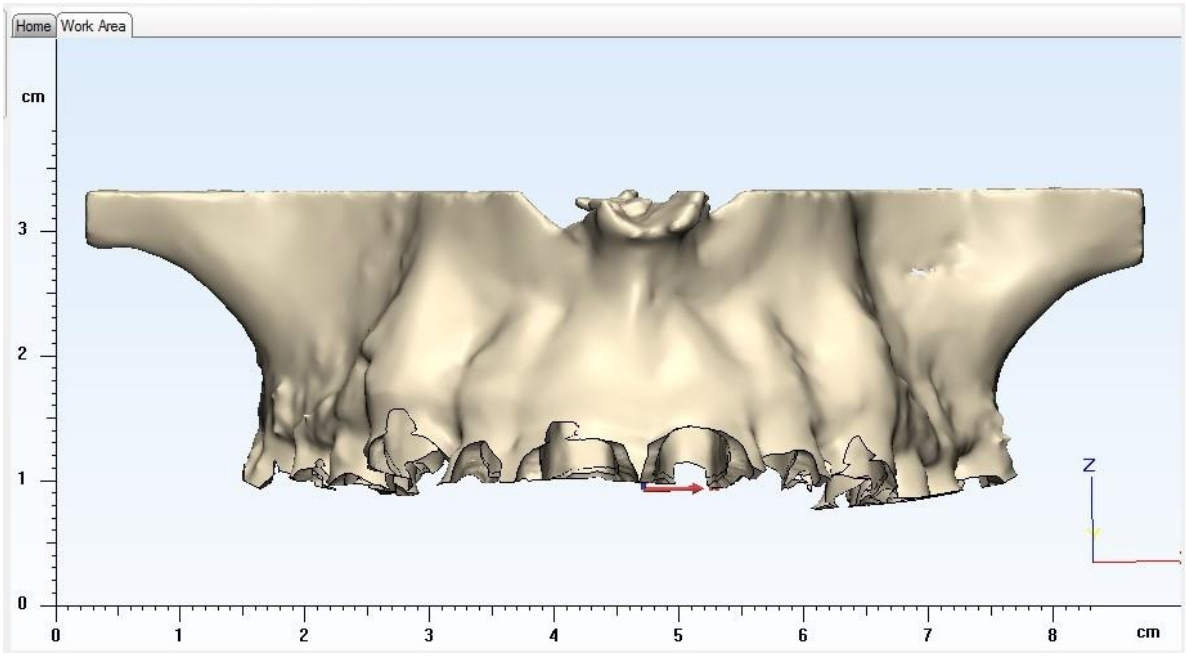

Figure VIII-52: Maxillary Bone

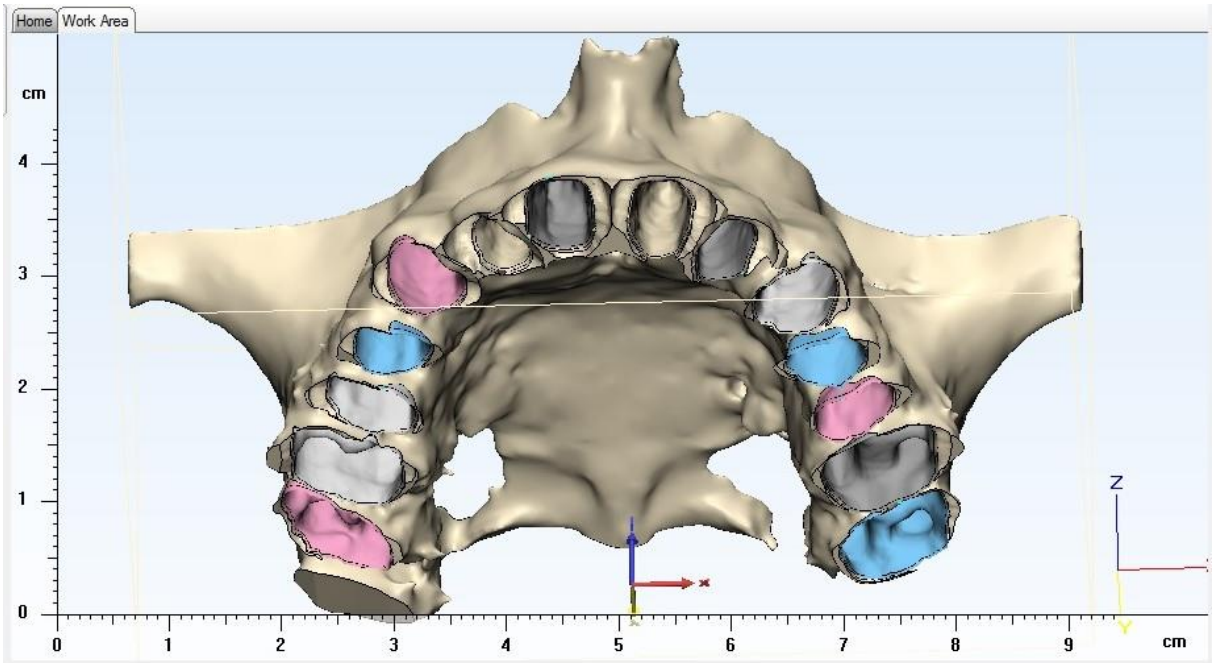

Figure VIII-53: Maxillary Bone with Periodontal Ligaments

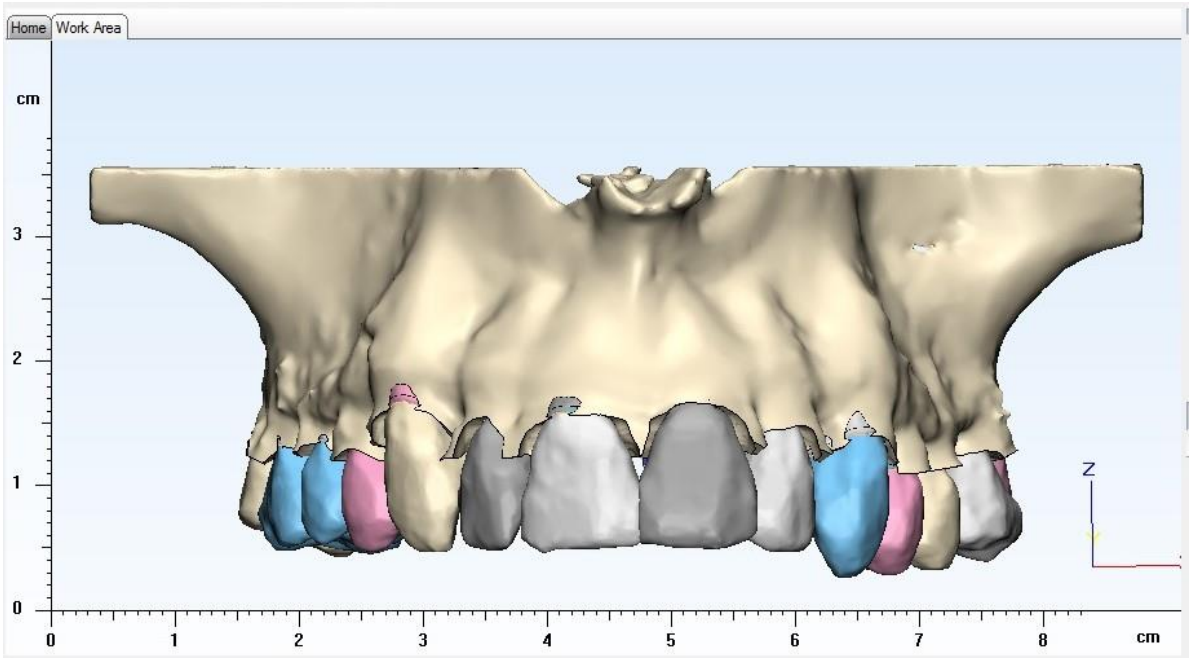

Figure VIII-54: Teeth, Periodontal Ligaments, and Bone together

J. Patient 10 – 37.3 year old female

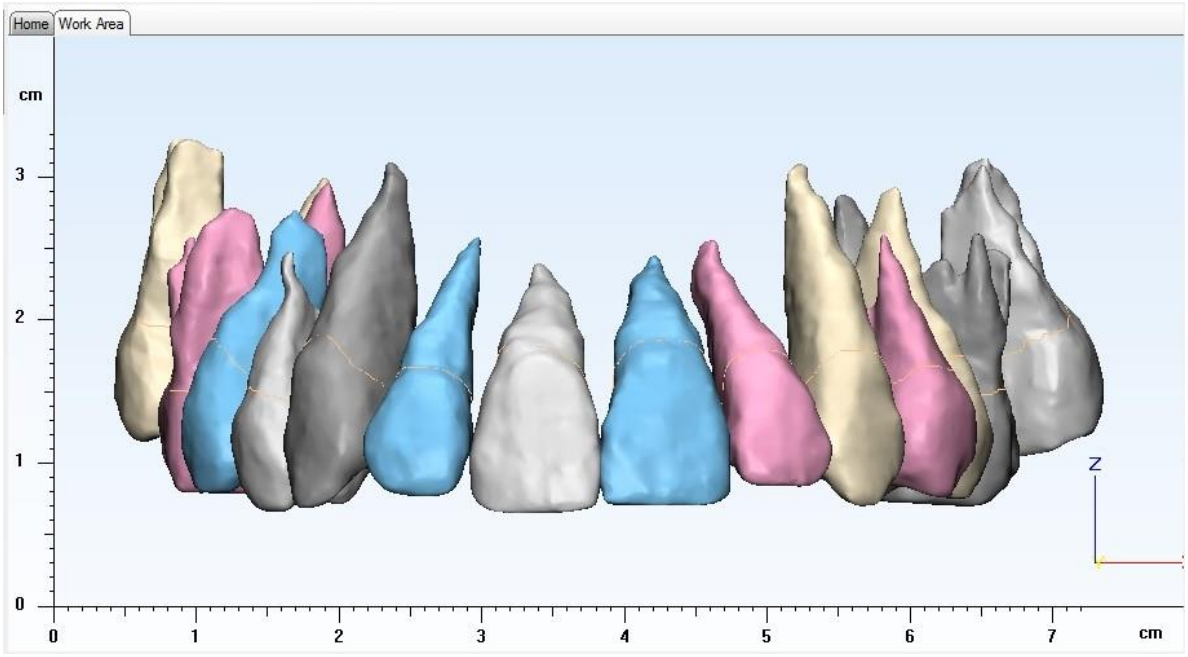

Figure VIII-55: Teeth

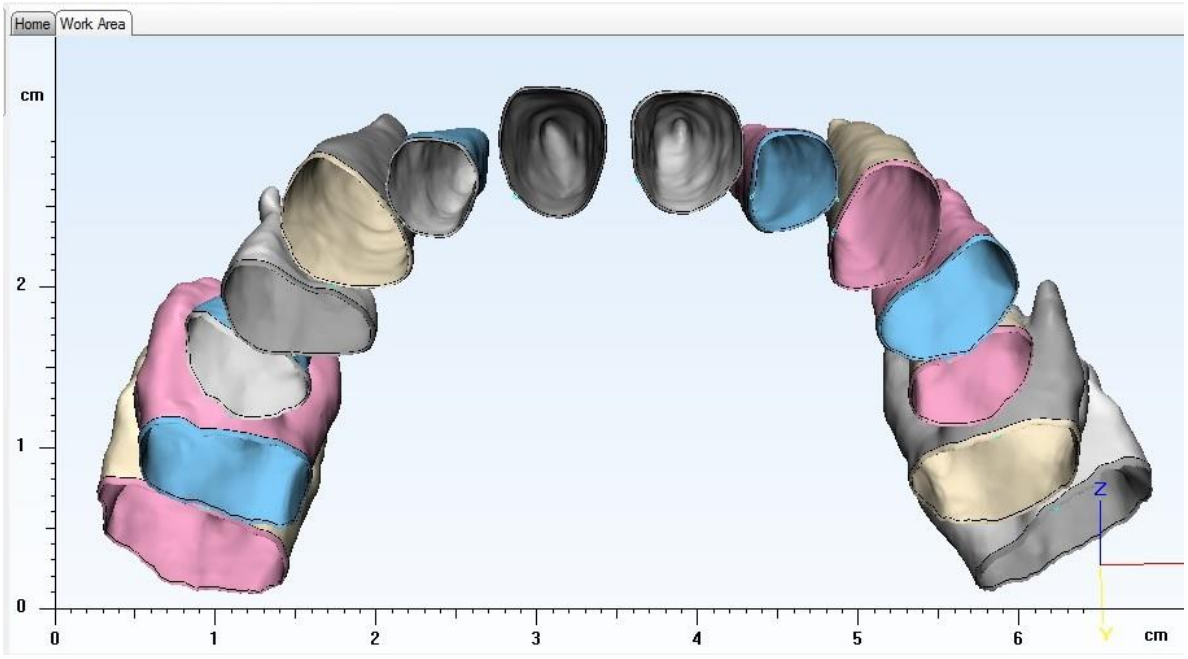

Figure VIII-56: Periodontal Ligaments

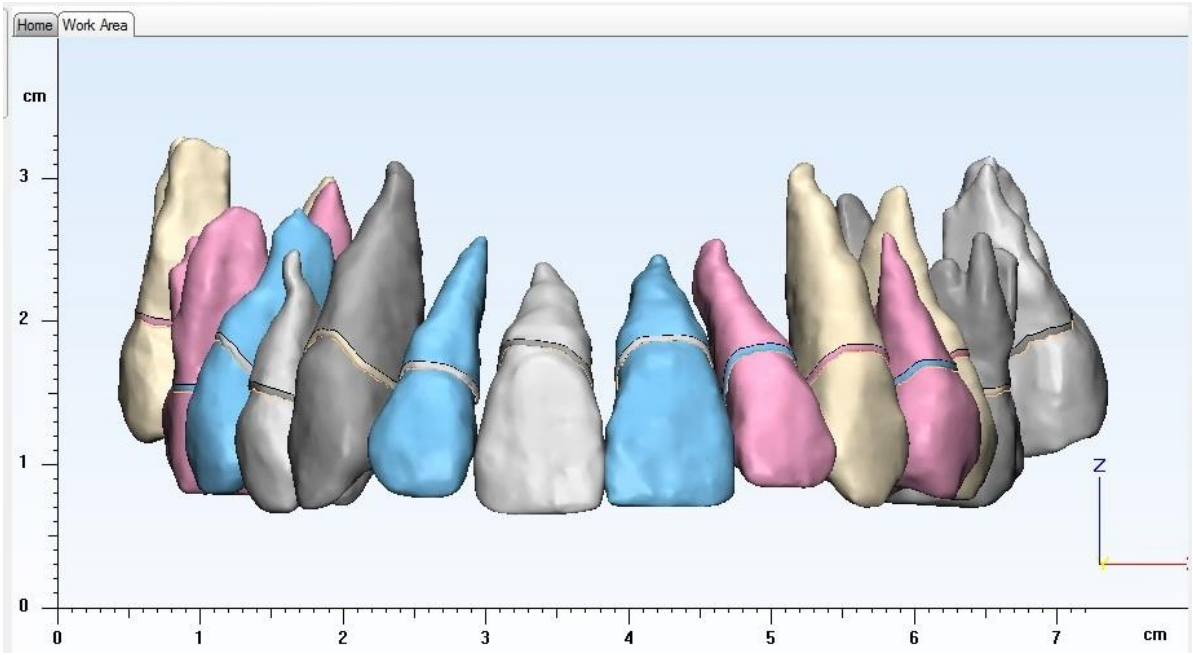

Figure VIII-57: Teeth and periodontal ligaments

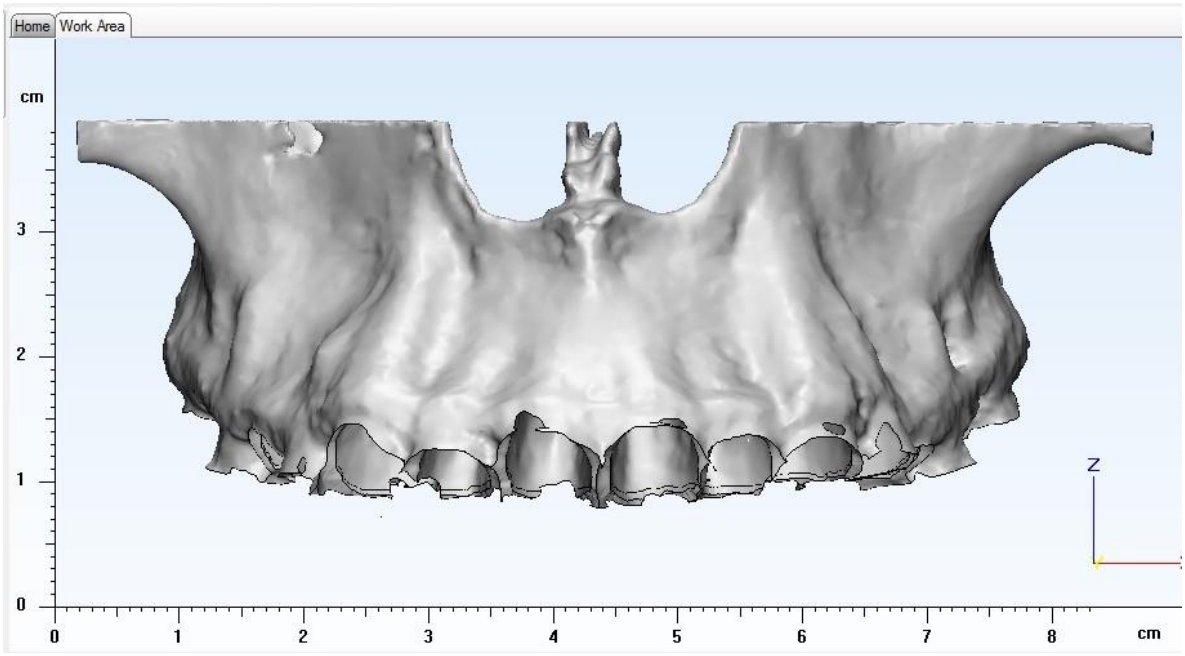

Figure VIII-58: Maxillary Bone

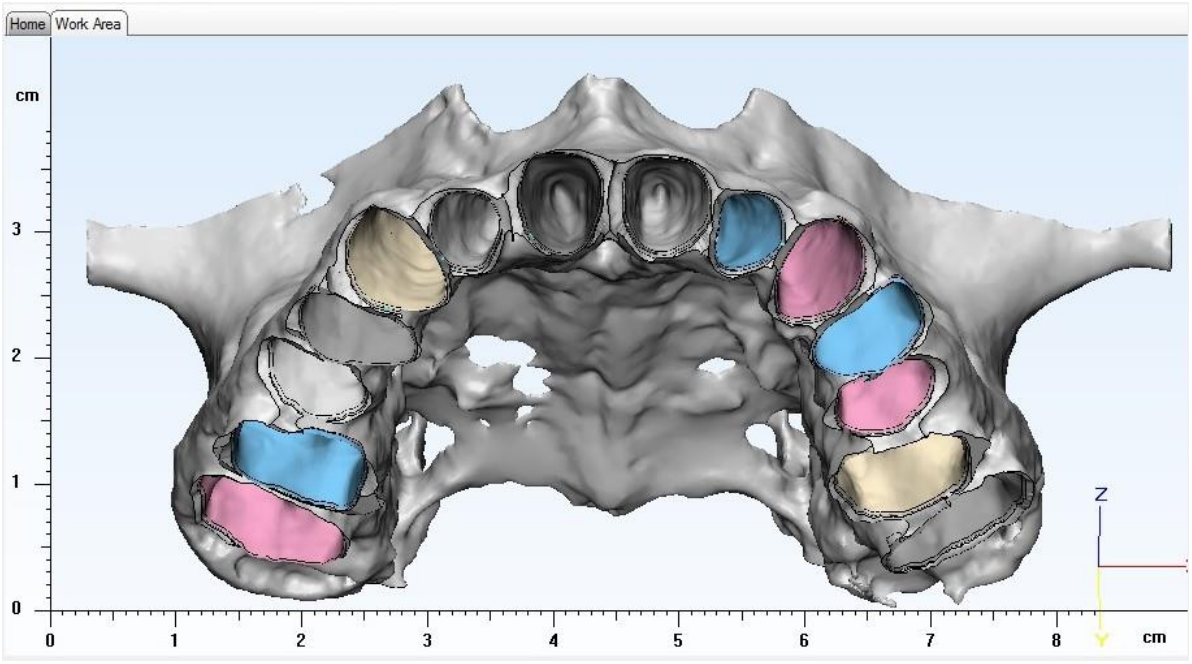

Figure VIII-59: Maxillary Bone with Periodontal Ligaments

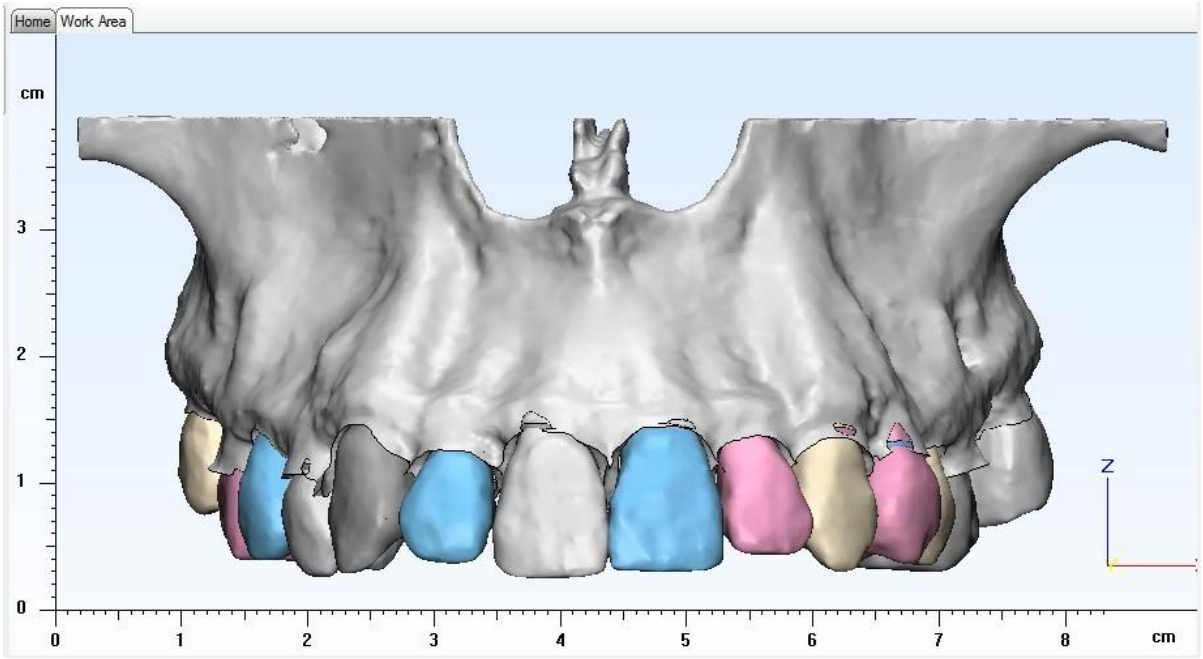

Figure VIII-60: Teeth, Periodontal Ligaments, and Bone together